LIMESTONE DISSOLUTION KINETICS IN UPFLOW REACTOR SYSTEMS

by

Ulrich Robin Christopher Kornmüller

A thesis submitted in partial fulfilment of the requirements for the degree of Master of Science in the Faculty of Engineering, University of Cape Town.

Department of Civil Engineering
University of Cape Town

September 1995

DECLARATION BY CANDIDATE

I declare that this thesis is my own work and it has not been submitted for a degree at another university.

U. R. C. Kornmüller

Signed by candidate

September 1995

SYNOPSIS

Waters derived from the Table Mountain sandstones are soft and acidic. Consequently they tend to be highly aggressive to cement materials and corrosive to metals. Full stabilization is normally effected using lime and carbon dioxide, this however is expensive and inappropriate in many rural areas. Partial stabilization effected by passing the water through limestone (calcium carbonate) granules appears to be a practical means of reducing aggression and corrosion problems associated with these waters. In this process calcium carbonate into the water increases the pH and the Alkalinity and calcium content. Feasibility of the process in part depends on the rate at which limestone dissolves into the water. This investigation addresses the problem of modelling the kinetics of the dissolution process and calibrating the model by experimentation.

Dissolution rates of Bredasdorp limestone granules were measured using an upflow packed bed reactor. Granule size was varied from 3,55mm to 8,05mm and loading rate from 3 m/hr to 38 m/hr.

The dissolution process was found to be diffusion controlled, and in the pH region $5 \leq pH \leq 9$, of the form

$$\frac{d[Ca^{2+}]}{dt} = k_{D.C.\ compound} \left\{ k'^{\frac{1}{2}}_{sp\,c} - [Ca^{2+}]^{\frac{1}{2}} [CO_3^{2-}]^{\frac{1}{2}} \right\}$$

where [ ] = molar concentration

$k'_{sp\,c}$ = apparent solubility product for $CaCO_3$

$k_{D.C.\ compound}$ = compound rate constant, which varies with temperature, ionic strength, granule size and hydraulic characteristics (loading rate) and includes a surface area term.

The dependence of $k_{D.C.\ compound}$ on loading rate and granule size was found to be

$$k_{D.C.\ compound\ (\phi)} = 0{,}0021 \frac{LR}{\phi} + 0{,}0044$$

where ϕ = nominal mean granule size (mm)

LR = loading rate (m hr^{-1})

ACKNOWLEDGEMENTS

My sincere appreciation and gratitude to:

Associate Professor R.E. Loewenthal, under whose supervision this research was conducted, for his support and encouragement.

Dr Nick Marais, for his advice regarding numerical methods.

Miss Bernadette Mentor and **Mr Graeme Evers** for their cheerful assistance in the laboratory especially with the many titrations.

Mr Eike von Guerard and **the workshop staff**, for making the experimental apparatus.

Water Research Commission and the **CSIR** for their financial support.

Mr Grant Mackintosh of the **CSIR** for his encouragement.

Mr Craig Peters of **Bontebok Lime Works** for supplying the Bredasdorp limestone granules.

TABLE OF CONTENTS

CHAPTER 1

INTRODUCTION

Typically raw waters derived from the Table Mountain sandstone regions of the eastern and southern seaboards of South Africa are extremely soft and acidic. Furthermore, dissolved humic substances derived from decaying vegetation impart a colour component to these waters in many areas. The general problem arising with these waters is one of aggressive attack to cement and corrosive attack to metal pipes and structures containing such waters.

Aggression involves attack by the water on cementitious materials in that free lime and some aluminium silicates dissolve readily. This results principally in two adverse effects. Firstly, the integrity of cement type pipes is lost resulting in pressure bursts; for concrete water retaining structures shrinkage cracks are exacerbated leading to failure. Secondly, for reinforced concrete structures the concrete cover is removed exposing the steel to a corrosive environment.

Corrosion of metals by soft acid waters presents in two different ways - either a low pH which causes acid corrosion of the metal, or on the other hand at higher pH ($pH \geq 7$) the low calcium and carbonate species concentrations (low buffer capacity) result in large tubercle formation over cathodic areas. This adversely affects flow characteristics and also creates an environment to harbour iron oxidizing bacteria. Loss of function and the eventual destruction of the conduit is the end result.

It is generally accepted that these soft acidic waters should be chemically treated to both remove humic materials and stabilize them to create a non-aggressive and non-corrosive end product.

Removal of humic substances is effected usually by the processes of coagulation, flocculation (at $pH \sim 6$) and sedimentation. Chemicals commonly used to effect the first two processes are salts of either aluminium (eg. aluminium sulphate and sodium aluminate) or iron (eg. ferric chloride). The optimum pH at which these processes are conducted are $pH \approx 5{,}5$ for aluminium salts and $pH \approx 6{,}5$ for ferric salts; pH control for the coagulation and flocculation processes is achieved by lime dosing either before or immediately after the metal salt dosing point. As the turbidity of these soft waters is generally low, water authorities serving smaller and/or less affluent communities often distribute these waters with minimal further treatment thereby creating an aggression/corrosion problem.

The aggressive properties of a water can be terminated by adjusting its chemical characteristics to a state where it is saturated or slightly supersaturated with respect to $CaCO_3$. Corrosion rates within a metal distribution network can be reduced and perhaps even halted altogether if a dense precipitate scale is formed on the metal surface adjacent to the water. Such passivation is effected if sufficient calcium and carbonate species have been introduced during the stabilization process and generally, this occurs only with very hard waters with pH in the region $7 \leq pH \leq 7,7$. From an economic point of view, treatment of a soft water both to be supersaturated and have $pH \leq 7,7$ requires extremely high chemical dosages and is impractical. Consequently, for softer waters, large metal pipes in the system are lined with cement mortar and the water treated to be non-aggressive, ie. supersaturated with respect to $CaCO_3$ (Loewenthal *et al* 1986). For the smaller pipes for a water treated to be non aggressive, attack in copper will not occur at the higher pH, and attack of iron pipes is reduced sufficiently to be cost effective.

Quality standards for stabilized water require that

i) the water is saturated or slightly super saturated with respect to $CaCO_3$,

ii) calcium and Alkalinity values should not be less than about 50 mg/ℓ as $CaCO_3$

iii) the dissolved oxygen concentration should be greater than about 4 mg/ℓ (as O_2).

Several methods are available for attaining the desired final quality, each of which will be more or less appropriate depending on the costs associated with the chemicals to be used. These include the conventional approaches such as lime and carbon dioxide dosing whereby the Alkalinity, calcium content and pH of the water are raised by chemical dosing (eg calcium hydroxide) to attain the desired Alkalinity and calcium content, carbon dioxide is then added to lower the pH so that a required degree of super saturation is attained. This type of stabilization procedure is well documented and understood (Loewenthal *et al* 1986, Loewenthal and Marais 1976). Control of the process requires a well qualified staff and reliable monitoring equipment. Larger water authorities have the resources and expertise to ensure successful operation of such plants, however due to the economy of scale these resources are beyond the reach of most smaller communities. In addition, as it takes some time for the effects of soft water attack to become evident it is often difficult to convince the relevant authorities to fund an adequate water stabilization program. Thus, few small local water authorities stabilize water prior to distribution. This results in both a shortened lifespan of the reticulation network and unacceptably high annual repair costs as well as a cost associated with water loss through leaks.

In light of the above, there seems to be a lack of tried and tested appropriate low cost, low maintenance solutions to the stabilization problem for soft acidic waters. Contact

stabilization is one possible solution that has been available since the earliest attempts to ameliorate the effects of soft water attack on reticulation systems.

Treatment of domestic water by contact with a bed of marble chips to reduce it's corrosivity was first documented in 1906 in Frankfurt, Germany. However as a positive precipitation potential cannot be achieved using such a system, full benefits of passivation cannot be realized. Attempts at stabilization using chemicals such as sodium carbonate, bi-carbonate and lime gained in popularity and by 1912 Tillmans and Heublin reported that soft water attack on iron was halted through lime stabilization (Reijnen 1979).

Although treatment of soft water by contact with limestone has not gained much popularity, several studies have been conducted into this process. One of the more noteworthy of these being an investigation by Lawson and Snyders (1962). They proposed a stabilization process where excess lime flour (finely ground $CaCO_3$) was suspended in continuously agitated water. In order to increase the dissolution potential and accelerate the dissolution process they investigated two techniques. Firstly, via addition of CO_2 to the suspension, and secondly, via addition of mineral acid (H_2SO_4). Both produced effluents high in calcium and Alkalinity. Subsequent blending with raw water was effected to reduce the volume to be treated. Addition of small amounts of lime (calcium hydroxide) for final pH adjustment was effected to produce a supersaturated effluent. Addition of mineral acid was preferred from an economic standpoint regarding cost of chemicals. A pilot plant was established at Worcester, South Africa, but was later abandoned presumably due to loss of Acidity because of CO_2 loss at the low pH values at which the process operated and carry over of limestone powder with the effluent (Mills 1984).

A possible solution to the stabilization problems faced by the smaller less affluent communities may be found in a vertical upflow packed bed reactor for the following reasons:

i) the problem of CO_2 (ie. Acidity) loss at the lower pH values is minimized as there is ample opportunity for the CO_2 to redissolve into the water during its path through the reactor,
ii) some measure of filtration is provided by the packed bed preventing excessive carry over of fines,
iii) cost of chemicals is reduced by replacing lime and CO_2 with either limestone (calcite) chips or granules,
iv) maintenance is minimal beyond periodic replacement of limestone granules and removal of insoluble impurities present in the dissolving limestone.

Although such a process produces a slightly under saturated water, it is expected to greatly reduce the aggressive properties of the water thereby substantially reducing the potential for

aggressive attack to the reticulation network. Further, the effluent will have pH $\geq$ 8 and corrosive attack to copper will not occur and rate of attack on ferrous materials greatly reduced. Clearly if such packed limestone granule beds are to be used, design of such process requires that the kinetics be quantified.

Various studies, usually from a geological standpoint, have been undertaken to determine reaction rates for the dissolution of limestone. A number of kinetic models have been proposed (See Chapter 3).

In essence mineral dissolution is usually a diffusion controlled process (Stumm and Morgan 1981) the rate of which varies with flow characteristics (higher flow rates leading to high species diffusion), surface area of dissolving mineral and degree of under saturation of the bulk solution. With regard to the surface area term the most reactive limestone depends not only on the possession of large surface area per unit volume (ie. high porosity) but also on the geochemical characteristics of the mineral itself. In this regard metamorphosed limestone, such as marble, does not react as fast as an unmetamorphosed limestone. The limestone utilized in this study was selected from a deposit in Bredasdorp, South Africa because of its friable porous and unmetamorphosed characteristics.

The study focuses on an investigation into the kinetics of dissolution of the Bredasdorp limestone, particularly for application in the partial stabilization of soft waters for smaller communities. The primary objectives of the investigation are;

i) to identify a kinetic model that describes the dissolution process, and
ii) to calibrate the model so that it can be used to predict the rate kinetics for dissolution of the Bredasdorp limestone (calcite).

The document is set out using the following format:
Chapter two describes fundamental weak acid (base) aqueous chemistry that forms the foundation for the investigation.
Chapter three addresses the chemistry of calcium carbonate dissolution in the aqueous environment and various kinetic models used to describe the process.
Chapter four describes the experimental investigation. A kinetic model is selected and the kinetic constants particular to the Bredasdorp limestone are reported.
Chapter 5 includes conclusions and recommendations for practical implementation and future research.

REFERENCES

Lawson S.P & Snyders R. (1962) Lime Acid Reaction for Water Stabilization. *Jour. AWWA* vol 54, Feb., pp 176-180.

Loewenthal R.E. & Marais G.v.R. (1976) *Carbonate Chemistry of Aquatic Systems: Theory and Application*, vol 1. Ann Arbour Sci. Publishers, Michigan.

Loewenthal R.E., Wiechers H.N.S. & Marais G.v.R. (1986) *Softening and Stabilization of Municipal Waters.* Water Research Commission, Pretoria.

Mills R.D.W.B. (1984) Stabilization of Calcium Carbonate deficient waters. *MSc thesis* U.C.T. Cape Town.

Reijnen G.K. (1979) Marmerontzuring, een oud proces met nieuwe perspectieven. H_2O vol. 12, Part 13 pp 290-295.

Stumm W. & Morgan J.J. (1981) *Aquatic Chemistry 2nd ed.* Wiley, New York.

CHAPTER 2

WEAK ACID (BASE) CHEMISTRY

INTRODUCTION

pH in aqueous environments is controlled by interactions between dissolved, gaseous and solid weak acid species. In terrestrial waters the weak acid system that dominates is the carbonate system, to an extent that in most cases other weak acid (base) systems may be neglected. The carbonate system in water is comprised of the carbonate species (molecularly dissolved carbon dioxide, carbonic acid, HCO_3^-, CO_3^{2-} species) and the water species (H^+ and OH^-). It is the interaction between these species that controls pH in natural terrestrial waters.

In this chapter aqueous phase equilibrium chemistry is applied to the carbonate system with two principal objectives. Firstly, characterization of the carbonate system in solution. This involves measuring values of selected parameters such that carbonate species concentrations can be determined. Secondly, prediction of change in state arising from some form of chemical dosing. This aspect may involve either specifying the type and amount of chemical dosage and determining the final state, or the initial and final states are specified and the chemical dosage must be determined. In both cases the approach will be to utilize equilibrium chemistry as the basis from which the development is effected.

EQUILIBRIUM EQUATIONS

Relationships between dissolved carbonate species ($H_2CO_3^*$, HCO_3^- and CO_3^{2-}) and water species (H^+ and OH^-) are governed by a set of thermodynamic equilibrium equations all of which must be satisfied simultaneously;

Thermodynamic equilibrium equations for water:

$$(H^+)\ (OH^-) = k_w \qquad (2:1)$$

for the carbonate system:

$$\frac{(H^+)\ (HCO_3^-)}{(H_2CO_3^*)} = k_{c1} \qquad (2:2)$$

$$\frac{(H^+)\ (CO_3^{2-})}{(HCO_3^-)} = k_{c2} \qquad \textbf{(2:3)}$$

Where k_w, k_{c1} and k_{c2} = thermodynamic equilibrium constants
( ) = activity of species

Values for the equilibrium constants k_w, k_{c1} and k_{c2} are temperature dependent, and are well documented in the literature (see Appendix A).

Referring to the above equations, the species in the equilibria expressions, (Eqs. 2:1 to 2:3), are expressed in the activity form; however in practice, with the exception of the H^+, most species are measured in the concentration (molar) form.

Concentration is a measure of the amount of substance per unit volume. On the other hand, activity is linked to chemical potential and through this to free energies of formation of species, free energies of reactions and equilibrium constants. In short, concentration is the norm in dealing with mass balance while activity is linked to equilibrium equations. However concentration and activity are not independent of each other.

The relationship between concentration and activity of a particular species in essence depends on the charge and ionic radius of a species, matrix and total concentration of charges in the solution and the nature and temperature of the solvent. The magnitude of these effects is termed the activity coefficient of the species, f_x, where

$$(X) = f_x\ [X] \qquad \textbf{(2:4)}$$

where f_x = activity coefficient for species X
[X] = molar concentration of species X

In practice it is not possible to determine activity coefficients of individual species without making non-thermodynamic assumptions. However, in solutions with low concentrations of charges, i.e. dilute solutions, useful semi-empirical methods have been proposed for their estimation. Invariably these estimates are based on the Debye - Hückel or some modification of this equation, for example the Davies equation. This type of equation is usually considered applicable for solutions with Total Dissolved Solids < 4000 mg/ℓ, ie. solution ionic strengths < 0,1 mole/ℓ (Loewenthal *et al* 1986).

The Davies equation is as follows:

$$\log f_i = - A z_i^2 \left(\frac{\mu^{1/2}}{1 + \mu^{1/2}} - 0{,}3\ \mu\right) \qquad (2:5)$$

where f_i = activity coefficient for species i
z_i = charge on species i
i = 1 if monoprotic, i = 2 if diprotic
μ = ionic strength (mole/ℓ)
A = temperature dependent constant

The temperature dependant constant, A, can be estimated as follows:

$$A = 1{,}825 \cdot 10^6\ (78{,}3\ T)^{-1{,}5} \qquad (2:6)$$

where T = temperature in °Kelvin

In Eq. 2:5 the effect of total charges in solution are reflected in the parameter ionic strength, μ, which can be determined if the type and concentration of ions in solution is known

$$\mu = \frac{1}{2} \sum_{i=1}^{n} c_i z_i \qquad (2:7)$$

where c_i = concentration of species i (moles/ℓ)
z_i = charge on species i

In the practical situation analysis of ionic species will rarely be available and empirical means are usually used to estimate ionic strength, eg. that of Langelier (1936), based on measured total dissolved salts concentration (S_d),

$$\mu = 2{,}5 \cdot 10^{-5}\ S_d \qquad (2:8)$$

or using conductivity measurements as proposed by Russell; (Snoeyink & Jenkins 1980)

$$\mu = 1{,}6 \cdot 10^{-5}\ Sc \quad \text{or} \quad \mu = 1{,}6 \cdot 10^{-3}\ Sc_m \qquad (2:9)$$

where Sc = Solution conductivity (μS/cm)
Sc_m = Solution conductivity (μS/m)
S_d = Total inorganic dissolved solids (mg/ℓ) (< 1000 mg/ℓ)

The work reported here deals with waters with very low dissolved salt concentrations and as such, the Davis equation is used to estimate activity coefficients.

Activity coefficients determined as above can now be applied to reformulate the equilibrium equations (Eqs. 2:1 to 2:3) in any desired format which may include species expressed in either or both concentration or activity units.

APPARENT EQUILIBRIUM EQUATIONS AND CONSTANTS

In practice the most useful form for weak acid species is the concentration form because this form is invariably linked to measurement through mass balance parameters. On the other hand the proton activity is usually measured via pH. Consequently the useful form of the equilibrium expression is with weak acid species on the concentration scale and the proton species on the activity scale.

Transforming each of Eqs. 2:1 to 2:3 to the desirable format gives, for water:

$$(H^+)\ [OH^-] = \frac{k_w}{f_m} = k_w' \qquad \textbf{(2:10)}$$

and for the carbonate system:

$$\frac{(H^+)\ [HCO_3^-]}{[H_2CO_3^*]} = \frac{k_{c1}}{f_m} = k_{c1}' \qquad \textbf{(2:11)}$$

$$\frac{(H^+)\ [CO_3^{2-}]}{[HCO_3^-]} = \frac{k_{c2}\ f_m}{f_d} = k_{c2}' \qquad \textbf{(2:12)}$$

where f_m, f_d = activity coefficient, subscripts m and d refer to mono- and diprotic states
k_{c1}', k_{c2}' = 1st and 2nd apparent equilibrium constants of the carbonate system respectively

Examining the equilibrium equations (Eqs. 2:10, 2:11 and 2:12) there are 5 unknowns (ie. (H^+), $[OH^-]$, $[H_2CO_3^*]$, $[HCO_3^-]$ and $[CO_3^{2-}]$) and 3 equations, thus in order to calculate all the unknown species concentrations, at least 2 of the variables must be measured. (This of course assumes that the values for the apparent equilibrium constants are known).

Considering the five unknowns in the above equations, the proton activity is measured directly using pH probes (usually standardized against NBS buffers). pH is defined as follows:

$$pH = -\log_{10}(H^+) \quad \text{or} \quad 10^{-pH} = (H^+) \tag{2:13}$$

Considering the remaining four parameters, direct measurement of any of these is not possible in the normal situation. However other system parameters each of which can be described in terms of dissolved carbonate and water species can be introduced. These include mass parameters and various capacity parameters.

MASS BALANCE EQUATION FOR THE CARBONATE SYSTEM

The total dissolved inorganic carbon C_T, is the sum of the various dissolved carbonate species concentrations, ie.

$$C_T = [H_2CO_3^*] + [HCO_3^-] + [CO_3^{2-}] \tag{2:14}$$

where [ ] = molarity of species (mole/ℓ)

By introducing the mass balance equation the fundamental problem (that of more unknowns than equations) has not changed as we have increased the number of equations by one and have introduced one more unknown. However if an inorganic carbon analyzer is available, C_T can be measured, and together with pH constitute sufficient information to speciate the solution.

The discussion above indicates that for a water with a known C_T value and some fixed ionic strength and temperature (ie. fixed k′ values), it is possible to formulate each of the weak acid species concentrations as functions of C_T and pH, ie:

For $H_2CO_3^*$ species

$$[H_2CO_3^*] = \frac{C_T}{\left\{1 + \frac{k'_{c1}}{(H^+)} + \frac{k'_{c2}\,k'_{c1}}{(H^+)^2}\right\}} \tag{2:15}$$

similarly for HCO_3^- species

$$[HCO_3^-] = \frac{C_T}{\left\{ \frac{(H^+)}{k'_{c1}} + 1 + \frac{k'_{c2}}{(H^+)} \right\}} \qquad (2:16)$$

and for CO_3^{2-} species

$$[CO_3^{2-}] = \frac{C_T}{\left\{ \frac{(H^+)^2}{k'_{c2}\,k'_{c1}} + \frac{(H^+)}{k'_{c2}} + 1 \right\}} \qquad (2:17)$$

For a known C_T a set of general equations can be produced expressing the logarithms of each of the species concentrations as a function of pH. These equations can be used to plot the so called *log[species]- pH* diagram (see Figure 2:1).

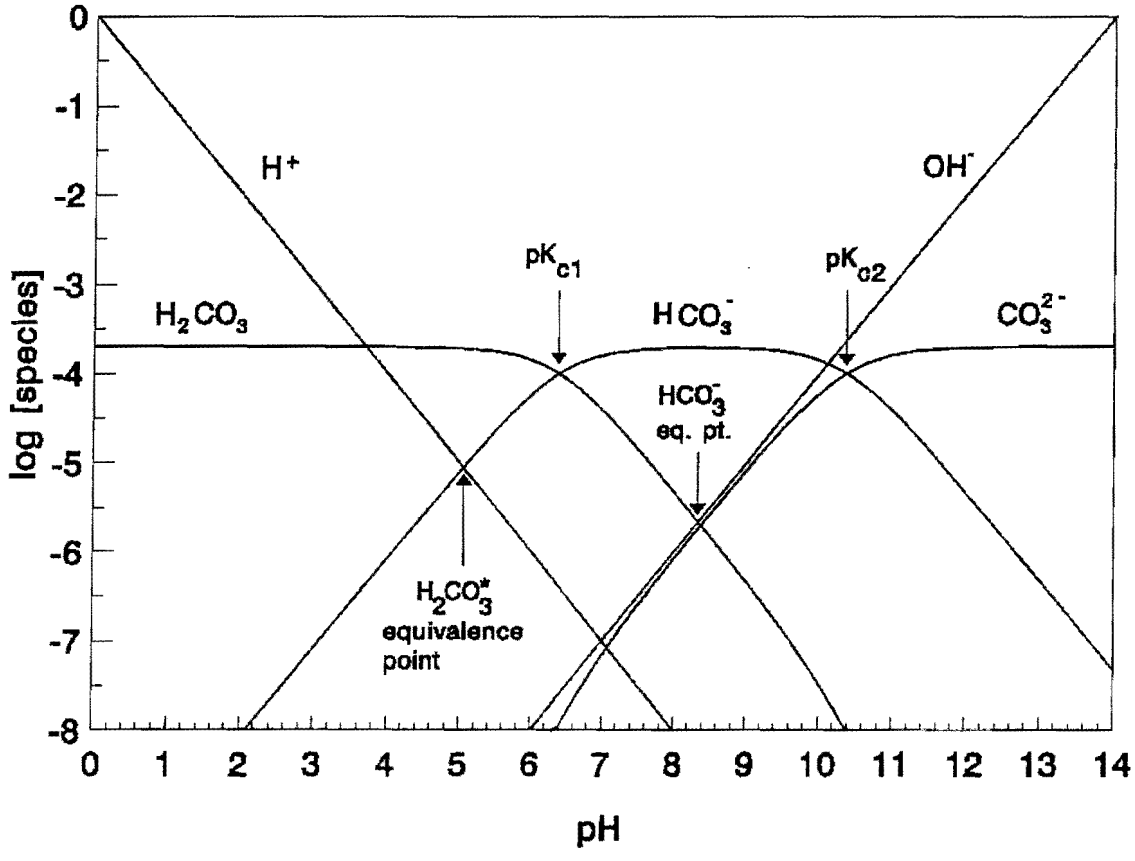

Figure 2:1: *log[species]-pH* diagram for carbonate system, C_T = 0.0002 moles/l.

An inorganic carbon analyzer is an expensive item of equipment and is not found in many

laboratories. Where this equipment is not available, some other system parameter needs to be measured (together with pH) to define the state of the water. In this regard the capacity parameters Alkalinity and Acidity have attained importance (Loewenthal *et al* 1989, 1991).

CAPACITY PARAMETERS - ALKALINITY AND ACIDITY

Over the years the terms "alkalinity" and "acidity" have been applied to a variety of different capacity parameters, the following section is included to define the meanings assigned to these terms in the work presented here.

If a carbonate species is added to pure water, either as a salt (eg. HCO_3^-, CO_3^{2-}) or as a gas (CO_2), the solution formed is known as an equivalent solution, with the pH established at the equivalence point for the particular weak acid species added. The carbonate species added to the water is termed the reference species, and the solution itself is termed an equivalent solution. If a strong base (acid) is added to this equivalent solution the pH will increase (decrease) above (below) the equivalence point of the solution. The mass concentration of base (acid) added to the solution to effect this change is known as the alkalinity (acidity) of the solution with respect to the original equivalent solution established by addition of the reference species to pure water.

Using the Arrhenius definition of an acid (ie. an acid when added to water releases protons (H^+)), the above definition can be rephrased as; ***alkalinity (acidity) is the proton accepting (donating) capacity of the solution relative to some reference state.***

It is possible to derive equations linking alkalinity (acidity) to each of the carbonate species ($H_2CO_3^*$, HCO_3^- and CO_3^{2-}) and the water species (H^+ and OH^-). These equations are given below, their derivations can be obtained from Loewenthal and Marais (1976).

$$\begin{aligned} H_2CO_3^* \text{ alkalinity} &= 2[CO_3^{2-}] + [HCO_3^-] + [OH^-] - [H^+] \\ &= - H_2CO_3^* \text{ acidity} \end{aligned} \qquad \textbf{(2:18)}$$

where [ ] = concentration on the molar scale

Similarly using HCO_3^- or CO_3^{2-} as reference species (addition of sodium carbonate or sodium bicarbonate) the following expressions can be obtained

$$\begin{aligned} HCO_3^- \text{ alkalinity} &= [CO_3^{2-}] + [OH^-] - [H_2CO_3^*] - [H^+] \\ &= - HCO_3^- \text{ acidity} \end{aligned} \qquad \textbf{(2:19)}$$

$$CO_3^{2-} \text{ alkalinity} = -2\,[H_2CO_3^*] - [HCO_3^-] - [H^+] + [OH^-] \quad (2:20)$$
$$= -\,CO_3^{2-} \text{ acidity}$$

Conventionally the $H_2CO_3^*$ alkalinity is written "**Alkalinity**" and the CO_3^{2-} acidity as "**Acidity**", and is the nomenclature used throughout this work.

It must be remembered that the above alkalinities (acidities) are a measure of the mass concentration of acid (base) required to bring the pH of a solution to a specified equivalence point. Thus a relationship between mass and capacity parameters exists.

INTERDEPENDENCE BETWEEN MASS AND CAPACITY PARAMETERS AND pH

The total carbonate species, C_T can be determined from a pair of alkalinity, acidity values as long as they are determined with respect to different reference species. The sum of an alkalinity, acidity pair with adjoining reference species is C_T, eg.

$$H_2CO_3^* \text{ alk} + HCO_3^- \text{ acidity} = C_T \quad (2:21)$$

and with reference species two protons apart is $2C_T$, eg.

$$H_2CO_3^* \text{ alk} + CO_3^{2-} \text{ acidity} = 2\,C_T \quad (2:22)$$

As each of the weak acid species can be written in terms of C_T and pH, (Eqs. 2:15, 2:16 and 2:17), it is clear that if two of the three parameters Alkalinity, Acidity and pH are known, the aqueous system is fully characterized. This is depicted graphically in Deffeys type diagrams which are constructed for a specific temperatures and ionic strengths (Loewenthal and Marais 1976, Loewenthal *et al* 1986).

The interdependence between pH, Alkalinity and Acidity is established via the equilibrium equations (Eqs. 2:10 to 2:12) and the equations for the capacity parameters Alkalinity (Eq. 2:18) and Acidity (Eq. 2:20), to give

$$\text{Acidity} = \text{Alk}\left[\frac{1 + 2\times10^{(pH - pK_{c1}')}}{1 + 2\times10^{(pK_{c2}' - pH)}}\right] - 10^{(pH - pK_w')} + 10^{(-pH)} \quad (2:23)$$

CHANGE IN MASS AND IN CAPACITY PARAMETERS WITH DOSING

The various forms of alkalinity and acidity discussed above change in a simple stoichiometric manner with the mass concentration of a chemical dosage (or removal) (Loewenthal et al 1986). The corresponding changes in pH are however more complex and need to be calculated using equilibrium considerations.

From the definitions of Alkalinity and Acidity above, the changes in ;the parameters Alkalinity and Acidity with chemical dosage are as follows:

$$\Delta \text{ Alkalinity} = \text{Alk}_{\text{added}} = 2[CO_3^{2-}]_{\text{added}} + [HCO_3^-]_{\text{added}} + [OH^-]_{\text{added}} - [H^+]_{\text{added}} \quad \textbf{(2:24)}$$

$$\Delta \text{ Acidity} = \text{Acid}_{\text{added}} = 2[H_2CO_3^*]_{\text{added}} + [HCO_3^-]_{\text{added}} - [OH^-]_{\text{added}} + [H^+]_{\text{added}} \quad \textbf{(2:25)}$$

where Δ indicates a positive change
From Eq. 2:22, the corresponding change in C_T is given by;

$$\Delta C_T = \frac{1}{2} \Delta \text{ Alk}_{\text{added}} + \frac{1}{2} \Delta \text{ Acid}_{\text{added}} = [H_2CO_3^*]_{\text{added}} + [HCO_3^-]_{\text{added}} + [CO_3^{2-}]_{\text{added}} \quad \textbf{(2:26)}$$

A rigorous proof of the above relationships from basic chemical relationships is given by Loewenthal and Marais (1976). These simple stoichiometric changes in the mass and capacity parameters with addition of the various carbonate and water (H^+ and OH^-) species form a useful basis for predicting either the condition of a water after dosing or to determine the dosage to achieve a desired resultant condition.

MEASUREMENT OF ALKALINITY

Ideally, to determine the alkalinity of a water with respect to a specific reference species, a titration should be carried out to the equivalence point of the selected reference species. The alkalinity being a measure of the strong acid added to the sample to reach that selected equivalence point. The problem often arising in this regard hinges around identifying the selected equivalence point.

The $H_2CO_3^*$ equivalence point varies with C_T which is initially unknown, consequently the end point to the titration is unknown. For waters with Alkalinity $\geq$ 30 mg/ℓ as $CaCO_3$, various procedures have been developed for the best estimate of the endpoint to the titration

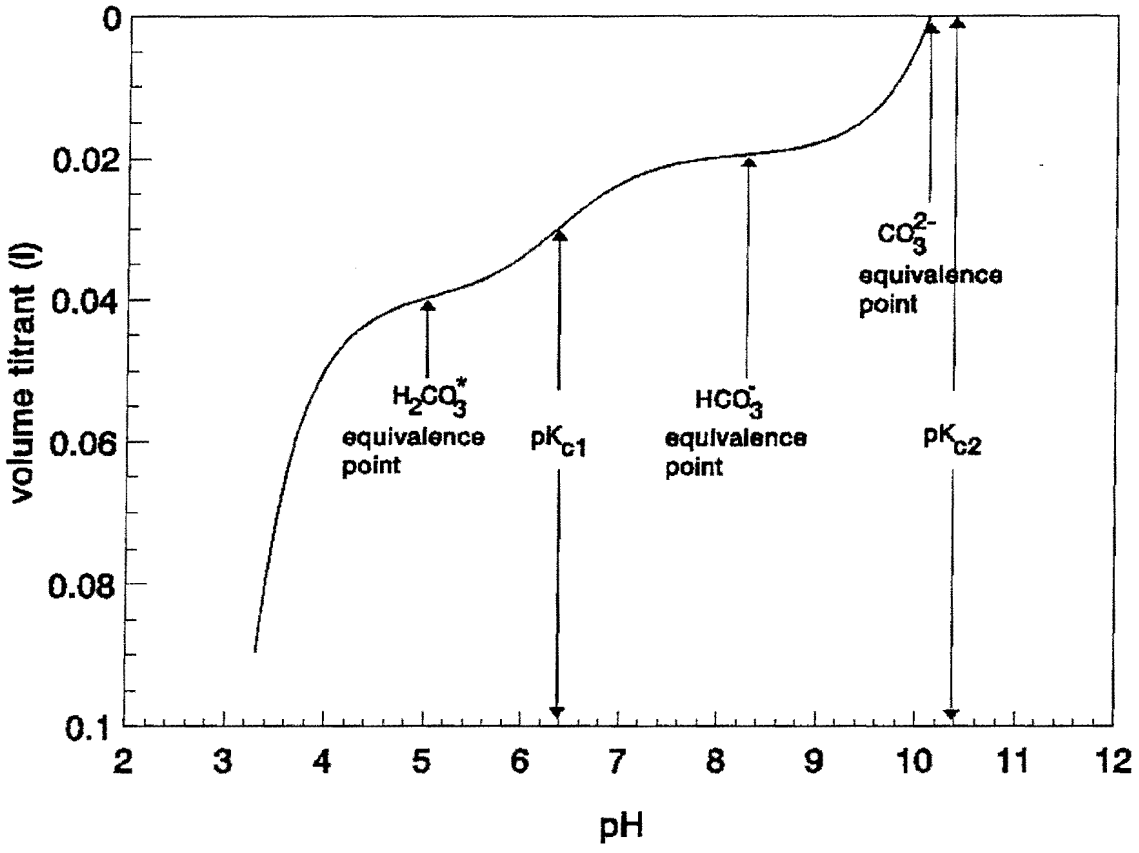

Figure 2:2: *Volume of titrant versus pH* curve for a 1 ℓ sample of 0,0002 mole/ℓ $NaCO_3$ solution titrated with 0,001 mole/ℓ HCl.

(and hence the Alkalinity value), see Standard Methods (1985). For waters with Alkalinity $\leq$ 30 mg/ℓ Alkalinity measurement should be effected using Gran titration methods (Gran 1952, Loewenthal *et al* 1986).

Where a potentiometric titration (ie pH measurement) is carried out, this data can be used to plot a *volume of titrant versus pH* curve. Certain inflection points are observed (see Figure 2:2). A maximum slope occurs at the pK values, and a minimum slope at the equivalence points. The slope of the *volume of titrant versus pH* curve thus gives an indication of the error in titrating to any particular pH value, a maximum slope indicating maximum possible error and vice versa. The slope of this curve introduces the concept of buffer capacity.

BUFFER CAPACITY

The buffer capacity of a water is a measure of the amount of strong acid or base required to change the pH by a predetermined amount. The more strong acid (base) required to effect this change, the better buffered is the water.

$$\text{Buffer capacity} = \beta = \left(\frac{\partial C_B}{\partial pH}\right)_{C_T} = -\left(\frac{\partial C_A}{\partial pH}\right)_{C_T} \qquad (2:27)$$

where C_B = quantity of strong base added (moles/ℓ)
C_A = quantity of strong acid added (moles/ℓ)

thus β is always a positive number and equals the sum of the buffer capacities for weak acid subsystems plus that for water itself (Butler 1962).

Butler showed that if $\frac{K_2}{K_1}$ is very small ($\frac{K_2}{K_1} \leq 5\ \%$), a polyprotic acid such as the carbonate system may be considered as a mixture of two monoprotic acids of equal concentrations. (For the carbonate system $\frac{K_{c2}}{K_{c1}} \approx 0.0001$) (Loewenthal and Marais 1976).

The buffer capacity for the carbonate system then approximates to

$$\beta = \beta_{H_2CO_3^*/HCO_3^-} + \beta_{HCO_3^-/CO_3^{2-}} + \beta_{H_2O}$$
$$= \frac{2{,}303\ C_T (H^+) K'_{c1}}{(K'_{c1} + (H^+))^2} + \frac{2{,}303\ C_T (H^+) K'_{c2}}{(K'_{c2} + (H^+))^2} + 2{,}303\left((H^+) + \frac{K'_w}{(H^+)}\right) \qquad (2:31)$$

A buffer capacity diagram for a solution with $C_T = 0.0002$ mole/ℓ is shown in Figure 2:3. The points of maximum buffer capacity of the carbonate subsystem corresponds to the pK_c' values. The water subsystem imparts very strong buffering at pH values less than 4 pH units and greater than 9,5 pH units.

Areas of minimum buffering capacity corresponds to the $H_2CO_3^*$ and HCO_3^- equivalence points. There is another minimum in the buffer capacity of the carbonate subsystem corresponding to the CO_3^{2-} equivalence point but in the combined buffer capacity diagram this minimum is masked by the high buffer capacity of the water subsystem.

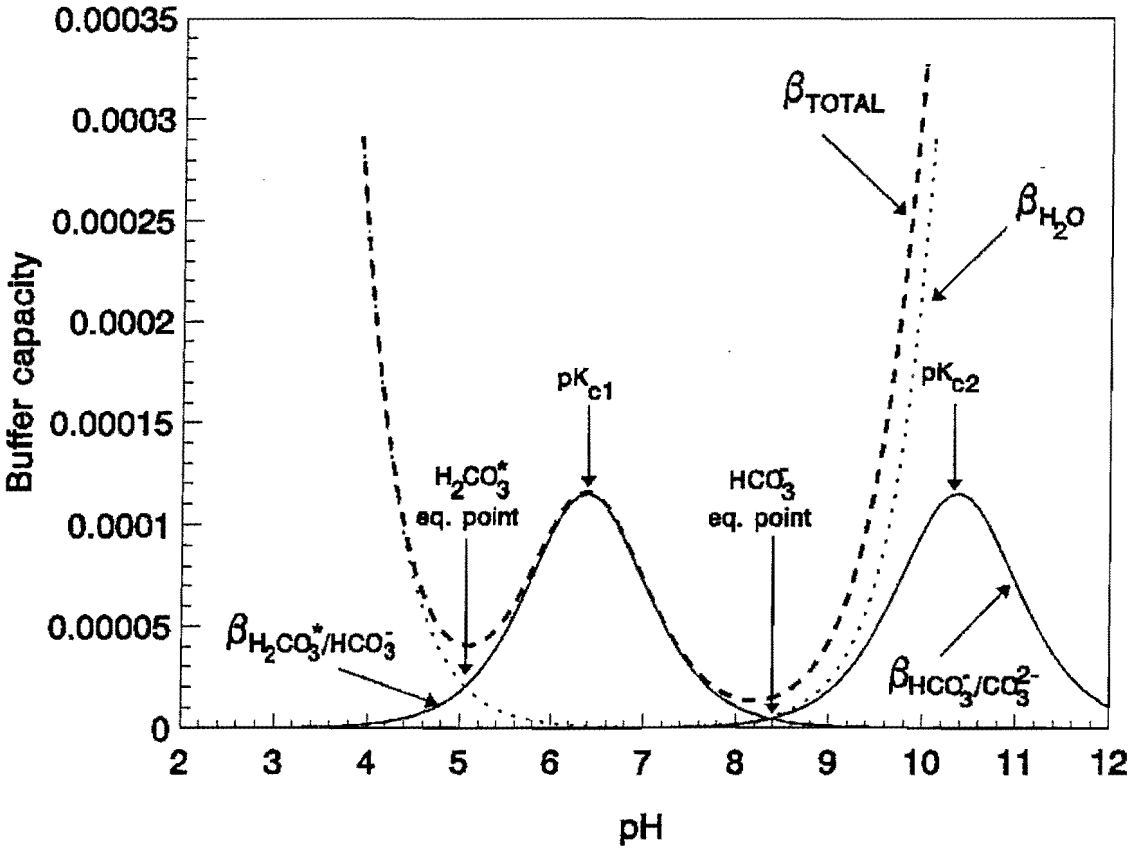

Figure 2:3: *Buffer capacity versus pH* curve for the carbonate system, C_T = 0,0002 moles/l.

REFERENCES

Gran G. (1952) Determination of the Equivalence Point in Potentiometric Titrations. Part 2. *The Analyst*. Vol. 77, pp 661-671.

Langelier W.F. (1936) The analytical control of anti-corrosion water treatment. *Jour. AWWA*. vol. 28, pp 1500.

Loewenthal R.E., Wentzel M.C., Ekama G.A. & Marais G.v.R. (1991) Mixed weak acid/base systems Part 2 - Dosing estimation, aqueous phase. *Water S.A.* vol. 15, No. 1, pp 3-24.

Loewenthal R.E., Ekama G.A. & Marais G.v.R. (1989) Mixed weak acid/base systems Part 1 - Mixture characterisation. *Water S.A.* vol. 15, No. 1, pp 3-24.

Loewenthal R.E., Wiechers H.N.S. & Marais G.v.R. (1986) *Softening and Stabilization of Municipal Waters.* Water Research Commission, Pretoria.

Loewenthal R.E. & Marais G.v.R. (1976) *Carbonate Chemistry of Aquatic Systems: Theory and Application.* Ann Arbour Sci. Publishers, Michigan.

Snoeyink V.L. & Jenkins D. (1980) *Water Chemistry.* Wiley, New York.

Standard Methods for Examination of Water and Wastewater, (1985), 16th ed., Publ. American Public Health Ass., American Water Works Ass., Water Pollution Control Federation, Washington.

CHAPTER 3

CHEMISTRY OF CALCIUM CARBONATE DISSOLUTION

INTRODUCTION

In this chapter the aqueous phase is brought into contact with calcium and carbonate species in the solid phase.

The concept of equilibrium between species in the aqueous and solid phases (ie. two phase equilibrium) is addressed as well as the solubility product equation describing this state. The solubility product equation is then used to introduce the concept of under and super saturation of a solution with respect to a solid phase.

A critical review is then presented of the various methods currently used to describe saturation state for example the Langelier saturation index and the calcium carbonate precipitation potential.

Whereas the rate to equilibrium between the various species in the aqueous phase is extremely rapid, interphase equilibrium is attained relatively slowly. Various models describing the kinetics of attainment of interphase equilibrium for solutions with the solid phase, that is various models for describing kinetics of calcium carbonate precipitation/dissolution are presented.

SOLID-AQUEOUS PHASE EQUILIBRIUM

When solid calcium carbonate is added to water, dissolution and precipitation reactions occur between species in the solid and aqueous phases. The reactions involved in the dissolution/precipitation of calcium carbonate can be represented as follows:

$$CaCO_{3\,(solid)} \underset{r_d}{\overset{r_p}{\rightleftharpoons}} Ca^{2+}_{(aqueous)} + CO_3^{2-} \qquad (3:1)$$

where r_d = dissolution (forward) reaction rate

r_p = precipitation (reverse) reaction rate

When the rate of the forward and reverse reactions are equal, the solution is said to be saturated with respect to calcium carbonate. At saturation, an equilibrium state exists

between dissolved and solid calcium carbonate species. This equilibrium state can be described using the so called solubility product equation, ie.

$$(Ca^{2+})\,(CO_3^{2-}) = k_{spc} \qquad (3:2)$$

where ( ) = activity of species (mole/ℓ), ie active mass concentrations
k_{spc} = an equilibrium constant which depends on temperature

Note: If the solid (reactant) is in it's pure form, it is by definition in the standard state and the activity is equal to unity.

The effects of ionic strength on equilibrium can be estimated by writing the solubility product equation in terms of concentration and activity coefficients ie.

$$[Ca^{2+}]\,[CO_3^{2-}] = \frac{k_{spc}}{f_d^2} = k'_{spc} \qquad (3:3)$$

where k_{spc} & k'_{spc} = thermodynamic and apparent solubility product constants for calcium carbonate respectively
f_d = activity coefficient for divalent ions which varies with ionic strength (see Chapter 2)

The effects of temperature on the calcium carbonate solubility product have been determined by numerous researchers. Loewenthal & Marais (1976) formulated the following equation from data reported by Larson & Buswell (1942) in the temperature range 0 °C to 80 °C

$$pK_{spc} = 0{,}01183 \times T + 8{,}03 \qquad (3:4)$$

where T = temperature, in degrees Celsius

Truesdell and Jones (1973) presented the relationship

$$pK_{spc} = 10{,}710 - \frac{698{,}61}{T_k} \qquad (3:5)$$

where T_k = temperature, in degrees Kelvin

Wiechers (1978) is of the opinion that the latter formulation is preferable, as their value at 25 °C is closer to that predicted by Langmuir (1968).

The above solubility product values were determined without taking into account ion pairing effects between calcium and carbonate species in solution. Consequently, this effect is

reflected in this solubility product value, ie. species concentrations in Eq. 3:3 reflect the sum of free and ion paired (total) species concentrations. However, this approximation is adequate for normal terrestrial waters where complexing of calcium and CO_3^{2-} by other ions in the solution is negligible.

If ion pairing is to be incorporated in computations then the solubility product function determined by Plummer & Busenberg (1982) should be used, ie.

$$\log k_{sspc} = -171{,}9065 - 0{,}077993\ T_k + \frac{2839{,}319}{T_k} + 71{,}595 \log T_k \qquad (3:6)$$

where T_k = temperature, in degrees Kelvin

The investigations reported here were for very soft waters and consequently ion pairing has been neglected so that Eqs. 3:4 and 3:5 were used where necessary.

SATURATION STATE

The rate at which equilibrium is attained between the solid and aqueous phases is extremely slow compared to attainment of equilibrium between species in the aqueous phase only. Consequently, for water in contact with solid calcium carbonate the solution may be either under or super or just saturated with respect to calcium carbonate. The states of under and super saturation may exist for protracted lengths of time. The calcium carbonate saturation state of a water describes the condition of the water with respect to the above states.

In terms of the solubility product equation Eq. 3:3, saturation state can be described by the relative saturation index, Ω , as follows.

$$\Omega = \frac{[Ca^{2+}]\ [CO_3^{2-}]}{k'_{sp\ c}} \qquad (3:7)$$

If $\Omega = 1$ the water is just saturated
If $\Omega > 1$ the solution is supersaturated and precipitation will occur with time
if $\Omega < 1$ if solid calcium carbonate is present, dissolution will occur with time

From the water treatment point of view it is important that the saturation state be known and if necessary adjusted prior to distribution (Loewenthal *et al* 1986).

In this context two problems arise, the first a qualitative one, the second a quantitative one. As far as the qualitative description of saturation is concerned referring to Eq. 3:7 values for k'_{spc}, Ca^{2+} and CO_3^{2-} need to be known. The first two can be obtained directly however, as shown in Chapter 2, the CO_3^{2-} concentration cannot be measured directly and needs to be determined from some other analytical measurement, in particular pH and Alkalinity. In this regard the work of Langelier (1936) pioneered a rapid means of assessing saturation state.

Langelier's saturation index, SI, is the difference between the actual pH of the water and the theoretical pH of the water at which it would be saturated for the measured Alkalinity and calcium concentrations. viz.

$$SI = pH_{actual} - pH_s$$
$$pH_s \approx pK'_{c2} - pK'_{spc} + p[\text{Alkalinity}] + p[Ca^{2+}] \qquad \textbf{(3:8)}$$

where pH_{actual} = measured pH of the water
pK'_{c2} = apparent equilibrium constant as defined in Eq. 2:12
pK'_{spc} = apparent solubility product for calcium carbonate
[ ] = molar concentration
If SI < 0 the water is super saturated
If SI > 0 indicates under saturation

Langelier stressed that the index is merely a qualitative description of the saturation state. The numerical value determined for the SI has no bearing on the amount of calcium carbonate that can dissolve/precipitate from the solution (Loewenthal *et al* 1986). Qualitative assessments of saturation state are not sufficient quality criteria by which to effectively monitor the treatment of water prior to distribution. To this end a quantitative description of saturation state is required. The calcium carbonate precipitation potential facilitates an accurate prediction of the amount of solid calcium carbonate that can precipitate from or dissolve into aqueous solution.

The *calcium carbonate precipitation potential* defines the mass of $CaCO_3$ that can dissolve/precipitate from the water given the initial Alkalinity and pH and calcium concentration, assuming that temperature and ionic strength effects have been considered and incorporated into the apparent equilibrium constant.

It has been shown previously that the chemical state of water containing carbonate species only can be uniquely determined if any two of the parameters Alkalinity, Acidity or pH are known. By considering such an aqueous solution in contact with solid calcium carbonate the

only species introduced/removed into/from the system are Ca^{2+} and CO_3^{2-}. By introducing the solubility product equation, expressed in concentration form (Eq. 3:3), one more equation and one more unknown viz. $[Ca^{2+}]$, have been introduced to the characterization problem, thus the system of equations describing the chemical state of the water remains consistent.

There is a direct stoichiometric relationship between the amount of calcium carbonate dissolving/precipitating and the corresponding changes in both Ca^{2+} concentration and Alkalinity in the solution. However this does not hold for the individual weak acid species, CO_3^{2-}, involved in the dissolved/precipitation reaction, as this component of calcium carbonate speciates in solution and varies with pH according to the single phase equilibrium chemistry described previously (see Chapter 2). Because of this complex relationship between the solution species involved in the dissolution/precipitation reaction, it has not been possible to develop a single elegant equation that can be used to calculate the precipitation potential from the measured parameters Alkalinity (or Acidity), pH and calcium. To this end iterative procedures involving successive approximations have been developed, to determine the precipitation potential. Computer programs such as "*Stasoft*" have been written to facilitate these calculations (Friend & Loewenthal 1992).

In addition to the computerized methods for determining the precipitation potential various graphical techniques have been developed in the past for use when computer facilities were not readily available. The Modified Caldwell-Lawrence (MCL) diagram is probably the most frequently used as it is not only easy to use but imparts a good insight into the changes that the capacity parameters experience in attaining a metastable or equilibrium state. The MCL diagram is a three-phase (aqueous, solid, gaseous) equilibrium diagram for use for the carbonate system. Separate graphs are available for various ionic strengths (or Total Dissolved Solids ie. TDS) and for different temperature ranges. The ordinate represents the solution Acidity while the abscissa, the difference between the solution Alkalinity and the calcium concentration (ie. Alkalinity minus Calcium or AMC). Sets of curves representing pH, Alkalinity and calcium values are plotted on these axes. The calcium line that passes through the intersection point of given pH and Alkalinity values is the calcium concentration that the water should have if it were saturated.

The theory involved in the construction of such diagrams is given by Loewenthal and Marais (1976) and examples of its use by Loewenthal *et al* (1986). Unfortunately the parameters of Alkalinity, Acidity and the calcium concentration must be reported in units of mg/ℓ as $CaCO_3$ which reduces the graphs usefulness in a fully metricated environment.

DISSOLUTION KINETICS

The rate at which a mineral dissolves in aqueous solution is influenced by a number of factors such as temperature, chemical composition, physical and chemical properties of the dissolving mineral and the manner in which the mineral is brought into contact with the solution.

Models to describe the kinetics of calcium carbonate precipitation/dissolution have been developed by numerous authors. However, most of the work was done from a geological standpoint with the view to describing limestone formations. Many of these models are totally empirical (Dorange & Guetchidjan (1978), Sjöberg (1976), Mills (1984)), however in some cases mechanistic models have been postulated, for example Plummer *et al* (1979) and van Cappellen *et al* (1993).

Dorange and Guetchidjan (1978), investigated the dissolution of marble chips. Their observations indicated that the dissolution rate is linearly linked to the degree of mineral undersaturation, ie.

$$\frac{d[Ca^{2+}]}{dt} = k_{(D+G)}\, S \left([Ca^{2+}]_{sat} - [Ca^{2+}]\right) \qquad \textbf{(3:9)}$$

where $\frac{d[Ca^{2+}]}{dt}$ = rate of dissolution reaction

$[Ca^{2+}]$ = concentration of Ca^{2+} in the bulk solution

$[Ca^{2+}]_{sat}$ = saturation equilibrium concentration of Ca^{2+} in the mono-layer

$k_{(D+G)}$ = dissolution rate constant used in the Dorange and Guetchidjan equation ($m\ s^{-1}$)

S = surface area of $CaCO_3$ crystals per unit volume in the solution

Subsequent investigations by many researchers (Morse (1983), Sjöberg (1976), Rickard & Sjöberg (1983), Compton and Daly (1987) and Plummer *et al* (1978)) in this field have shown that such a first order reaction does not give a general description of dissolution kinetics of calcium carbonate. Similarly, Nancollas and Reddy (1971), Wiechers *et al* (1975) and Sturrock *et al* (1976)) showed that this type of equation does not model calcium carbonate precipitation kinetics.

Reddy and Nancollas (1970) postulated that the rate of precipitation in any seeded solution is proportional to the surface area of seed and the degree of supersaturation (viz. the

concentration of the zero ion pair, $CaCO_3^0$), of the bulk solution. They presented a second order model (Eq. 3:10 below) for the net precipitation rate.

$$- \frac{d[Ca^{2+}]}{dt} = k_{(R+N)} S \left\{ [Ca^{2+}] [CO_3^{2-}] - \frac{K_{sp\,c}}{f_d^2} \right\} \quad \textbf{(3:10)}$$

where $k_{(R+N)}$ = dissolution/precipitation rate constant used in the Reddy and Nanchollas equation ($m^{-2}\ s^{-1}$)

$k_{sp\,c}$ = Thermodynamic solubility product for $CaCO_3$

f_d = activity coefficient for the divalent ion

Wiechers et al (1975) also utilized this form of equation to describe precipitation kinetics in surface controlled processes, ie. processes independent of mixing phenomena. However, these authors noted an inconsistency in the model in that the rate constant depended on the initial pH of the solution where $5 \leq pH_{initial} \leq 9$. Sturrock *et al* (1976) reexamined surface controlled calcium carbonate precipitation kinetics. They found that the inconsistencies arising in the Reddy and Nancollas model as observed by Wiechers *et al*, could be bypassed using the theory of Davies and Jones (1955) developed originally for AgCl precipitation kinetics. Davies and Jones hypothesised that precipitation kinetics for surface controlled processes depend on the charge established at the crystal growth site(s) and the surface area of crystal. Using this hypothesis, Sturrock *et al* formulated the following equation for calcium carbonate precipitation kinetics processes governed by surface controlled reactions and with bulk solution pH in the region $5 \leq pH \leq 9$ as,

$$- \frac{d[Ca^{2+}]}{dt} = k_{(D+J)} S f_d^2 \left\{ [Ca^{2+}]^{\frac{1}{2}} [CO_3^{2-}]^{\frac{1}{2}} - \left(\frac{k_{sp\,c}}{f_d^2} \right)^{\frac{1}{2}} \right\}^2 \quad \textbf{(3:11)}$$

where $k_{(D+J)}$ = precipitation rate constant used in the Davies and Jones equation ($mole^{-1}m^4s^{-1}$)

This approach resolved the inconsistencies observed by Wiechers *et al* relating to the dependency on initial pH.

Mills (1984) attempted to apply the Davies and Jones hypothesis to the dissolution of limestone chips in acidified terrestrial waters ($pH_{initial} \leq 2{,}5$). He found no agreement for the initial dissolution rate up to pH of approximately 5. In order to model the process more closely he incorporated an additional term dependent on the proton activity in the bulk solution, ie.

$$-\frac{d[Ca^{2+}]}{dt} = k_{(M1)}\, f_d^2 \left\{ [Ca^{2+}]^{\frac{1}{2}}\, [CO_3^{2-}]^{\frac{1}{2}} - \left(\frac{k_{spc}}{f_d^2} \right)^{\frac{1}{2}} \right\}^2 + k_{(M2)}\, (H^+)^{0,584} \qquad (3:12)$$

where $k_{(M1)}$, $k_{(M2)}$ = dissolution rate constants used by Mills, includes surface area effects for a particular pebble size

Mills showed that the second term above dominates calcium carbonate dissolution kinetics where pH $\leq$ 4,5, at higher pH values the second term becomes negligible and kinetics is governed by the first term.

An important criticism that can be levelled at the work reported by Mills is that he did not investigate whether he was dealing with a surface controlled or a diffusion controlled process. That is, he did not investigate the effects of variable mixing energy on the dissolution kinetics. This omission has important implications because the first term in his equation was formulated for surface controlled reactions (Sturrock *et al* (1976)), such surface controlled reactions should be independent of mixing energy.

Furthermore virtually all his experimental data was in the low pH region, $2,5 \leq pH_{initial} \leq 5$, where the proton activity term totally dominated dissolution kinetics and very little correlation is reported for the higher pH region, 5 $\leq$ pH where the first term dominates.

The first point above has been reassessed in this investigation using an upflow reactor system and limestone granules from Bredasdorp. The experimental configuration and control is described in detail in Chapter 4. The effects of mixing energy on the observed rates of dissolution were investigated by varying the flow characteristics in the pH region 5 $\leq$ pH $\leq$ 9 . The plot of the observed rate versus the Sturrock *et al* function was closely linear and equal to the rate constant $k_{(D+I)}$ in Eq. 3:11. However, the rate constant $k_{(D+I)}$ varied with flow rate (see Chapter 4). This observation indicates that dissolution rate is not controlled by surface phenomena (as required in the formulation of the Sturrock *et al* equation) but by transport/diffusion phenomena between the surface of the dissolving mineral and the bulk solution. Summarizing, Eq. 3:11 was developed for surface controlled precipitation/dissolution phenomena ie. processes independent of mixing energy, clearly this equation and the underlying theory in its formulation are inappropriate in the description of dissolution phenomena.

Stumm and Morgan (1981) and others propose that for mineral dissolution processes the kinetics is best described by a first order type of equation, ie.

$$\frac{d[Ca^{2+}]}{dt} = k_{(S+M)}\, S \left\{ c_{sat} - c \right\} \qquad (3:13)$$

where $k_{(S+M)}$ = dissolution rate constant used in the Stumm and Morgan equation
c_{sat} = concentration of dissolved mineral in solution at saturation
c = concentration of dissolved mineral in solution

The rate constant $k_{(S+M)}$ in Eq. 3:13 above depends on a number of factors including the physical characteristics of the dissolving mineral and the hydraulic flow characteristics, ie. flow rate.

The form of this equation appears to have been derived from Fick's first law. In a quiescent aqueous environment, the driving force of the molecular diffusion process is the concentration difference between two regions of solution at some distance, ℓ, from each other and according to Fick's first law, it is a first order equation of the following form:

$$Flux_i = \frac{D_i}{\ell} \left(\Delta c_i \right) \qquad (3:14)$$

where $Flux_i$ = flux of ion species,i
D_i = diffusion coefficient of species i
Δc_i = concentration difference of species i
ℓ = distance across which concentration difference has been measured

It should be noted that the diffusion coefficient, D_i, increases with the mobility of ions. That is, it will have a higher value for the more mobile H^+ ion than for say Ca^{2+}. In most practical situations the water body is not quiescent, with the bulk of the liquid undergoing some form of turbulence due to the flow regime of the system. From pipe flow theory it is known that a quiescent layer of water exists at the wall of the pipe, slightly further from the wall, laminar flow begins to occur, with the velocity increasing with distance from the wall, until some boundary is reached at which the flow becomes turbulent. The thickness of this quiescent and laminar flow region, known as the boundary region, reduces with an increase of the turbulence in the bulk liquid.

By analogy a similar situation can be envisaged at the surface of solid calcium carbonate particles dissolving in an agitated (by means of stirring, say) aqueous medium. The model suggests that the chemical reaction rate at the surface of the solid calcium carbonate is sufficiently high to maintain a thin mono-layer located immediately adjacent to the solid in an equilibrium condition with respect to the mineral. Transport of dissolution products from

this layer to the turbulent bulk liquid must be by means of diffusion through the boundary layer. In this case the distance ℓ, in Eq. 3:14 should be replaced by the thickness of the boundary layer, δ, which is dependent on the flow regime in the bulk solution. The difference between the equilibrium activity in the mono-layer and the active concentration (activity) of the corresponding species in the bulk solution is the force driving the process.

$$\begin{aligned} \text{Rate} &= \frac{k_d}{\delta}\frac{S}{V}\left\{a_{eq} - a\right\} \\ &= \frac{k_d}{\delta}\frac{S}{V}\left\{(CaCO_3)_{(eq)\pm} - (CaCO_3)_{\pm}\right\} \\ &= k_{d\,(hyd)}\, S\left\{(Ca^{2+})_{eq}^{\frac{1}{2}}(CO_3^{2-})_{eq}^{\frac{1}{2}} - (Ca^{2+})^{\frac{1}{2}}(CO_3^{2-})^{\frac{1}{2}}\right\} \\ &= k_{d\,(hyd)}\, S\left\{k_{sp\,c}^{\frac{1}{2}} - (Ca^{2+})^{\frac{1}{2}}(CO_3^{2-})^{\frac{1}{2}}\right\} \end{aligned} \qquad \textbf{(3:15)}$$

where a_{eq}, a = equilibrium activity and activity of species
( ) = activity of species, moles/ℓ
δ = thickness of boundary layer
k_d = dissolution rate constant
$k_{d\,(hyd)}$ = dissolution rate constant including hydrodynamic effects

This equation is identical in form to the equation proposed by Sjöberg (1976) based on observations of calcium carbonate dissolution in solution in the region $5 \leq pH \leq 9$, ie.

$$\frac{d[Ca^{2+}]}{dt} = k_{(S)}\, S\left\{k'^{\frac{1}{2}}_{sp\,c} - [Ca^{2+}]^{\frac{1}{2}}[CO_3^{2-}]^{\frac{1}{2}}\right\} \qquad \textbf{(3:16)}$$

where $k_{(S)}$ = dissolution rate constant used in the Sjöberg equation (ms^{-1})
$k'_{sp\,c}$ = apparent solubility product for $CaCO_3$

or in terms of the relative saturation, Ω, as:

$$\frac{d[Ca^{2+}]}{dt} = k_{(S)}\, S\left\{1 - \Omega^{\frac{1}{2}}\right\} \qquad \textbf{(3:17)}$$

where Ω = relative saturation index

Alternatively this equation can be written in terms of mean ionic concentration in which case it appears very similar to Eq. 3:13 of Stumm and Morgan (1981), ie.

$$\frac{d[Ca^{2+}]}{dt} = k_{(S)}\, S \left\{ c_{sat(products)} - c_{(products)} \right\} \qquad \textbf{(3:18)}$$

where $c_{sat\ (products)}$ = saturation equilibrium concentration of dissolution products
$c_{(products)}$ = concentration of dissolution products in bulk solution

The above equation appears to have obtained wide acceptance as a model describing calcium carbonate dissolution kinetics in the pH region $5 \leq pH \leq 9$. However, outside this pH range and under extraordinary environmental conditions (such as high partial pressure of carbon dioxide) other considerations need to be addressed.

Plummer *et al* (1979) proposed that calcium carbonate dissolution kinetics may be dominated by either or both the proton activity and carbonic acid species concentrations in the bulk solution. That is, when either H^+ activity and or $H_2CO_3^*$ concentration in the bulk solution are sufficiently high, these species accelerate reactions at the crystal surface thereby accelerating the overall dissolution reaction.

$$\frac{d[Ca^{2+}]}{dt} = k_{(P1)}\, S\, a_{H^+} + k_{(P2)}\, S\, a_{H_2CO_3^*} + k_{(P3)}\, S\, a_{H_2O} \qquad \textbf{(3:19)}$$

where $k_{(P1)}$, $k_{(P2)}$, $k_{(P3)}$ = rate constants used in the Plummer *et al* equation
a = activity in the bulk solution

According to Plummer *et al* the first term in Eq. 3:19 is significant only for pH less than about 5, and the second term for $\bar{p}CO_2$ greater than 0.1 atmospheres. Their third term, formulated as a function of the activity of water links to the dissolution rate in pure water. This term however does not appear to be linked to the typical diffusion controlled type of equation introduced above (Eq. 3:18).

With respect to dissolution rate, they observed that the H^+ attack (ie. the first term in Eq. 3:19) depended on stirring rate, reflecting a transport controlled process. However, the CO_2 and water dependence of the dissolution rate (ie. the second and third terms respectively) did not appear to be significantly affected by stirring. This would indicate dissolution processes which are not diffusion controlled. By including terms describing the dissolution of calcium carbonate due to high concentrations of H^+ and/or $H_2CO_3^*$ in Eq. 3:15, the dissolution model becomes:

$$\frac{d[Ca^{2+}]}{dt} = k_1 S \left\{ k'^{\frac{1}{2}}_{spc} - [Ca^{2+}]^{\frac{1}{2}} [CO_3^{2-}]^{\frac{1}{2}} \right\} + k_2 S [H^+] + k_3 S [H_2CO_3^*] \quad \textbf{(3:20)}$$

where k_1, k_2, k_3 = rate constants

Each of the three rate constants in the above equation (ie. k_1, k_2 and k_3) depend on a number of factors including the physical characteristics of the dissolving mineral and the hydraulic flow characteristics, ie. flow rate. As far as the physical characteristics of the mineral are concerned calcium carbonate occurring in natural deposits may vary from a dense metamorphosed marble through a pure non metamorphosed chalk to a friable impure permeable form. In general each calcium carbonate deposit will give rise to different rate constants. For natural terrestrial waters usually only the first term is of any significance and it is this term which is investigated in this work.

In the following chapter the validity of the use of Eq. 3:20 to model calcium carbonate dissolution into typical soft Cape waters is investigated.

REFERENCES

Compton R. G. & Daly P. J. (1987) The Dissolution/ Precipitation Kinetics of Calcium Carbonate: An Assessment of Various kinetic Equations using a Rotating Disk Method. *Journal of Colloid and Interface Science*. vol. 115, no. 2, pp 493 - 498.

Davies C.W. & Jones A.C. (1955) The precipitation of silver chloride from aqueous solutions. *Trans. Faraday Soc.* vol. 51, pp 812-817.

Dorange G. & Guetchidjan A.C.R. (1978) *Acad. Sci. Paris Ser.* C286, pp 159.

Friend J.F.C. & Loewenthal R.E. (1992) *Chemical Conditioning of Low- and Medium-Salinity Waters: Stasoft version 3.* Water Research Commission, Pretoria.

Langelier W.F. (1936) The analytical control of anti-corrosion water treatment. *Jour. AWWA.* vol. 28, pp 1500-1521.

Langmuir D. (1968) Stability of Calcite based on Aqueous Solubility Measurements. *Geochimica et Cosmochimica Acta.* vol. 32, pp 835 - 851.

Larson T.E. & Buswell A.M. (1942) Calcium carbonate saturation index and Alkalinity interpretations. *J. AWWA.* vol. 34, pp 1667-1684.

Loewenthal R.E., Wiechers H.N.S. & Marais G.v.R. (1986) *Softening and Stabilization of Municipal Waters.* Water Research Commission, Pretoria.

Loewenthal R.E. & Marais G.v.R. (1976) *Carbonate Chemistry of Aquatic Systems: Theory and Application.* Ann Arbour Sci. Publishers, Michigan.

Mills R.D.W.B. (1984) Stabilization of Calcium Carbonate deficient waters. *MSc thesis* U.C.T., Cape Town.

Morse J.W. (1983) The kinetics of calcium carbonate dissolution and precipitation. *Mineralogical Society of America, Short Course on Carbonates: Mineralogy and Chemistry* pp 227-264.

Nancollas G. H. & Reddy M. M. (1971) The Crystallization of Calcium Carbonate.II Calcite Growth Mechanism. *Journal of Colloid and Interface Science.* vol. 37, no. 4, Dec., pp 824 - 830.

Plummer L. N. & Busenberg E. (1982) The solubilities of calcite, aragonite and vaterite in CO_2-H_2O solutions between 0 and 90°C, and an evaluation of the aqueous model for the system $CaCO_3$-CO_2-H_2O. *Geochimica et Cosmochimica Acta.* vol. 46, pp 1011-1040.

Plummer L. N., Parkhurst D. L. & Wigley T. M. L. (1979) Critical Review of the Kinetics of Calcite Dissolution and Precipitation. in Jenne E.A., *Chemical Modelling in Aqueous Systems: Am. Chem. Soc. Symposium Ser.* pp 537 - 573.

Reddy M. M. & Nancollas G. H. (1970) The Crystallization of Calcium Carbonate.I Isotopic Exchange and Kinetics. *Journal of Colloid and Interface Science.* vol. 36, no. 2, June, pp 166 - 172.

Rickard D. & Sjöberg E. L. (1983) Mixed Kinetic Control of Calcite Dissolution Rates. *American Journal of Science.* vol. 283, Oct., pp 815 - 830.

Sjöberg E. L. (1976) A fundamental equation for calcite dissolution kinetics. *Geochimica et Cosmochimica Acta* vol. 40, pp 441-447.

Stumm W. & Morgan J.J. (1981) *Aquatic Chemistry 2nd ed.* Wiley, New York.

Sturrock P.L.K, Loewenthal R.E & Marais G.v.R. (1976) Calcium Carbonate precipitation kinetics, Part 1. *Water S.A.* vol. 2, no. 3, pp 101-109.

Truesdell A.H. & Jones B.F.(1973) *WATEQ, a computer program for calculating chemical equilibrium of natural waters.* NTIS, report no. PB-220 464.

van Cappellen P., Charlet L., Stumm W. & Wersin P. (1993) A surface complexation model of the carbonate mineral-aqueous solution interface. *Geochimica et Cosmochimica Acta* vol. 57, pp 3505-3518.

Wiechers H.N.S. (1978) *Engineering aspects of Calcium Carbonate and Magnesium Hydroxide precipitation in waste water reclamation.* Phd thesis U.C.T., Cape Town.

Wiechers H. N. S., Sturrock P. & Marais G. v. R. (1975) Calcium Carbonate Crystallization Kinetics. *Water Research.* vol. 9, pp 835 - 845.

CHAPTER 4

CALCITE DISSOLUTION KINETICS - EXPERIMENTAL INVESTIGATION

INTRODUCTION

Researchers investigating dissolution kinetics of calcium carbonate minerals have used a number of laboratory systems in order to investigate the kinetics of the process. Principally, three systems are identified:

i) pH stat method. In this method pH of the solvent is kept constant by addition of standard mineral acid. The rate of acid addition is recorded and linked to dissolution rate. In order to approximate a constant ionic strength solution during the process, experiments are conducted in high ionic strength medium such as 0,1M KCl. Carbonate species are removed to a degree by sparging. This system is most frequently used in conjunction with a rotating disc of the dissolving mineral. This provides an easily defined hydraulic system which can be varied by altering the rotational speed. The surfaces of the calcium carbonate sample require careful pretreatment and consequently the method is suitable for either dense metamorphosed calcium carbonate minerals eg. marble or minerals with a uniform crystal structure, that is the various forms of spar. This type of system is ideal for investigating the effects of diffusion when the solution saturation state is far from equilibrium (Sjöberg & Rickard 1984, Plummer *et al* 1970).

ii) Free drift batch test method. In this method investigation is conducted by monitoring pH of the solution containing known quantities of finely ground calcium carbonate in suspension. Change in pH in with time is related to the dissolution/precipitation rate provided initial CO_3 acidity is known (and remains constant). Constant ionic strength solutions are again often approximated using a similar technique as described above. The influence of surface area effects on the dissolution rate can be investigated by varying the amounts of calcium carbonate powder in suspension. These systems are frequently used when the solution saturation state is close to equilibrium (Plummer *et al* 1979).

iii) Semi-plug flow reactor method. In this method investigations are carried out by allowing the solvent to pass through a reactor containing calcium carbonate granules. Samples are drawn at intervals along the length of the reactor and the calcium

concentration (and pH, Alkalinity etc.) measured. The spacial changes in water quality can be related to calcium carbonate dissolution kinetics. The hydraulic conditions and mineral surface area are not as easily defined as in the two systems above, but can be altered by changing the flow rate through the system and the mean particle size of the reactor contents respectively (Mills 1984).

The investigation reported here utilized limestone obtained from a quarry near Bredasdorp, Western Cape, South Africa. The porous friable nature of the Bredasdorp limestone ruled out the possibility of making use of the pH stat and free drift batch test methods. As transport mechanisms were expected to be rate controlling (see Chap. 3), the complexities of determining and varying the hydraulic conditions in systems of type ii) above rendered it unsuitable for this investigation. In addition, energy requirements of a full scale suspended media reactor would probably be prohibitive. The semi plugflow reactor method was considered to be most representative of the likely full scale applications of the system to partial stabilization with limestone. Some measure of control over the surface area could be obtained by uniformly packing the reactor with a range of "single size granules" for the different experiments.

Having selected the most appropriate method of investigation, it was then necessary to identify system parameters to be measured so that rates could be determined. As limestone (calcium carbonate) is the dissolving mineral, referring to Chapter 3, analyses requires measuring (knowing) both Ca^{2+} and CO_3^{2-} concentrations with time. Calcium concentrations are relatively easily determined, but there are some problems in determining CO_3^{2-} (and other carbonate species) especially for a soft acidic water. As an inorganic carbon analyzer was not available, choice of which parameters should be measured to determine CO_3^{2-} concentration was any two of the three Alkalinity, pH and Acidity. Alkalinity is accepted as a reliable and relatively easily measurable parameter. The second parameter selected was pH (see Chap. 2).

To ensure that Alkalinity and pH measurement could be used to give an accurate description of the in-situ CO_3^{2-} concentration in the reactor, one needs to identify factors which may cause the values of these parameters to change during sampling and measurement. In this regard the principle factor would appear to be loss or gain of CO_2 from the sample.

CO_2 exchange with the atmosphere will have no effect on the value of the Alkalinity parameter. However, Acidity will change (see Chap. 2). Consequently pH will change with CO_2 exchange and affect the calculated value for CO_3^{2-}. Clearly it would be advantageous to measure pH directly inside the reactor. This was achieved using a sampling unit described

later.

A further possible problem arising from loss of CO_2 from solution was escape of this gas from solution within the reactor forming gas pockets; alternatively introduction or loss of CO_2 into the reactor during sampling procedure.

The former was obviated by selecting an upflow reactor configuration. This ensured that any CO_2 dissolved in the water remained within the bulk liquid in its path through the reactor. This also provided contact opportunity for re-dissolution should gas release occur at the bottom of the reactor. The second problem was overcome by adhering to a contra-flow sampling sequence.

Ionic strength effects were taken into account simply via change in TDS.

A description of the equipment and the analytical methods used is presented below.

EQUIPMENT AND ANALYSES

The equipment common to most of the investigations is described in this section followed by a short descriptions of the analytical chemistry methods that were used during this investigation.

Reactor and accessories

The overall arrangement of the test equipment is shown in Figure 4:1. The basic elements comprised of:

i) A vertical upflow reactor together with its accessories;
ii) A flow meter, overhead constant head tank, pipework and valves to supply the reactor with a constant flow of water;
iii) Two supply tanks of $1m^3$ and $2m^3$ capacity each, a pump and an air compressor.

Reactor

Reactor

The reactor consisted of a vertical, 105mm internal diameter clear PVC tube 1500mm in length (see Appendix B Figure B:1). The inner end caps were conically shaped to distribute the flow evenly into the reactor. A No. 10 stainless steel wire mesh was fitted at the ends

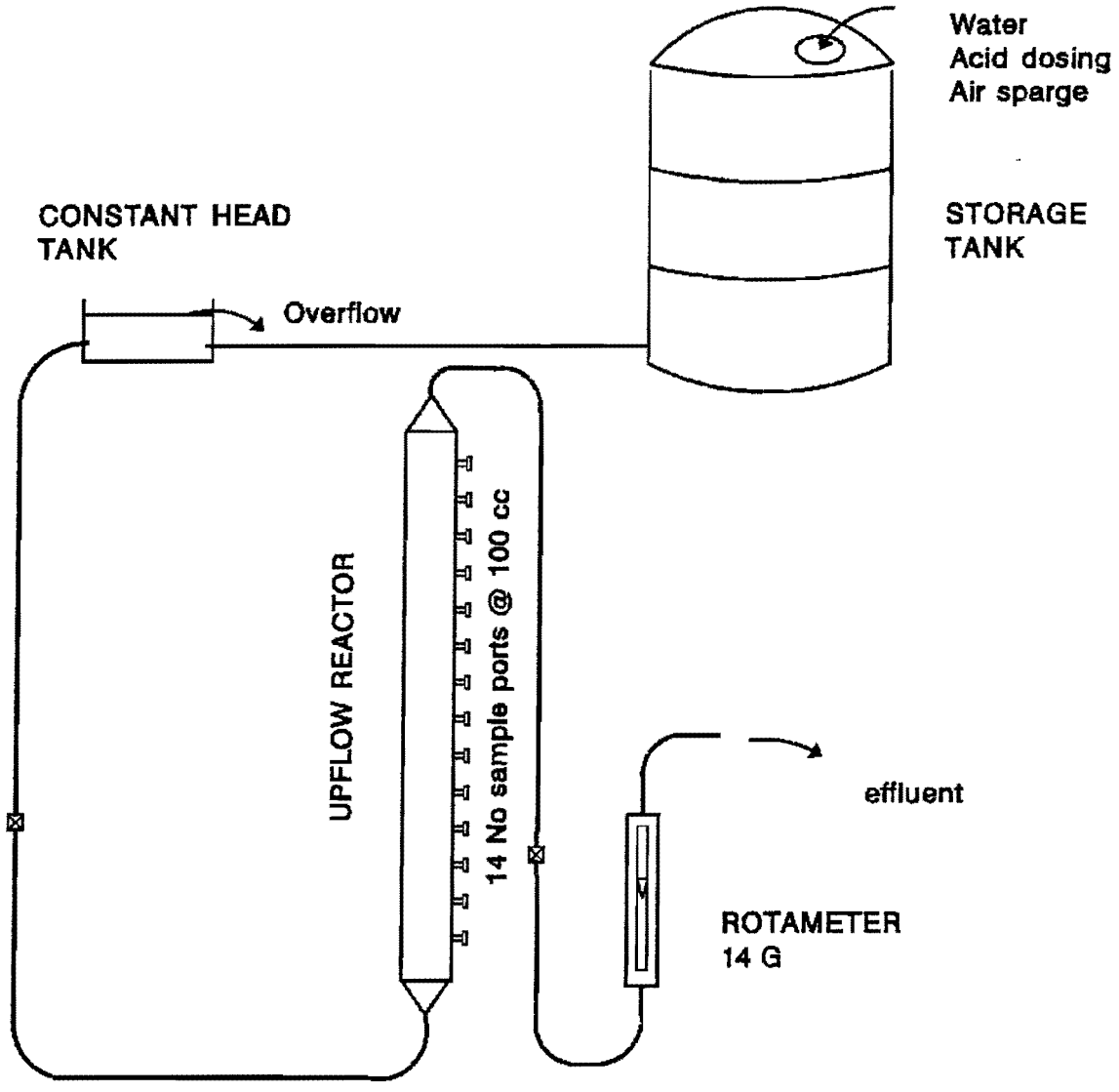

Figure 4:1: Arrangement of test apparatus to measure $CaCO_3$ dissolution rate.

of the reactor for two reasons. Firstly, to prevent the limestone samples from clogging the inlet zone. This also identifies the entry level to the reactor. Secondly, to prevent particle washout. Fourteen sampling ports were spaced equally, 100mm apart, along the length of the reactor. When not in use, these ports were kept closed by PVC stoppers held in place by tight fitting "O" rings.

Sampling unit

In order to obtain meaningful in-situ pH measurements it was necessary to measure this parameter before the sample was exposed to the atmosphere. This was effected by allowing the sampling stream to flow through a sealed sampling container with only a very small outlet area open to the atmosphere.

The sampling unit is shown in Figure B:2. It consisted of a clear PVC cylinder with 185mℓ volume. This clipped into a sample port by means of an inlet nozzle at its base. Flow through the unit was controlled by means of a stopcock fixed to the inlet nozzle. The lid of the unit was provided with three openings, two of which were designed to provide close fits for the pH and the temperature probes. The third opening acted as the outlet.

Sampling and pH observation were effected by plugging this device into a sample port, adjusting the flow volume to the desired rate, usually 75 mℓ/min, and allowing a number of residence times to pass. The contents of the sample unit were then poured into plastic containers for the other analysis later. Sampling was always effected sequentially from the top port downwards (ie. counterflow) to obviate interference between successive samples.

Manometer tubes

Two 9mm internal diameter clear PVC tubes were vertically mounted and extended above the constant head tank. The fittings at the lower ends of these tubes were such that they could be clipped simultaneously into any two sampling ports. This allowed measurement of the difference in hydrostatic head between two ports.

Conductivity recording equipment

To determine the rate at which a plug of fluid passes through the packed bed, conductivity readings with respect to time were required. These readings were obtained at the upper end cap of the reactor, ie. as close as possible to where the water emerges from the packed bed.

A PVC unit with a suitable bore into which a conductivity probe could be fitted was screwed into the upper end cap of the reactor. A sampling stream was directed through this unit and flowed annularly over the sensing rings of the conductivity probe. A short distance after the sensing rings an outlet tube intercepted the main sampling tube at 90°. The flow stream was controlled by a needle valve and rotameter series 1100 flow meter.

The conductivity meter was a Hanna Instruments model HI 8820 bench conductivity meter which had been converted to give a 0 to 2 Volts analog output. This signal was amplified to 0 to 10 Volts and read into a personal computer using a PC 30B data input card. This system enabled conductivity readings to be recorded at a rate of 1 reading per second. In addition, a facility existed whereby markers could be introduced into the electronic record. This was used to indicate when events, such as the introduction of tracer to the system, occurred. Data sets consisting of time, conductivity and a marker value were continuously obtained and which could be processed with the aid of any normal spreadsheet package.

Calibration of the conductivity meter was unnecessary as readings were only required relative to each other. the flow meter was calibrated in the usual fashion for such instruments, the calibration curve is shown in Appendix C.

Flow control

Flow meter

A Rotameter *metric 14G* flow meter (operating range approximately from 0,3ℓ/min to 5,3ℓ/min) was mounted downstream from the reactor just prior to the discharge point from the system. The Rotameter was calibrated prior to use yielding calibration curves such as that shown in Appendix C.

Constant head tank

In order to reduce the effect of flow surges through the system a PVC constant head tank of 15 ℓ capacity was used. It was constructed with a broad weir leading to an overflow trough, the outlet of which was directed to the raw water storage tank. The constant head tank was designed to cover a large range of overflow rates with negligible change in hydrostatic head.

Outlet

The outlet consisted of a 15mm diameter galvanized metal pipe located immediately after the flow meter and fixed directly to it. This pipe was allowed to discharge horizontally to the atmosphere. A nonflexible pipe was used to prevent inadvertent hydrostatic head changes during experiments.

Miscellaneous

Tanks

Tanks of a 2,5m^3 and a 1m^3 capacity were used to provide storage for the feed water. Both tanks were lined with black PVC to reduce biological growth.

Aeration

A 0,25kW electric motor driven compressor acted as an air source for a sparging device in the 2,5m^3 storage tank. Air from the compressor was delivered via clear 9mm PVC tubing to four frittered glass diffusers anchored by means of PVC weights to the bottom of the tank.

Sizing of Limestone granules

Standard laboratory test sieves were used to size the limestone granules. Sieve sizes used were 9,4mm, 6,7mm, 4,7mm, 2,4mm, 1,7mm and 1,168mm.

Chemical analyses

Parameters that were routinely measured in any particular experiment included temperature, pH, conductivity, calcium concentration and Alkalinity. Equipment and methods used were as follows.

pH and temperature

Two pH meters, model Hanna Instruments HI 8417, were used in conjunction with HI 1131 combined glass electrodes. Temperature was measured to within 0,1 °C. pH calibration was against standard N.B.S. buffer solutions, nominally pH 4 and pH 7 (HI 7004 and HI 7007 respectively). The instruments were calibrated before every major experimental run. After calibration probes were thoroughly rinsed with distilled water and placed in a large stirred beaker containing water of the type to be tested for at least five minutes. This allowed probes to acclimatize to the low buffer capacity water used in the experiments.

pH observations at sampling ports were effected using the sampling units described earlier. This device minimized the effects of CO_2 exchange between sample solution and the atmosphere (air).

Conductivity

Conductivity of samples was measured using a Hanna Instruments model HI 8820 bench conductivity meter. The instrument was calibrated for low conductivity waters against a nominal 84μS standard solution at 25 °C.

Calcium concentration

Calcium concentrations were determined using an EDTA titration method (0,01M EDTA solution univAR grade manufactured by Saarchem Laboratory chemicals and Merck). The indicator/reagent was the Hardness - (Calcium hardness) uniLAB indicator tablet manufactured by Saarchem (Standard Methods 1985).

Alkalinity

Alkalinity determinations were effected using Gran titrations in the pH range $4 > pH > 3$ with standardized HCl titrant (Loewenthal *et al* 1989).

The acid was dispensed using a Metrohm Herison Multi-Bürette model L485 which dispenses with an accuracy of 0,01 mℓ. Each batch of HCl (manufactured by BDH Ltd.) was standardized against a standard Na_2CO_3 solution.

EXPERIMENTAL INVESTIGATION - GENERAL COMMENTS & OBJECTIVES

In Chapter 3 it was shown that kinetics of limestone (calcium carbonate) dissolution could be modeled by an equation of the form given by Eq. 3:19 provided that the mechanism is diffusion controlled. Further, for pH in the region $5 \leq pH \leq 9$ and $\bar{p}CO_2 \leq 0,1$ atmospheres, the first two terms are negligible so that the rate equation now becomes Eq.4:1 below.

$$\frac{d[Ca^{2+}]}{dt} = k_1 \left\{ k_{spc}^{/\frac{1}{2}} - [Ca^{2+}]^{\frac{1}{2}} [CO_3^{2-}]^{\frac{1}{2}} \right\} \qquad \textbf{(4:1)}$$

The rate constant, k_1, varies with temperature, ionic strength, granule size, physico-chemico properties of the mineral **and** the hydraulic characteristics (flow rate).

Alternatively if the mechanism is surface controlled the rate equation in the region $5 \leq pH \leq 9$ and $\bar{p}CO_2 \leq 0,1$ atmospheres reduces to Eq. 4:2 ie.

$$\frac{d[Ca^{2+}]}{dt} = k_{(D+J)} f_d^2 \left\{ [Ca^{2+}]^{\frac{1}{2}} [CO_3^{2-}]^{\frac{1}{2}} - \left(\frac{k_{spc}}{f_d^2} \right)^{\frac{1}{2}} \right\}^2 \qquad \textbf{(4:2)}$$

where the rate constant $k_{(D+J)}$ varies with temperature, ionic strength, granule size and the physico-chemico properties of the mineral but *not* with the hydraulic characteristics.

The initial investigation involved determining whether the process is diffusion or surface controlled. Clearly this requires determining whether dissolution kinetics in the system are controlled by hydraulic characteristics. That is whether the rate constants in Eq. 4:1 and Eq. 4:2 above vary with flow rate, if so then the process is diffusion controlled and Eq. 4:1 is valid, if not then it is surface controlled and Eq. 4:2 applies.

The experimental investigation therefore was divided into two sections. The first, an investigation into the mechanism of rate control. The second, determination of the effects of limestone granule size and flow rate on the rate constant (for limestone from one particular quarry).

In both of the objectives outlined above, the same experimental apparatus was used. Consequently, first it is necessary to describe briefly procedures used in effecting a particular experiment using the upflow reactor.

DETERMINATION OF THE RATE CONSTANT

The upflow reactor described in the previous section was extensively used to investigate the dissolution behaviour of limestone granules under various flow conditions for specific initial water quality parameters. During the course of the investigation a range of different conditions were held constant while others were varied and visa versa, but in essence the experimental and analytical procedure remained unchanged throughout. The next sections describe experimental and analytical procedures adopted.

Experimental procedure

Experimental procedure involved preparing a water to a predetermined specific initial state, loading the reactor with limestone granules and then allowing the water to pass through the reactor at a certain predetermined flow rate. Samples were taken at various ports along the side of the reactor during the run. The procedures used are set out below.

Preparation of Raw Water

A number of waters were used in the investigation. Theses included tap water (which was adjusted chemically prior to use), rain water and terrestrial water derived from a Table Mountain sandstone region.

Tap Water

For economic reasons many of the experiments were carried out using tap water which was adjusted prior to its use to Acidity and Alkalinity values (and hence pH) approximating a raw terrestrial water derived from a Table Mountain Sandstone region.

Tap water supplied by the municipality of Cape Town has pH $\pm 9,1$ calcium concentration ± 35 mg/ℓ as $CaCO_3$ and a precipitation potential of approximately 2mg/ℓ as $CaCO_3$.

Pretreatment involved filling the $2,5m^3$ tank with the tap water and then dosing it with mineral acid to reduce Alkalinity, followed by aeration to reduce Acidity by removing CO_2.

The raw water tap supply varied slightly in quality with time. In order to ensure some measure of consistency in water quality from one batch to another, pH of the water, after aeration was maintained at approximately pH 4. Aeration was continued for a minimum of twelve hours after the last increment of acid had been added. Provided no significant change in pH was detected over this period, the water was considered to be sufficiently stable for use in the reactor.

Rain water

A limited amount of rainwater was collected from the roof of the laboratory during the winter months (the high rainfall season in the Western Cape). As large quantities of distilled water are difficult to produce, this was a reasonable substitute. This water was stored in the $1m^3$ and $2,5m^3$ storage tanks and received no pretreatment.

Table Mountain water

A few experiments were conducted making use of a typical soft acidic water representative of that found in the rivers of the Western Cape . This water was transported to the laboratory from Constantia Nek water treatment plant supply. This water has low Total Dissolved Solids (TDS $\pm$ 75 mg/ℓ, pH $\pm$ 6,5, Alkalinity $\pm$ 5 mg/ℓ as $CaCO_3$ and a variable carbon content due to dissolved humic substances. The water was used without pretreatment of any form and variances in the quality of the batches of water, especially with respect to humic substances, had to be accepted.

Preparation of Limestone Granules

Crushed, pre-sieved granular limestone was obtained from a limestone quarry near Bredasdorp, Western Cape, South Africa.

In any particular dissolution test conducted, the limestone granules used were of some nominal mean diameter. Sizing to obtain mean diameter was effected using standard soil analysis sieves and a sieve shaker. The upper and lower sieves were used to select the higher and lower diameters for any particular selected mean size. Four mean granular sizes ere obtained, they were 8,05 $\pm$ 1,35 mm, 5,70 $\pm$ 1,00 mm, 3,55 $\pm$ 1,15 mm and 1,43 $\pm$ 0,27 mm.

The limestone obtained from Bredasdorp is very friable and invariably enmeshes small particles even after sieving. These small particles were removed prior to experimentation by placing the granules on a sieve (the smaller of the two sieve sizes used) and washing under a jet of water. This process was carried out just prior to use. Secondary removal of the small particles was effected in filling the reactor.

Filling the reactor

The uniform packing of the limestone granules in the reactor is essential to ensure similar opportunities for dissolution along the flow path. Furthermore because of the friable nature of the limestone, the filling procedure had to be effected in a fashion which prevented further breakup of the granules. The following filling procedure was adhered to.

The upper reactor end cap was removed and the reactor inlet connected to the constant head tank. The maximum possible flow of water was then directed through the reactor, spilling to waste at the upper end. Small quantities of sized and washed granules were dropped in at the top of the reactor to settle through the up flowing water. The reactor was constantly lightly tapped at the zone where the granules came to rest to ensure a uniform packing density. This technique of filling the reactor had the following advantages:

i) granules settled with a similar velocity throughout the reactor thus avoiding denser packing at the bottom of the reactor than at the top.

ii) the slower settling velocity reduced the impact at the bottom of the reactor, reducing damage arising from the friable nature of the material.

iii) in passing through the upward flowing water any remaining dust on the granules tended to be washed off. A zone of larger dust particles tended to appear ahead of the advancing front of settled and packed granules and was eventually washed out of the reactor.

iv) the light but consistent tapping applied at the zone where the granules came to rest resulted in a slightly tighter packing than would have been achieved by merely allowing the particles to settle. This ensured that the granules were firmly packed against the wall of the reactor, thereby helping to prevent short circuiting at the periphery of the packed bed.

v) it prevented air from being trapped in pockets in the limestone media.

Once full, the end cap was replaced and connected to the pipework. The reactor was kept full of water to avoid trapping air pockets in the media.

Starting and operating the reactor

A number of precautions were taken prior to start-up and during each experimental run.

Prior to startup the pipes leading to the upflow reactor where cleared of any entrapped air by flushing to waste. Effects of air entrainment through sampling was prevented by the contra-flow sampling procedure described previously.

The reactor was run for at least an hour before samples where taken to ensure that the reactor was operating at a steady state condition. The pH at the uppermost sampling port was continuously monitored during this period. When the pH showed a constant value a steady state was assumed. The time taken to reach this steady value varied but rarely took longer than twenty minutes.

The sampling unit allowed in-situ pH measurements to be taken, thereafter the contents of the sampling unit was filtered immediately through 0,45μm filter paper. This was done to prevent continued dissolution of any grains of limestone that may have been inadvertently washed into the sampling unit. The sample was then stored in plastic sample containers for further analysis.

Estimation of Contact Time

In order to determine dissolution kinetics from the water quality data gathered during each experiment, the contact time between the water and the limestone has to be known. This time depends inter alia on flow rate, flow behaviour and porosity of the packed bed.

With regard to flow behaviour, in all probability the flow is likely to be pseudo plug flow. However, for the sake of convenience **true plug flow is assumed** in order to facilitate modelling the limestone (calcium carbonate) dissolution behaviour. It is accepted that true plug flow is an idealized condition, but in many instances packed column reactors are used to approximate this idealization (Levenspiel 1972). Deviation from the ideal may arise from a number of factors including flow channelling and the existence of stagnant regions. Flow channelling can be minimized by uniform packing throughout the reactor, thereby ensuring that no extra voids occur at the reactor walls. To this end, the filling procedure described previously was strictly adhered to. The potential for the formation of stagnant regions was reduced by the conical transitions at the end caps, which, together with the wire gauze supporting the limestone granules, ensured that the fluid flow was introduced uniformly over the entrance to the reactor.

With regard to the porosity, n, of the in-situ granules, this is the ratio of the total volume of voids in the reactor to the total volume occupied by the granules and voids. The total volume of voids in the reactor was determined assuming that all voids were occupied by water. By draining and measuring the amount of water contained within the volume of reactor occupied by the limestone granules the volume of voids in this space was determined. This was measured in two stages. Firstly, free water within the reactor was allowed to drain out of the reactor over a period of 12 hours, collected and measured. Secondly, the damp granules were weighed, dried in an oven for 24 hours at 105°C, and weighed again. The difference in the two weights allowed the volume of water that was still trapped in the voids of the granules to be calculated. The total volume of voids being the sum of these two quantities. This procedure is in line with accepted soil technology practice provided that no air bubbles are trapped in the granules. The procedure used for filling the reactor with

granules ensured that no air was trapped. The porosities determined are shown listed in Table 4:1 below. A porosity based on the volume of drained water alone also is shown.

Table 4:1: Porosity of the Bredasdorp limestone granules

Nominal Granule size (mm)	Porosity (by oven drying)	Porosity (by drip drying)
1,43	59,6 %	45,3 %
3,55	64,1 %	47,2 %
5,7	63,9 %	44,5 %
8,05	65,1 %	45,2 %

Once porosity is known, it is possible to determine average flow velocity through the medium. A relationship frequently used in soil technology to determine the average velocity of flow of water through a soil, $\bar{v}$, (Craig 1992) is

$$\bar{v} = \frac{\ell}{t_\ell} = \frac{q}{A \times 1000} \times \frac{1}{n} \qquad \textbf{(4:3)}$$

where $\bar{v}$ = average velocity of plug (m/min)

t_ℓ = time taken for fluid plug to pass through a distance ℓ of reactor (min)

ℓ = axial distance along reactor (m)

A = reactor cross sectional area (m^2)

q = flow rate through reactor (ℓ/min)

n = porosity

However, the relationship above is applicable only where the material itself is non-porous, and the porosity used is the packing porosity of the granules, ie. based on the inter granular voids only. Examination of individual Bredasdorp limestone granules reveals that the mineral has a very porous structure. This is confirmed by the difference in porosities indicated in Table 4:1 between the oven and the drip dried samples. The possibility therefore arises that there is a flow component through the granules themselves. In this event the mineral porosity (ie. the intra granular porosity) of the granule also must be taken into account when determining the flow path through a cross sectional area of the reactor. Because of this uncertainty together with the packing porosity, Eq. 4:3 will not provide an adequate approximation to the flow velocity through the packed granules.

In view of the potential complexities of the flow behaviour through the packed bed, tracer studies were undertaken in an attempt to obtain a direct measurement of flow velocities through the reactor.

Measurement of flow velocity

A tracer KCl solution was injected at a lower port of the reactor while recording the conductivity with time at the upper end cap. Tracer injection was by means of an ordinary 6mℓ medical syringe fitted with a 1mm diameter needle. Due to the friable nature of the limestone granules, the needle penetrated them with ease making it possible to inject the tracer near the centre of the reactor, thereby minimizing influences from the reactor sides.

Calibration of the conductivity meter was unnecessary as measurements were required relative only to some base conductivity value. Data logging with time was effected using a Personal Computer, which provided an accurate measure of time. On injection of tracer, a signal was sent to the computer to indicate the start of the observations. *Conductivity versus time* plots were produced for the various flow rates and tracer injection at the different ports. These are presented in Appendix D. The time taken by a plug to flow from injection point to the detector was measured from the electronic marker indicating the moment of injection to the centroid of the *conductivity versus time* plot (Levenspiel 1972). These times are shown in the relevant tables in Appendix D, together with the standard deviation of the conductivity readings about this time. The numerical procedures used to calculate this time and the standard deviation is set out also in Appendix D.

Referring to the *conductivity versus time* plots shown in Appendix D, these are slightly skewed to the right and have a fairly large standard deviation. Possible factors contributing to this behaviour were:

i) the reactor is not a perfect plug flow device and a certain degree of dispersion of the plug can be expected,

ii) injection of the tracer was not as a perfect pulse of zero time but in fact took a few seconds,

iii) unknown dispersion effects could exist at the end cap due to change in flow patterns, and

iv) an attenuation effect may arise due to the manner of abstraction of the sampling side stream.

With regard to deviation from perfect plug flow conditions (ie. i and ii above), this was assessed using a dimensionless quantity known as the vessel dispersion number, VDN,

(D/uL). It is generally accepted that values for VDN around 0,025 indicate an intermediate amount of dispersion, values around 0,20 indicate a large amount of dispersion (Levenspiel 1972). This number was calculated for the results of the tracer tests assuming a pulse type introduction of tracer (see Appendix D). The results indicate that in general intermediate dispersion occurred in the reactor and consequently it was assumed that the initial assumption of plug flow through the reactor is acceptable.

With regard to (iii) and (iv) above, to minimize the error due to end effects and sampling technique, a number of observations were conducted for any particular flow rate through the reactor. By plotting *depth of reactor bed (distance)* against *observed times* for a particular flow rate, a straight line plot was obtained which does not pass through the origin (because of end cap effects and sampling technique). These lines are shown in the *distance versus average time to centroid of trace* plots developed for each of the mean granule sizes in Appendix D (see Figures D:2, D:5, D:8 and D:11). However the slope of such a line represents the average velocity at which a plug passed through the reactor. The observations were repeated for a number of loading rates and the average velocity for each was determined. A *velocity versus flow rate* plot was obtained for each granule size (see Appendix D) and plotted on a common axis in Figure 4:2 below. The inverse of the average velocity, read off this graph for a particular loading rate, gives the time a plug of fluid takes to pass through a unit length of reactor.

Examining the *velocity versus flow rate* plots for the various granule sizes under investigation (Figure 4:2), it can be seen that the slopes of these plots, (corresponding to mean granule diameters of 8,05mm, 5,7mm and 3,55mm), decrease with decreasing granule size. However, investigation of the corresponding porosities revealed that the proportion of voids in each case is closely constant (regardless of whether one examines the porosity obtained before or after oven drying, see Table 4:1). This is to be expected as single size particles of similar shape would probably pack in similar proportions. Consequently, the observed differences in velocities with granule size would indicate a significant flow component through the granules arises from the mineral porosity.

The total porosity of the granules in the reactor has been determined from the volume of voids obtained by oven drying the granules. Some idea of the packing porosity of the granules themselves (ie. assuming no mineral porosity) has been derived by using the void volume determined by the drip drying technique. An indication of the extent to which the mineral porosity plays a role in determining the flow through the reactor, can be obtained by developing the concept of apparent porosity.

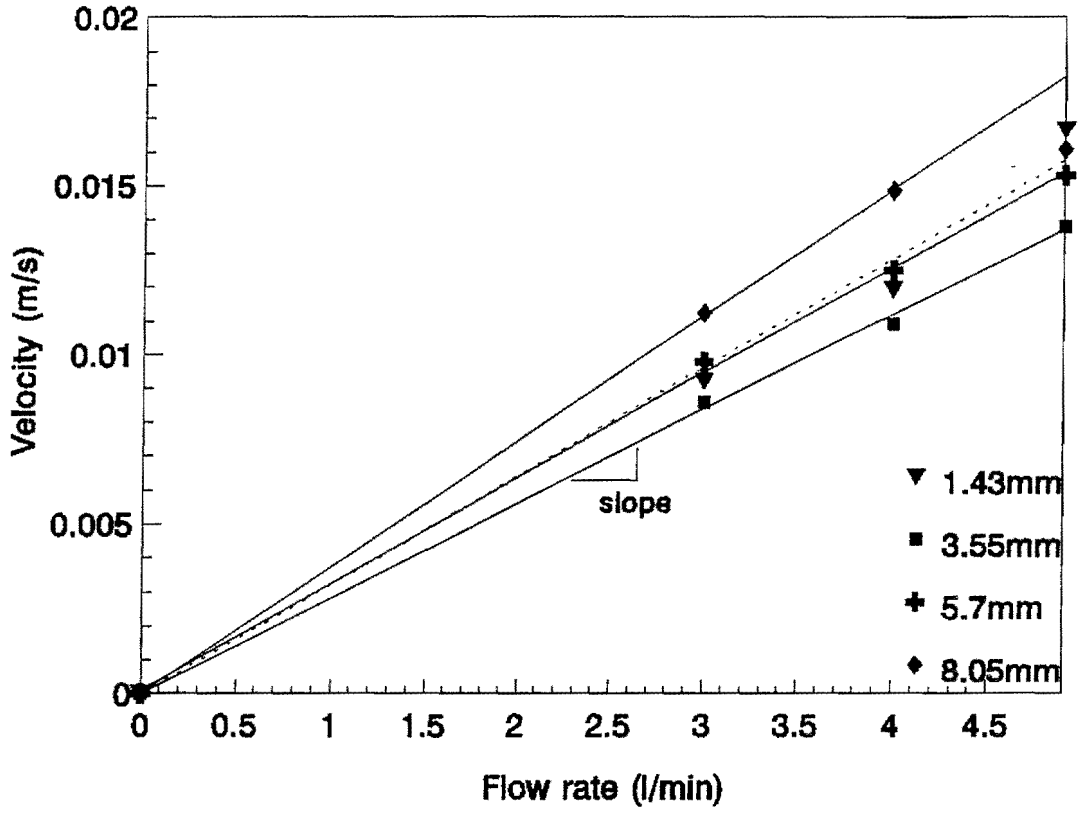

Figure 4:2 *velocity versus flow rate* plot for the various Bredasdorp limestone granules investigated.

Rearrangement of Eq. 4:3 to give an equation for porosity, n, in terms of the other parameters, yields,

$$n = \frac{q}{\bar{v} \times A \times 1000} \qquad (4:4)$$

The quantity $\frac{q}{\bar{v}}$ is the inverse of the slope of the *velocity versus flow rate* plot, thus by multiplying by the cross sectional area of the reactor, the apparent porosity is obtained. The closer this apparent porosity is to the total porosity, the greater is the flow component through the granules.

Accepting that there is a flow component through the granules, one would expect this component, indicated by the apparent porosity, to vary with the surface area of the granules used. A relationship linking total surface area of granules per unit volume, (S_v), to mean granule diameter, (D_m), is formulated as follows:

Considering first the granules alone, and assuming a mean granule diameter, (D_m): the volume of a granule, (V_g), is proportional to the mean granule diameter cubed

$$V_g \propto D_m^3$$
$$V_g = \text{constant}_1 \times D_m^3$$

and the surface area of a granule, (S_g), is proportional to the mean granule diameter squared

$$S_g \propto D_m^2$$
$$S_g = \text{constant}_2 \times D_m^2$$

Assuming uniform packing the number of particles per reactor volume, N, is inversely proportional to the volume of the granules

$$N = \frac{1}{V_g}$$
$$N \propto \frac{1}{D_m^3}$$
$$N = \text{constant}_3 \times \frac{1}{D_m^3}$$

Therefore the total surface area per reactor volume, (S_a), is

$$S_a = N \times S_g$$
$$S_a = \text{constant}_4 \times \frac{1}{D_m^3} \times D_m^2$$

$$S_a = \text{constant}_4 \times \frac{1}{D_m} \qquad (4:5)$$

A plot of the *apparent porosity versus inverse mean granule diameter* was drawn, see Figure 4:3 below. Referring to this plot, it can be seen that there is a fairly linear dependence of the apparent porosity on the inverse of the mean granule diameter and therefore on the surface area for the larger three granule sizes investigated.

However the smallest granule size deviates from the above behaviour. A possible explanation for this is that the shape of the smaller granules is no longer similar to that of the other three mean granule sizes and/or due to a change in hydraulic conditions reflected in a greater head loss through the reactor. From a practical point of view this granule size is unlikely to be used in reactors and in view of the discrepancy discussed above, will be excluded from further investigation.

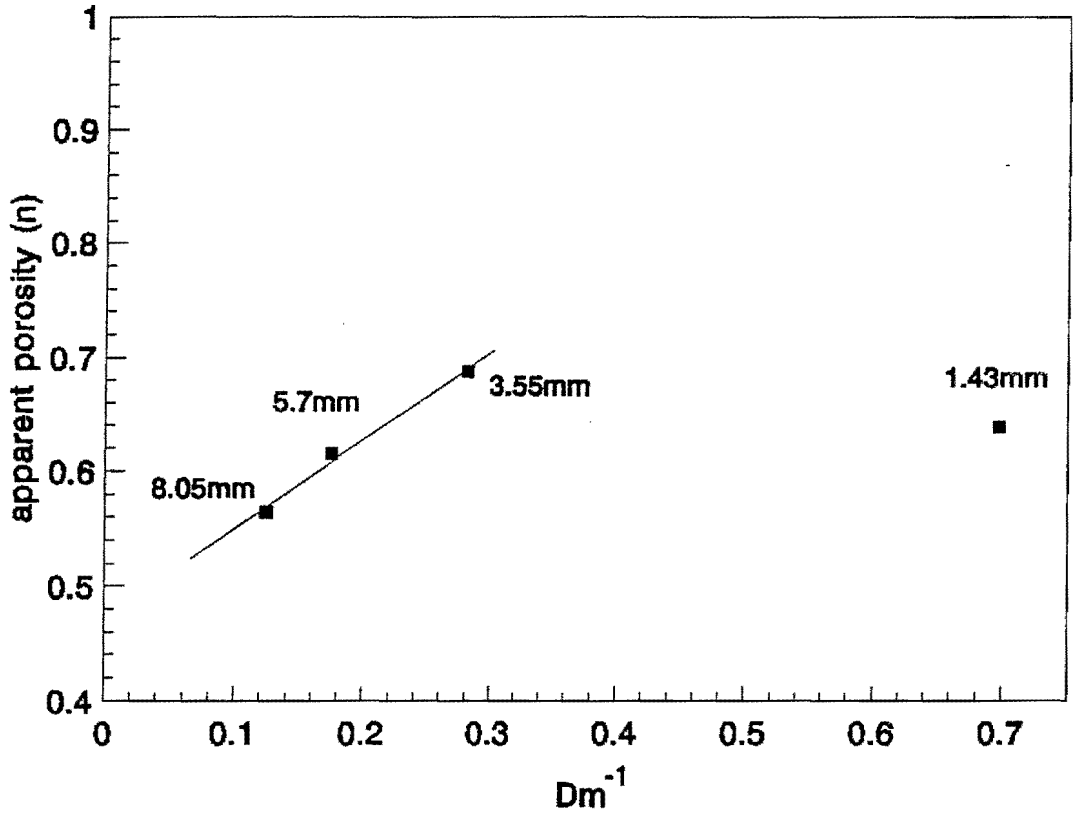

Figure 4:3 *Apparent porosity versus inverse mean granule size* plot for the range of Bredasdorp limestone granules investigated.

Having determined the flow velocities through the reactor at the various flow rates for each of the granule sizes, the average contact time can be calculated.

Estimate of average contact time

The contact time between successive sampling ports, which is required for the subsequent kinetic studies, is derived from the flow velocity. Eq. 4:3 is rearranged, and as the distance between port is known, the time taken for the fluid plug to pass through this distance can be calculated and is taken to be the contact time.

Analytical considerations

Examination of the rate equations, Eqs. 4:1 and 4:2, indicates that both are functions of the concentrations of Ca^{2+} and CO_3^{2-} in solution, ie.

$$\text{Dissolution rate} = k \,.\, S \,.\, f([Ca^{2+}], [CO_3^{2-}]) \qquad (4:6)$$

where k = rate constant and is influenced by different parameters, depending on the mechanism proposed.

S = surface area

$f([Ca^{2+}], [CO_3^{2-}])$ = a model function incorporating the products of the concentrations of the two species (see Eqs. 4:1 and 4:2).

Furthermore, if the surface area term is constant, it can be incorporated into the rate constant to give rate equations in terms of a "compound rate constant", $k_{compound}$. The compound rate constant is given by the slope of a plot of *dissolution rate versus the model function*. Thus for a particular set of experimental conditions, the value of $k_{compound}$ depends on the choice of model used to describe the dissolution reaction.

Dissolution rate versus model function plot

In order to effect a plot of limestone (calcium carbonate) dissolution rate against the model function, values for the dissolution rate and the Ca^{2+} and CO_3^{2-} concentrations need to be determined from some set of measurements at the sample ports. Each of these determinations is now considered in detail.

Dissolution rate determination

Provided that the flow in the reactor approximates plug flow conditions, dissolution rate can be determined either from calcium and/or Alkalinity measurement at successive ports along the reactor, provided that time of flow between ports is known. The analyses addressed earlier indicate that the assumption of plug flow conditions is reasonable.

The limestone dissolution rate at any port can be approximated by the difference between the calcium (Alkalinity) concentration of the port immediately downstream of the port in question and the one immediately upstream, divided by the time it takes a plug of water to pass through the distance between these ports. Thus to determine the dissolution rate at any port, n:

$$\left(\frac{d[Ca^{2+}]}{dt}\right)_{(n)} = \left([Ca^{2+}]_{(n+1)} - [Ca^{2+}]_{(n-1)}\right) \times \frac{\Delta d}{v} \qquad (4:7)$$

where Δd = distance between ports (n-1) and (n+1)
v = velocity of flow through the reactor

Model function determination

The two model functions investigated here are for a diffusion controlled process (ie. Eq. 4:8), and for a surface controlled process (ie. Eq. 4:9). That is, for the diffusion controlled process;

$$f(\text{diffusion model}) = \left\{ k'_{sp\ c}{}^{\frac{1}{2}} - [Ca^{2+}]^{\frac{1}{2}} [CO_3^{2-}]^{\frac{1}{2}} \right\} \qquad \textbf{(4:8)}$$

and, for the surface controlled process;

$$f(\text{surface model}) = \left\{ k'_{sp\,c}{}^{\frac{1}{2}} - [Ca^{2+}]^{\frac{1}{2}} [CO_3^{2-}]^{\frac{1}{2}} \right\}^2 \qquad \textbf{(4:9)}$$

Values for the model function at any particular port therefore requires knowing the concentrations of Ca^{2+} and CO_3^{2-}, temperature and ionic strength at that port. The calcium concentration, temperature and ionic strength can be measured as set out in the appropriate section. The concentration of CO_3^{2-} is determined indirectly from the measured Alkalinity and pH values at a particular port, ie., at port n,

$$[CO_3^{2-}]_{(n)} = \left(Alk_{(n)} - \frac{k_w'}{(H^+)_{(n)}} + \frac{(H^+)_{(n)}}{f_m} \right) \times \frac{k'_{c2}}{2\,k'_{c2} + (H^+)_{(n)}} \qquad \textbf{(4:10)}$$

where $[CO_3^{2-}]_{(n)}$ = concentration of CO_3^{2-} at port n. (moles/ℓ)
$Alk_{(n)}$ = Alkalinity at port n. (moles/ℓ)
k_w' = apparent equilibrium constant of the water subsystem
k_{c2}' = 2nd apparent equilibrium constant of the carbonate subsystem
$(H^+)_{(n)}$ = $10^{(-pH)}$ at port n.
f_m = activity coefficient for monoprotic species

Determination of the compound rate constant, $k_{compound}$

From a theoretical standpoint it should be possible to determine the compound rate constant from the slope of a plot of *dissolution rate* versus *model function*. However in practice this procedure proved unreliable because, small errors in the values of any of the parameters measured lead to large variability in dissolution rate and/or model function. Therefore, alternative techniques for determining $K_{compound}$ were investigated.

Examination of the proposed dissolution equations reveal that they are Ordinary simultaneous Differential Equations (ODE's). Numerical solutions to ordinary differential equations can be found by a variety of numerical methods, provided that an initial state has been characterised. These methods involve successive approximation techniques utilizing a particular rate equation together with known flow rate and initial characteristics of the water.

The initial value - Ordinary differential equation approach

In this approach the model equations are used together with an assumed rate constant and known initial states to predict the measured parameters along the length of the reactor. If the predicted parameters are sufficiently close to the observed values the model can be considered to be a fair representation of the dissolution process. One of the benefits of such an approach is that it provides a solution to some of the design problems. For example, the initial water quality is determined by measurement, and given any two of the three design parameters, flow rate, reactor diameter and reactor height the third can be determined to attain a desired effluent quality.

A number of techniques exist for the solution to such initial value problems (Gerald & Wheatley 1984). The simpler ones, such as Euler's method involve a series of steps, where each successive ordinate is calculated from the value of the rate function (slope of graph) at the previous ordinate. The accuracy of this type of method tends to improve as the step lengths are made smaller (Hahn 1989). This method tends to become impractical if the number of steps required for the desired accuracy becomes very large. Consequently this method was not considered suitable.

A variety of algorithms, under the general name of RUNGE-KUTTA exist which can be used to solve the initial value problem for Ordinary Differential Equations. This group of solution techniques is recognized as having the ability of predicting subsequent ordinates with a higher degree of accuracy with relatively few steps for initial value problems involving ODEs. In this regard a fourth order Runge-Kutta formula has often been found to suffice. An algorithm using this method for determining the rate constant, $K_{compound}$, is developed below.

Examination of the two dissolution models, ie. Eq. 4:8 and Eq. 4:9, shows that the rate at which the calcium concentration in the bulk solution changes with time t, is a function of the concentration of calcium and carbonate ions in solution. ie.

$$\frac{d[Ca^{2+}]}{dt} = f_1\,(t, [Ca^{2+}], [CO_3^{2-}], \text{constants}) \qquad (4:11)$$

Further, this rate equation can be formulated in terms of change in Alkalinity with time by recognizing the effects of $CaCO_3$ dissolution on both Ca^{2+} concentration and Alkalinity. In this regard, each mole of $CaCO_3$ dissolving increases Ca^{2+} concentration by one mole/ℓ and the Alkalinity by two mole/ℓ (see Eq. 2:24). This is given by,

$$\frac{d\,Alk}{dt} = 2\frac{d[Ca^{2+}]}{dt} = 2\,f_1\,(t, [Ca^{2+}], [CO_3^{2-}], \text{constants}) \qquad (4:12)$$

The CO_3^{2-} concentration in the above rate equation is characterized via the equilibrium equations and known (measured) values for any two weak acid parameters. For example, one may write $[CO_3]$ as a function of pH and Alkalinity or as a function of Alkalinity and Acidity. The pair selected would be those values most conveniently measured.

Thus Eq. 4:11 and Eq. 4:12 can be rewritten as;

$$\frac{d[Ca^{2+}]}{dt} = f_1\,(t, [Ca^{2+}], Alk, Acid, \text{constants}) \qquad (4:13)$$

$$\frac{d\,Alk}{dt} = 2\,f_1\,(t, [Ca^{2+}], Alk, Acid, \text{constants}) \qquad (4:14)$$

A third differential equation is available from the recognition that Acidity (with CO_3^{2-} as reference species) remains unchanged with $CaCO_3$ dissolution/precipitation, ie.

$$\frac{d\,Acid}{dt} = f_2\,(t, [Ca^{2+}], Alk, Acid, \text{constants}) \qquad (4:15)$$
$$= 0$$

Equations 4:13 to 4:15 are a set of three simultaneous ordinary differential equations, the solutions of which can be found numerically by means of the Runge-Kutta method provided the initial conditions and the constants are known. The first observed data point that falls within the criteria of $5 \leq pH \leq 9$ for which $[Ca^{2+}]$, Alkalinity and Acidity are known is used. This can be said to occur at time, $t = 0$. Subsequent values for these parameters can be predicted for any time, t, during which the plug of water remains within the reactor. In order to find the rate constant, $k_{compound}$, an algorithm was developed to determine the least sum of the squares of the difference between predicted and observed values along the length of the reactor. The algorithm used is set out in Appendix E. A computer program was

written to effect the calculations.

A few simplifications were adopted which facilitated algorithm development and also enhanced the computational speed of the algorithm. Furthermore, there are certain cautions that should be observed when applying the algorithm. These are discussed below.

Solution Ionic Strength

Solution ionic strength can be approximated from the measured conductivity readings by making use of Eq. 2:9. The measured conductivity of the solution samples obtained from each port showed (as was expected) an increased with residence time in the reactor. Thus as $CaCO_3$ dissolves into the solution there is an increase of solution ionic strength.

From the previous discussion of weak acid chemistry (Chapter 2) the mono- and divalent activity coefficients are required to determine values for the apparent solubility constant for calcium carbonate, k_{spc}', and the weak acid apparent equilibrium constants k_{c1}' and k_{c2}' and to calculate values for pH and $[CO_3^{2-}]$ from known (measured) values of Alkalinity and Acidity. The temperature dependence of the activity is obtained from Eq. 2:6. In any particular test, temperature change was small (ie. $\pm 0.2\,^{\circ}C$) and consequently was ignored.

Furthermore, the investigations were limited to soft waters so that solution conductivity seldom exceeded 30 mS/m even after passing through the reactor. For most experimental runs the difference between conductivities measured at the initial and the final ports used in the analysis (ie. in the range $5{,}5 \leq pH \leq 9$) seldom exceeded 3 mS/m. Using the approximation of Eq. 2:9, this corresponds to an increase in solution ionic strength of 0,0005 mole/ℓ. In addition to this low increase in solution ionic strength, the activity coefficients determined in Eq. 2:5 are not very sensitive to ionic strength (Loewenthal *et al* 1986). Thus an average ionic strength was determined from the average conductivity observed over all ports with pH readings in the desired range, for use in the algorithm. Sensitivity to variations in ionic strength was then tested by using various conductivity values in the algorithm. It was found that the values for the rate constant, $k_{compound}$ so determined, did not vary significantly when the values corresponding the to the initial and final measured conductivity for a particular experimental run were used.

Solution Acidity

In a previous section it has been shown that Acidity (with CO_3^{2-} as reference species) remains constant with $CaCO_3$ dissolution (also see Eq. 2:24). The solution Acidity is determined from the observed pH and Alkalinity at a port by making use of Eq. 2:23. This equation is sensitive to the values of pH that are used, therefore the solution Acidities calculated at each

port are expected to vary somewhat. In order to determine the best estimate for the solution Acidity, the Acidity at each port (within the prescribed pH range) was calculated from the observed pH and Alkalinity values, the average of these Acidity values, taken to be the initial (and final) solution Acidity. An underlying assumption to the above is that there are no impurities in the $CaCO_3$ granules that could impart significant Acidity to the solution. This assumption is supported to a large extent by the mineralogical analysis discussed later in this chapter.

Selection of initial and final ports for the analysis

A further analytical consideration relates to the choice of initial and final reactor ports over which the "least sum of the squares of the difference between predicted and observed values" procedure to determine $k_{compound}$ is carried out. It must be noted that the closer the initial and final observation ports are to each other, the lower the sum of the squares difference will tend to be, and, in the extreme, when the ports are adjacent to each other, this sum reduces to zero. Caution should be exercised to ensure that sufficient observation ports are selected for comparison with predicted values to ensure an adequate assessment of the model. To this end, the more observation ports that are included in the pH range under consideration (ie. $5{,}5 \leq pH \leq 9$) for comparison with the model, the more reliable the determined value of $k_{compound}$ will be.

DETERMINATION OF THE CONTROLLING MECHANISM OF DISSOLUTION KINETICS

Mineral dissolution phenomena usually are controlled by a diffusion mechanism, Stumm and Morgan (1981). In the previous chapter it was shown that for calcium carbonate dissolution a diffusion controlled mechanism in the region $5 \leq pH \leq 9$ leads to an equation of the form;

$$\frac{d[Ca^{2+}]}{dt} = k_{D.C.\ compound} \left\{ k'^{\frac{1}{2}}_{spc} - [Ca^{2+}]^{\frac{1}{2}} [CO_3^{2-}]^{\frac{1}{2}} \right\} \qquad \textbf{(4:16)}$$

where $k_{D.C.\ compound}$ = compound rate constant for a diffusion controlled reaction, which varies with temperature, ionic strength, physico-chemico properties of the mineral and hydraulic characteristics (flow rate) and includes a surface area term.

However, for calcium carbonate dissolution, some investigators have either explicitly postulated a surface controlled mechanism (Sjoberg 1976) or implicitly accepted a surface controlled mechanism by their choice of the equation describing kinetics (Mills 1984). Such a mechanism leads to an equation of the form utilized by Mills (1984), ie;

$$\frac{d[Ca^{2+}]}{dt} = k_{S.C.\ compound}\, f_d^2 \left\{ \left(\frac{k_{spc}}{f_d^2} \right)^{\frac{1}{2}} - [Ca^{2+}]^{\frac{1}{2}} [CO_3^{2-}]^{\frac{1}{2}} \right\}^2 \qquad \textbf{(4:17)}$$

where $k_{S.C.\ compound}$ = compound rate constant for a surface controlled reaction, which varies with temperature, ionic strength, physico-chemico properties of the mineral and includes a surface area term.

(Both these equations representing kinetics in regions where $5 \leq pH \leq 9$ and $\bar{p}CO_2 \leq 0{,}1$ atmospheres, see previous chapter).

To identify which of these two mechanisms controls dissolution, one needs to identify some measurable parameter which separates them. In this regard, a mineral dissolution phenomenon in which the kinetics varies with mixing energy (all other parameters being kept constant) is considered diffusion controlled. That is, where the compound rate constant in Eq. 4:16 varies with mixing energy between otherwise identical experiments, the process is diffusion controlled. This approach was used to identify the rate controlling mechanism in the investigation reported here.

Method

The reactor was loaded with single size granules of a nominal mean diameter. Acidified tap water was prepared and a set of experiments was carried out as described in the previous section. Mixing energy was varied by changing flow rates between experiments. The compound rate constant was determined for both model functions (ie. $k_{D.C.\ compound}$ and $k_{S.C.\ compound}$) and plotted against the loading rates.

Loading rate, LR, was selected because it is independent of cross sectional area of the reactor, ie.

$$LR = \frac{q \times 60}{A \times 1000} \qquad \textbf{(4:18)}$$

where LR = loading rate (m hr^{-1})
A = reactor cross sectional area (m^2)
q = flow rate through reactor (ℓ/min)

Results

Rate constants determined using the diffusion model were calculated for the set of experiments conducted on the 5,7mm mean size Bredasdorp limestone granules. The experimental data is shown in Appendix F (experiments 1 to 6). The experiments were all conducted at temperatures between 23,2°C and 24,4°C, ie. 23,8°C $\pm$ 0,6°C. A plot of compound rate constant(s) determined versus loading rate(s) is shown in Figure 4:4.

From Figure 4:4 it can be seen that the rate constant varies with loading rate, ie mixing energy. This indicates that the process is diffusion controlled. Consequently, an equation of the form shown in Eq. 4:16 is considered to represent the dissolution process. At this stage it is noted that the compound rate constant varies with both mixing energy and granule size.

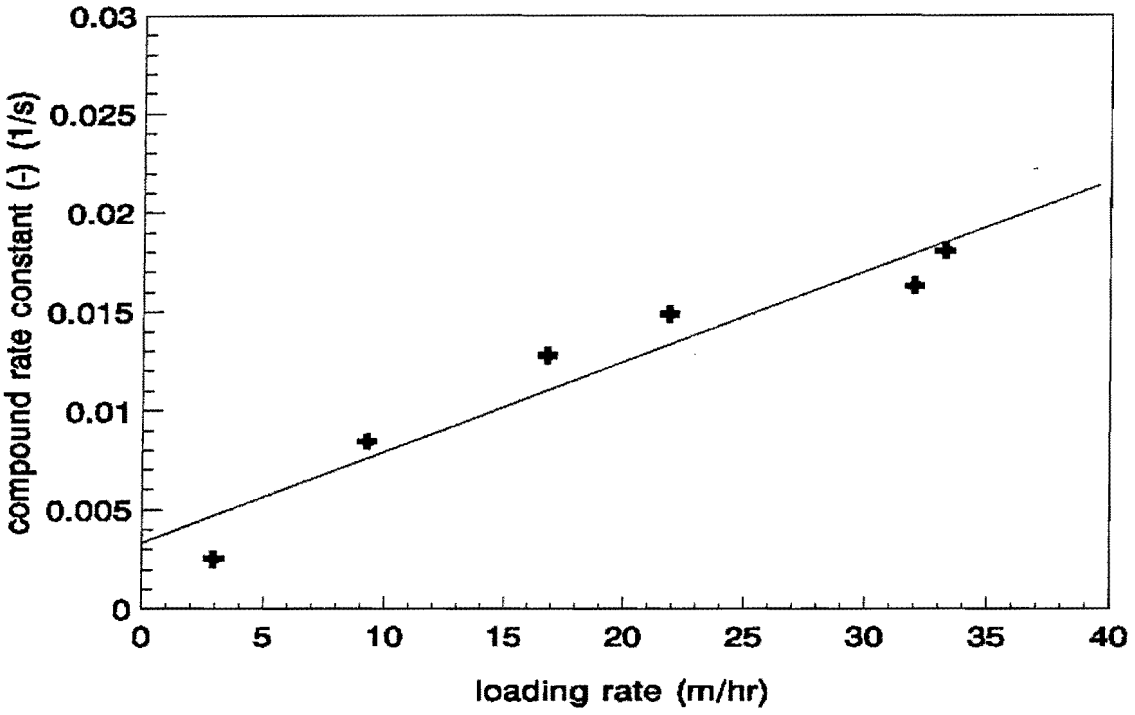

Figure 4:4: *Compound rate constant versus loading rate* plot for 5,7mm mean size Bredasdorp limestone granules in acidified tap water (T = 24°C ± 0,8°C).

EFFECTS OF GRANULE SIZE ON THE COMPOUND RATE CONSTANTS

The discussion above shows the dependence of the compound rate constant on loading rate for a single granule size. However, from Eq. 4:16 the mineral dissolution rate is proportional to a rate constant which incorporates a surface area term. Some idea of the nature of this interdependency is obtained from Eq. 4:5 where it is shown that the effects of surface area per unit volume of reactor is inversely proportional to the mean granules diameter. From this, it is expected that as the granule diameter increases/decreases the surface area term and hence the compound rate constant decreases/increases (ie. decrease/increase in mineral dissolution rates). This interdependency was investigated by experiment.

Acidified tap water was prepared as set out above and a set of dissolution rate experiments was carried out on two extra granule sizes (3,55mm and 8,05mm) in the packed beds. In each case mixing energy was varied by changing the flow rates between experiments. The experimental data is listed in Appendix F (experiments 7 to 18). All experiments were conducted at temperatures between 20,7°C and 24,3°C, ie. 22,5°C ± 1,8°C. The compound rate constant was determined using the diffusion controlled model function.

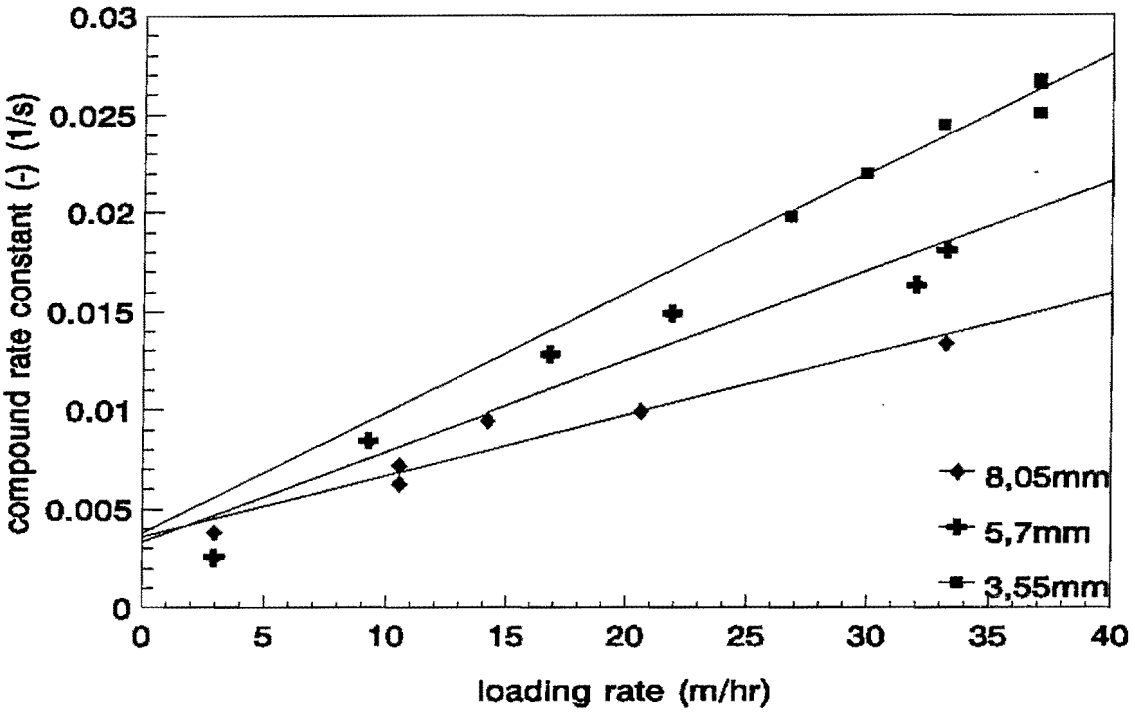

Figure 4:5: *Compound rate constant versus loading rate* plot for 3,55mm, 5,7mm and 8,05mm mean size Bredasdorp limestone granules in acidified tap water (T = 22,5°C ± 2°C).

In Figure 4:5 is shown plotted the compound rate constant versus the loading rate for the three granule sizes 3,55mm, 5,7mm and 8,05mm. This plot indicates a closely linear relationship between the compound rate constant and the loading rate for each nominal mean granule size. Linear regressions were carried out on this data in order to obtain the best fit line representing each of the data sets and are plotted in the diagram. Experimental data gives a compound rate constant which increases with decrease in granule size.

A linear dependence of the apparent porosity (and hence the flow characteristics of the reactor) on the inverse of the mean granule diameter was established in a previous section. This made it possible to simultaneously present the effects of both granule size and loading rate on the compound rate constant. A plot of $k_{compound}$ versus the ratio of loading rate to mean granule diameter is shown in Figure 4:6. In this form experimental data of all three granule sizes is closely linear. A linear regression was carried out to obtain an equation representing the effects of both granule size and loading rate on the compound rate constant giving,

$$k_{D.C.\ compound\ (\phi)} = 0{,}0021\ \frac{LR}{\phi} + 0{,}0044 \qquad (4:19)$$

where ϕ = nominal mean granule size (mm)
LR = loading rate (m hr^{-1})

It is reiterated that Eq. 4:19 is valid only for granules obtained from the Bredasdorp deposit and within the mean nominal granule size range of 8,05mm to 3,55mm.

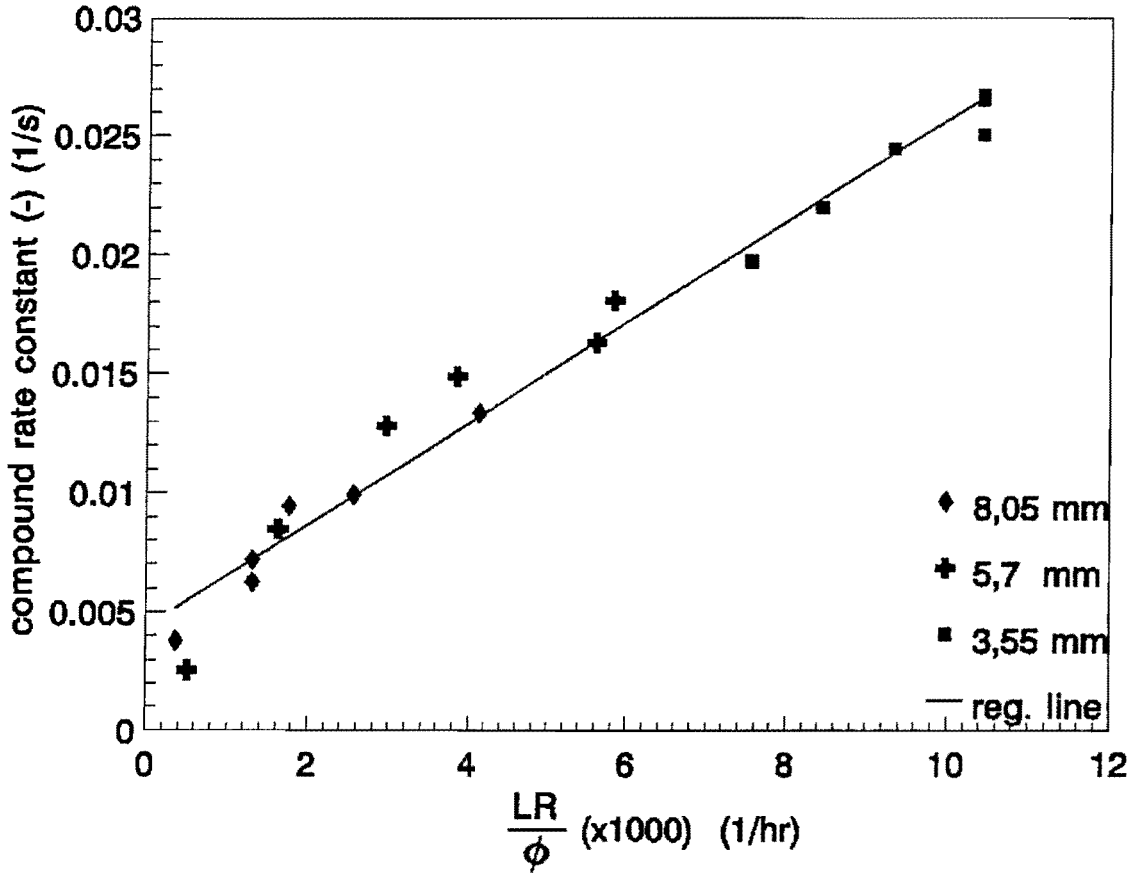

Figure 4:6: *Compound rate constant versus LR/ϕ* for all limestone granules investigated in acidified tap water (T = 22,5°C ± 2°C).

INFLUENCE OF WATER SOURCE ON THE COMPOUND RATE CONSTANT

Values for the compound rate constants for the Bredasdorp limestone were determined largely using chemically adjusted tap water (This arose because of various difficulties in transporting raw water to the laboratory). In this section the effects of using other waters are investigated. To this end two sets of experiments were conducted, each making use of a different natural water. In a first set of experiments, rain water - runoff collected from the laboratory roof, was used while in a second set of experiments a coloured water of varying organic carbon content (derived from one of the Table Mountain reservoirs) was used.

Rate constant measurement was effected using a similar procedure to that employed previously. In the first set of experiments, (ie. using rain water) 8,05mm Bredasdorp limestone granules were used (Appendix F experiments 22 to 25). In the second set of experiments (ie. using Table Mountain humic water) 5,7mm Bredasdorp limestone granules were used (Appendix F experiments 26 to 30). In each set of experiments the loading rate was altered between 10m/hr and 35m/hr.

Compound rate constants obtained from these experiments are shown superimposed on Figure 4:5 in Figures 4:7 and 4:8. Figure 4:7 shows the results for the experiments involving 8,05mm limestone granules and rain water, and Figure 4:8, the results of the experiments involving the 5,7mm limestone granules and Table mountain water. It is noted that these experiments were conducted at lower temperatures (between 12,5°C and 14,5°C) than those using acidified tap water (Figure 4:5).

Referring to Figure 4:7, the $k_{DC\ compound}$ values for the dissolution of the 8,05mm limestone granules in rain water plot very closely to the positions predicted by the acidified tap water experiments. This confirms that the dissolution by soft water such as rain water is adequately simulated by the use of acidified tap water provided due consideration is taken of activity coefficient effects. Further it is noted that temperature does not have a major influence on the predicted $k_{D.C.\ compound)}$ values.

Referring to Figure 4:8, for the dissolution of 5,7mm limestone granules in brown humic water, it can be seen that the compound rate constants determined between brown water and acidified tap water are only sometimes in agreement. For experiments marked 26 and 27, good agreement is obtained between the two waters. However, for the remaining experiments the compound rate constants are significantly lower than those corresponding to acidified tap waters.

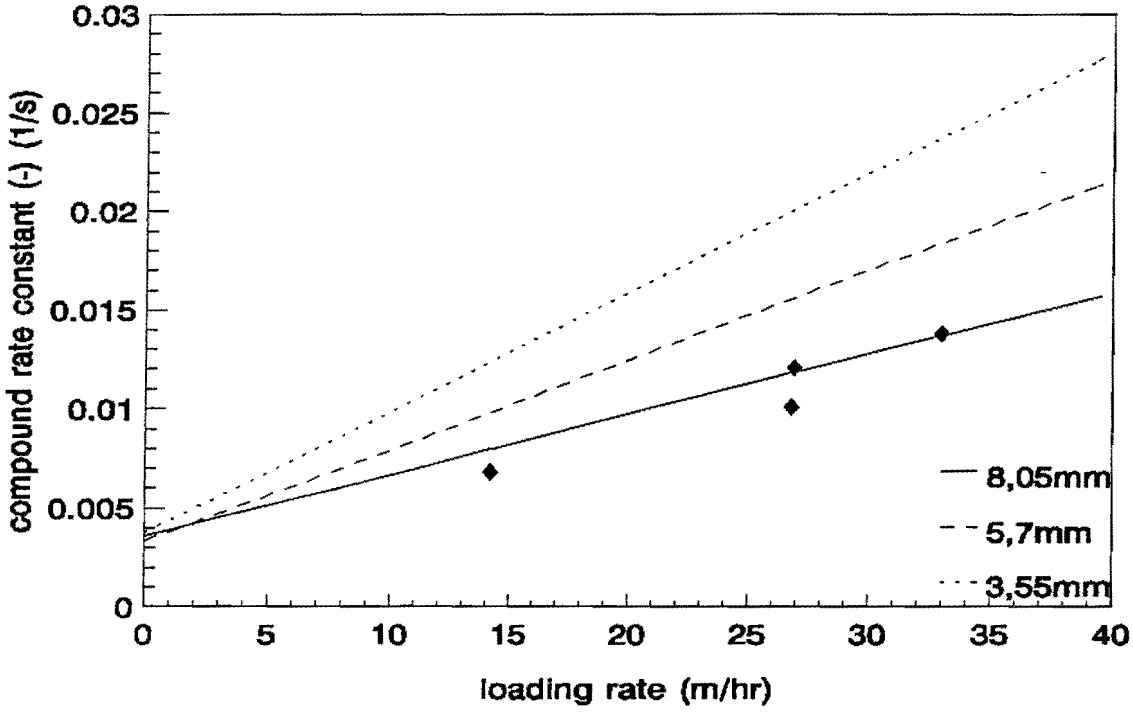

Figure 4:7 *Compound rate constant versus loading rate* plot for 8,05mm mean size Bredasdorp limestone granules in rain water.

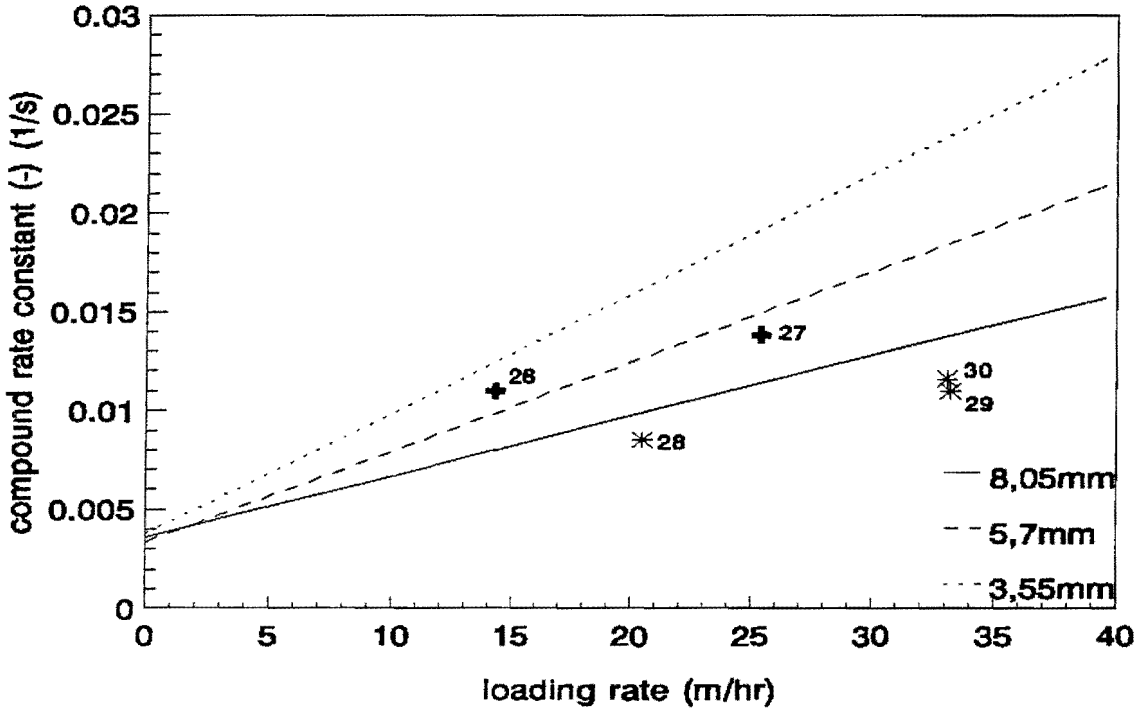

Figure 4:8: *Compound rate constant versus loading rate* plot for 5,7mm mean size Bredasdorp limestone granules using Table Mountain water.

Two possible explanations for this are proposed. First, experiments 27 and 28 were conducted at temperatures of 19,3°C ± 0,2°C while the latter experiments were conducted at 13,8°C ±1°C. However, the insensitivity to temperature of the rain water experiments above would tend to discount this explanation. Second, experiments (experiments 26 to 30) were interrupted for a period of two months after experiments 26 and 27 were completed. During this two month period the limestone granules remained submerged in the brown humic water resulting in humic substances (and perhaps biological growth) occurring on active dissolution sites of the mineral thereby decreasing the two phase reaction rates.

COMMENTS ON THE EXPERIMENTAL RESULTS

Referring to the data in Appendix F (experiments 1 to 30), in a number of experiments the calculated Acidity value increased with flow through the granule bed. This is contrary to what is to be expected from basic theory. In Chapter 2 it was shown that with calcium carbonate dissolution or precipitation Acidity (with reference species CO_3^{2-}) is unaffected.

The increase in calculated Acidity may arise either from some external source of Acidity (eg. CO_2 or mineral acid) or it may result from errors in measurement of either or both Alkalinity and pH.

With respect to an external source of Acidity, great care was taken to avoid CO_2 interaction with the air (see earlier in Chapter 4) and this interference effect was therefore rejected. A second alternative is that the Bredasdorp limestone is contaminated with a source of Acidity released on dissolution on waters with high redox potential. In this regard obvious sources are the minerals Fe_3O_4 and/or $FeCO_3$ and/or $MnCO_3$ entrapped in the limestone matrix. Dissolution of these minerals may release carbonates which do not affect Acidity, and manganous and ferrous species which would be oxidized and subsequently precipitate $Fe(OH)_3$ and/or MnO_2. This would result in Acidity increase and concomitant Alkalinity decrease. This hypothesis was discarded for two reasons. First the Alkalinity and calcium concentrations (on the equivalent scale) increased by closely equal amounts with dissolution through the bed. Second, X-ray fluorescence analysis of the limestone, see Table 4:2, indicated that Mn and Fe^{2+} exist only in trace amounts in the mineral.

With respect to errors arising in Alkalinity and/or pH measurement, an apparent increase in Acidity would require either an over estimate of Alkalinity or an under estimate of pH or both. With respect to Alkalinity measurement this was effected using Gran titration and there is no reason to suppose that a continuously increasing overestimate in measured Alkalinity should occur up the reactor.

Table 4:2: Mineralogical analysis by X-ray fluorescence of the Bredasdorp limestone deposit.

Mineral	Sample A	Sample B	Average
	% by weight	% by weight	% by weight
SiO	6.23	6.83	6.50
TiO_2	0.02	0.03	0.025
Al_2O_3	0.21	0.30	0.255
Fe_2O_3	0.25	0.35	0.30
MgO	0.59	0.64	0.615
Na_2O	0.02	0.03	0.025
K_2O	0.08	0.10	0.09
P_2O_5	0.05	0.05	0.05
CaO	~54*	~54*	~54*
CO_2	not analyzed		
	parts / million	parts / million	parts / million
Mn	10	14	12
Cr	14	17	15.5

* outside calibration range

With respect to pH measurement there is the possibility of a sluggish probe response arising in the very poorly buffered waters investigated. During a particular experimental run, pH observations were taken from the top of the reactor downwards (ie. in a direction against the flow) with observations moving from high pH zone with low buffer (ie. pH $\approx$ 8) through a zone of better buffer capacity (ie. pH $\approx$ 6,5) into a lower zone again with poor buffer capacity (pH $\approx$ 5) (see Figure 2:3). There is a possibility that the responsiveness of the probe is linked to buffer capacity (ie. slower response with lower buffer capacity). In the high pH region of lower buffer capacity an error of $\pm$ 0,3 pH units would have negligible effect on the calculated Acidity value whereas in the lower pH region, also with low buffer, an error of $\pm$ 0,3 pH units would have very significant effect on the calculated Acidity value. This type of trend is not observed with the troublesome experimental data and hence it is unlikely that sluggish pH response causes the observed Acidity increase trend on these particular experiments. This matter requires further investigation.

REFERENCES

Craig R.F. (1992) *Soil Mechanics 5th ed.*. Chapman & Hall, London.

Gerald C.F. & Wheatley P.O. (1984) *Applied numerical Analysis 3rd ed.*. Addison-Wesley, Reading Mass..

Hahn B.D. (1989) *Problem solving with True Basic 2nd ed.*. Juta & Co., Cape Town.

Levenspiel O. (1972) *Chemical reaction engineering 2nd ed.*. Wiley, New York.

Loewenthal R.E., Wiechers H.N.S. & Marais G.v.R. (1986) *Softening and Stabilization of Municipal Waters.* Water Research Commission, Pretoria.

Loewenthal R.E., Ekama G.A. & Marais G.v.R. (1989) Mixed weak acid/base systems Part 1 - Mixture characterisation. *Water S.A.* vol. 15, No. 1, pp 3-24.

Mills R.D.W.B. (1984) Stabilization of Calcium Carbonate deficient waters. *MSc thesis* U.C.T., Cape Town.

Plummer L. N., Parkhurst D. L. & Wigley T. M. L. (1979) Critical Review of the Kinetics of Calcite Dissolution and Precipitation. in Jenne E.A., *Chemical Modelling in Aqueous Systems: Am. Chem. Soc. Symposium Ser.* pp 537 - 573.

Sjöberg E. L. (1976) A fundamental equation for calcite dissolution kinetics. *Geochimica et Cosmochimica Acta* vol. 40, pp 441-447.

Sjöberg E. L. & Rickard D. T. (1984) Calcite Dissolution Kinetics: Surface speciation and the origin of the variable pH dependence. *Chemical Geology.* vol. 42, pp 119 - 136.

Standard Methods for Examination of Water and Wastewater, (1985), 16th ed., Publ. American Public Health Ass., American Water Works Ass., Water Pollution Control Federation, Washington.

Stumm W. & Morgan J.J. (1981) *Aquatic Chemistry 2nd ed.* Wiley, New York.

CHAPTER 5

GENERAL CONCLUSIONS AND RECOMMENDATIONS

This investigation deals with modelling of limestone granule dissolution in upflow reactors. It was established that the dissolution process is diffusion controlled and the following general equation models the rate:

$$\frac{d[Ca^{2+}]}{dt} = k_1 S f_d \left\{ k'^{\frac{1}{2}}_{spc} - [Ca^{2+}]^{\frac{1}{2}} [CO_3^{2-}]^{\frac{1}{2}} \right\} + k_2 S [H^+] + k_3 S [H_2CO_3^*] \quad (5:1)$$

where k_1, k_2, k_3 = rate constants
S = surface area

The first term of the equation is dominant in natural terrestrial soft water environments (in the range $5 \leq pH \leq 9$). The second and third terms of the equation represent dissolution phenomena dominated by high proton (low pH, $pH \leq 4$) and carbonic acid concentration ($pCO_2 \geq 0,1$ atmospheres) respectively.

Each of the rate constants depend on a number of factors including the physico-chemico characteristics of the mineral, flow characteristics, temperature and ionic strength. The physico-chemico characteristics of the mineral vary according to the geological history of the limestone deposit, hence these rate constants must be determined for a particular limestone (calcium carbonate) deposit. To this end the procedures described in Chapter 4 should be followed.

The model was applied to the dissolution of limestone from the Bredasdorp deposit in the soft waters representative of those found in the Western Cape. The last two terms of the model above, do not play a significant role in the dissolution of limestone in the natural waters relevant to this study, and were therefore not investigated further. The first term in the above rate equation thus became the focus of this study. For practical purposes, the surface area, S, and rate constant, k_1, were combined to form a compound rate constant, $k_{DC\ compound}$, which was found to vary with mixing energy (ie. hydrological conditions) for a specific granule size - an observation consistent with the diffusion controlled model. Thus the equation investigated is

$$\frac{d[Ca^{2+}]}{dt} = k_{D.C.\ compound}\ f_d \left\{ k'^{\frac{1}{2}}_{spc} - [Ca^{2+}]^{\frac{1}{2}} [CO_3^{2-}]^{\frac{1}{2}} \right\} \qquad (5:2)$$

where $k_{D.C.\ compound}$ = compound rate constant for a diffusion controlled reaction, which varies with temperature, ionic strength, physico-chemico properties of the mineral and hydraulic characteristics (flow rate) and includes a surface area term.

Limestone from the Bredasdorp deposit is friable and porous. The porosity influences the flow characteristics through the reactor. The velocity at which a plug of water progresses through the reactor was found to decrease with increase in the granule surface area per unit volume of reactor (ie. decrease in mean nominal granule size). Tracer tests were used to establish the actual residence time of a plug of water in the reactor. With this information it was possible then to measure the rate of $CaCO_3$ dissolution and hence determine the rate constant in the laboratory.

The dependence of the compound rate constant (for Bredasdorp limestone) on granule size and hydraulic conditions was investigated, and leads to the following empirical relationship,

$$K_{D.C.compound} = 0{,}0021 \frac{LR}{\Phi} + 0{,}0044 \qquad (5:3)$$

where ϕ = nominal mean granule size (mm)
in the range $3{,}55mm \leq \phi \leq 8{,}05mm$
LR = loading rate (m/hr)

A limited number of tests using rain water and Table Mountain water (ie. containing dissolved organic carbon), showed that use of the results obtained from the acidified tap water was justified when considering the soft waters of the Western Cape. Long term effects of humic substances, such as precipitation of humics and consequential armouring effects, were not investigated. However, long term tests ($\pm$ 100 days) conducted at the University of Cape Town into the dissolution of concrete pipes in humic waters, showed no armouring effects (Mackintosh 1990).

Practical application of the work reported here is limited because in practice a reactor will contain particles of varying size and these will change with time. In all probability, a grading will occur from small to large size up the reactor. However, design using the findings here for the rate constant based on size of granules added to the reactor will yield

a conservative result. That is reactions in practice may be expected to occur faster than those based on "startup" granule size. With regard to design, the algorithm developed here forms a useful tool for determining effluent quality given initial water characteristics, loading rate and hydraulic retention time.

In a number of experiments the calculated Acidity value increased with flow through the granule bed. This is contrary to what is to be expected from basic theory. the reason for this anomaly is at present still elusive.

With regard to future research, this investigation identifies a number of needs. These include,

i) Quantifying the kinetic behaviour of the other two terms.
ii) investigating the possibility for addition of mineral acid and/or CO_2 and blending to obtain a system dealing with smaller volumes.
iii) the long term effects of humic substances on dissolution rates need to be investigated.
iv) reasons for the sporadic observed increase in calculated Acidity through the reactor need to be explained.

REFERENCES

Mackintosh G.S. (1990) Aggressive water attack on carbonated cement materials. *MSc thesis* U.C.T., Cape Town.

APPENDIX A

THERMODYNAMIC EQUILIBRIUM CONSTANTS

Values for the weak acid dissociation constants and the calcium carbonate solubility product can be obtained from Table A:1 below.

TABLE A:1
WEAK ACID DISSOCIATION CONSTANTS AND CALCIUM CARBONATE SOLUBILITY PRODUCT AND THEIR TEMPERATURE DEPENDENCY.
$pK = (A/T) - B + C.T$ WHERE T IS IN °KELVIN. (TRUESDELL and JONES, 1973)

		pK 25°C	A	B	C
Water	pK_W	14,000			
Carbonate	pK_{c1}	6,352	3404,7	14,8435	0,03279
	pK_{c2}	10,330	2902,4	6,4980	0,02379
Henry's constant	pK_H	1,47	-1760,0	- 9,619	-0,00753
Calcium Carbonate	pK_{spc}	8,367	-698,61	-10,710	

The relationship between the thermodynamic equilibrium constants, k_x, and the dissociation constants, pK_x, is expressed as

$$10^{-pK_x} = k_x \qquad \textbf{(A:1)}$$

Note: pK_{spc} also incorporates ion pairing effects between Ca^{2+} and CO_3^{2-}.

APPENDIX B

EXPERIMENTAL APPARATUS

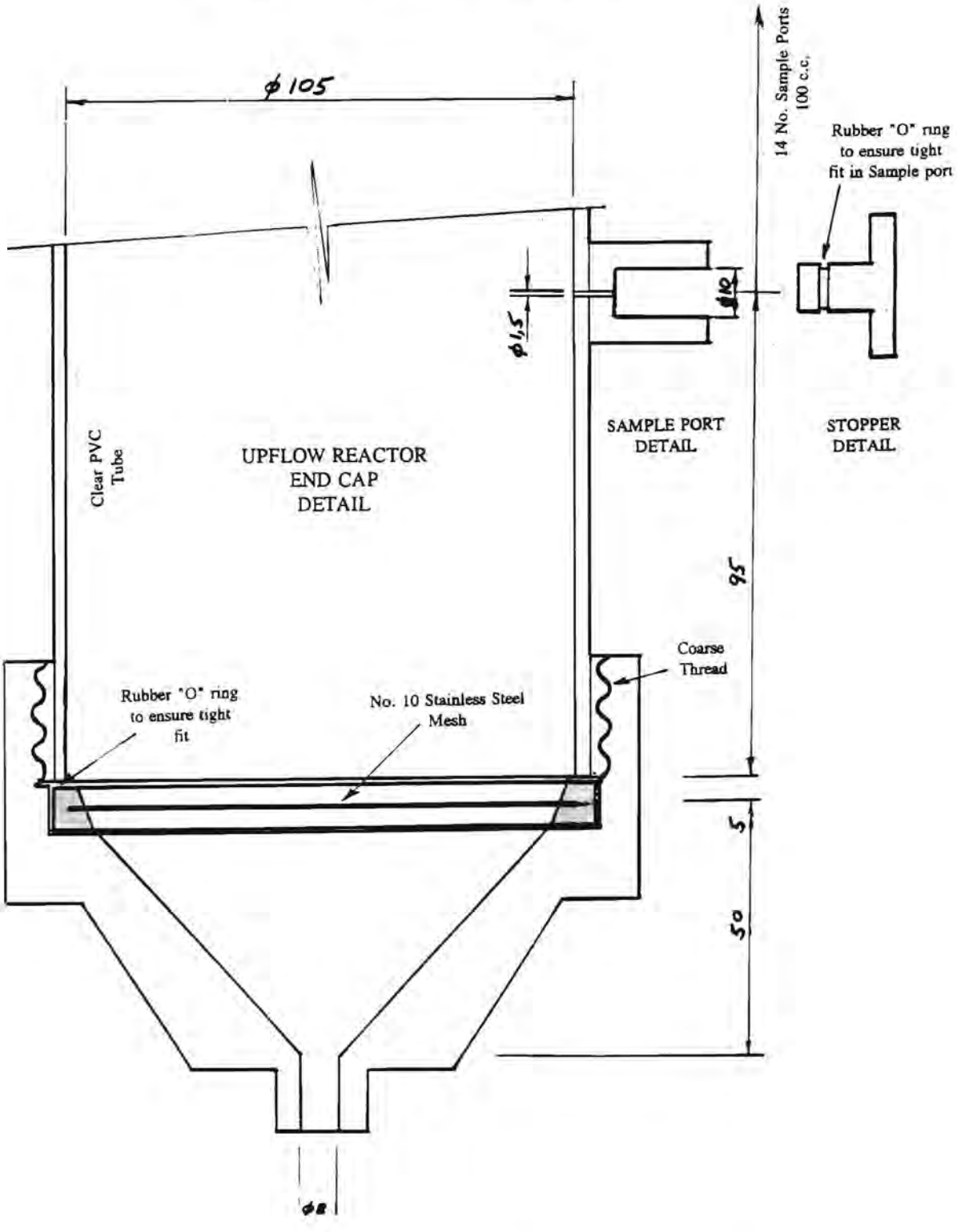

Figure B:1: Upflow reactor **END CAP DETAIL** 2off required (Upper and Lower)

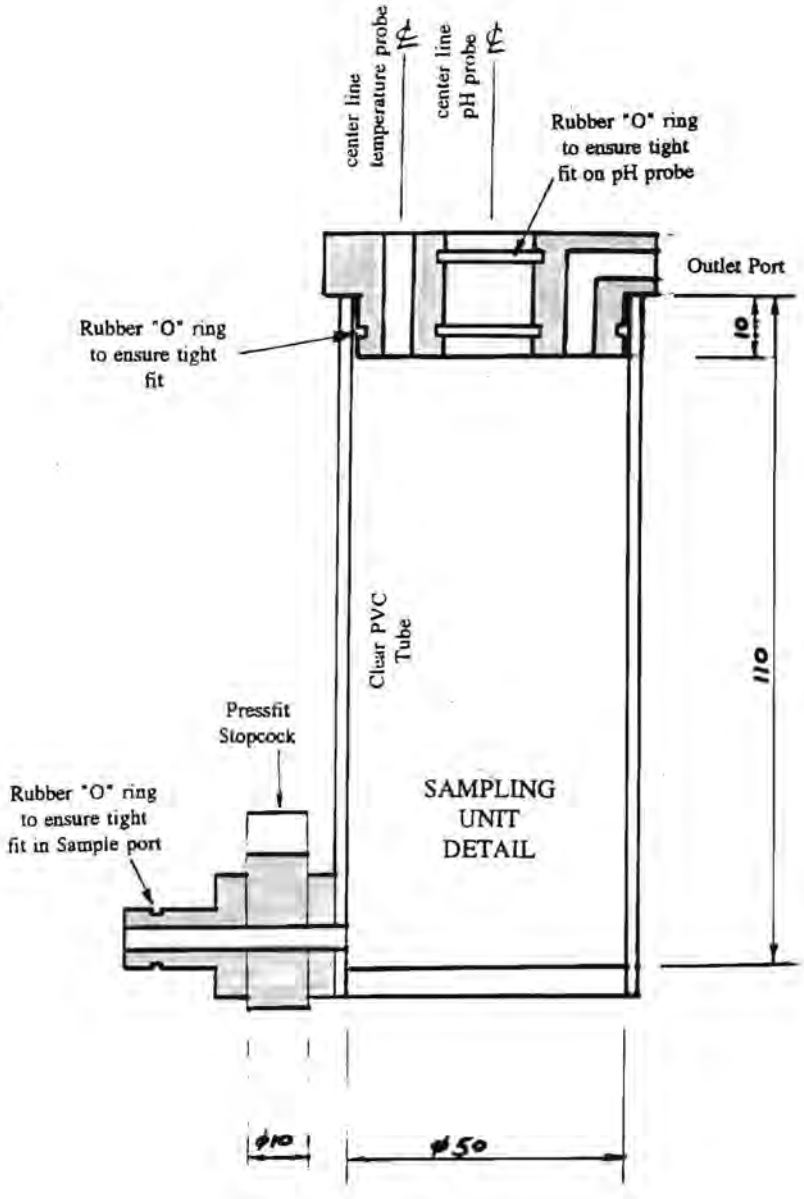

Figure B:2: SAMPLING UNIT DETAIL

APPENDIX C

FLOW METER CALIBRATION CURVES

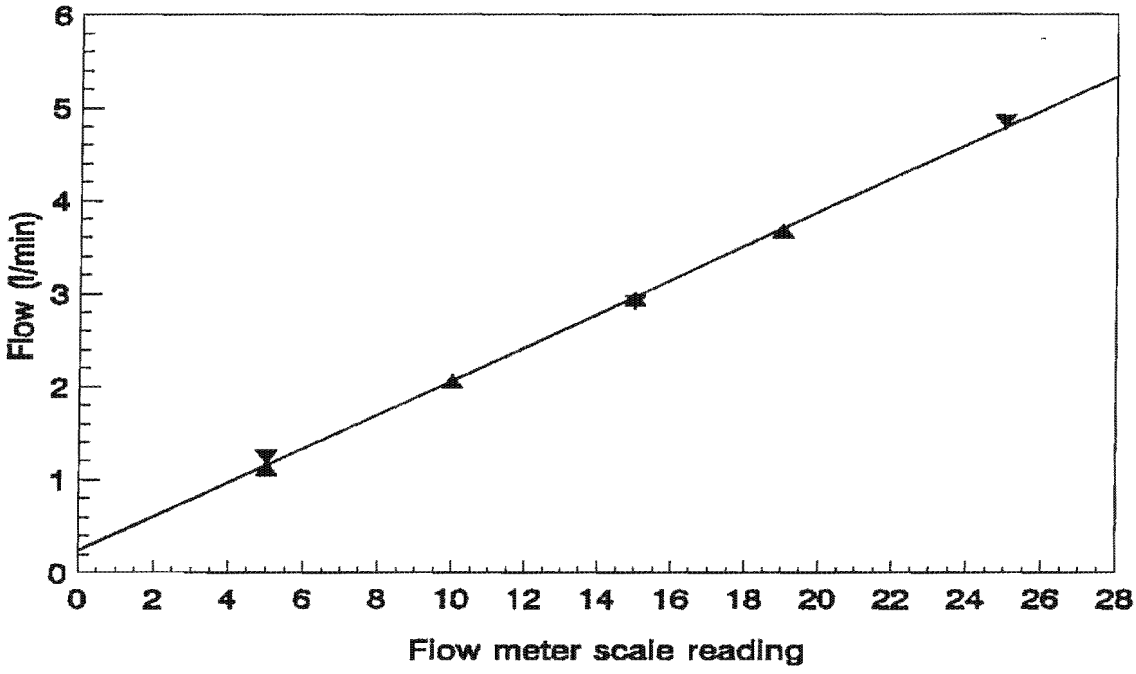

Figure C:1: Calibration curve for the Rotameter 14G flow meter.

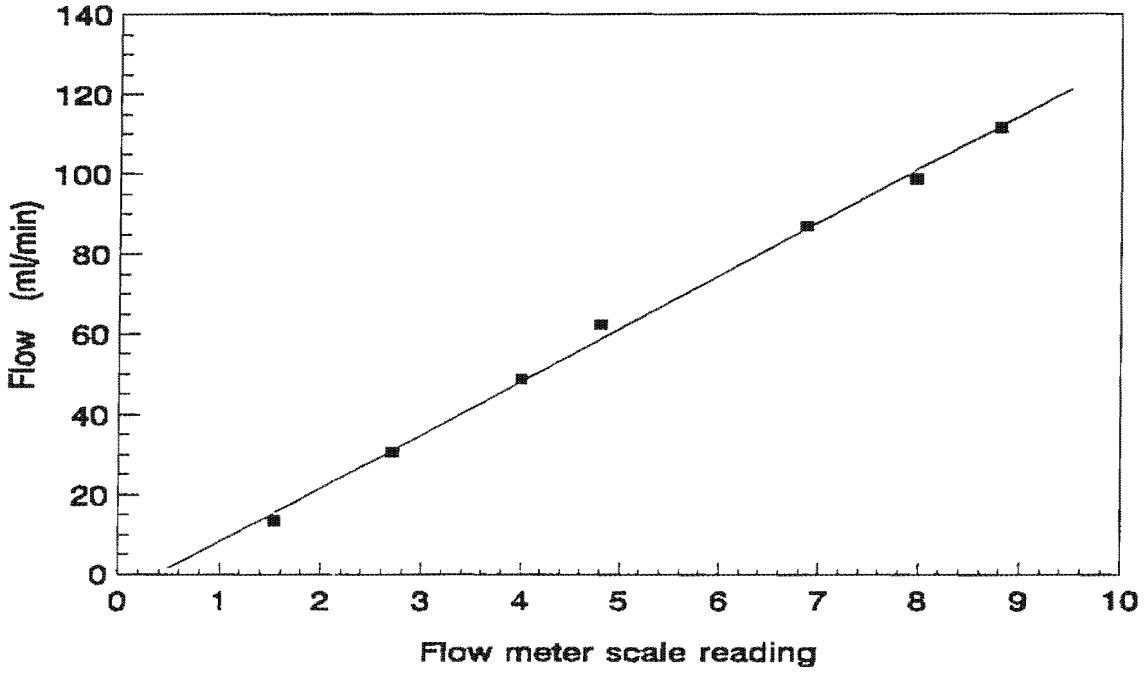

Figure C:2: Calibration curve for the Rotameter MFG 2-D-150 flow meter.

APPENDIX D

TRACER TESTS

TRACER INVESTIGATION TO DETERMINE THE AVERAGE CONTACT TIMES

This Appendix contains the data of the tracer experiments conducted on the Bredasdorp limestone (see Chapter 4). The results of the tracer experiments for 1,43mm, 3.55mm, 5.7mm and 8,05mm granule sizes are shown in Figures D:1, D:4, D:7 and D:10 respectively. Each Figure contains three separate graphs, one for each of three different flow rates investigated. Each graph shows *conductivity versus time* plots depicting tracer injected at various ports (generally ports 1, 4, 7, and 10). The moment of injection of tracer was plotted at Time = 0 in all cases.

A Personal Computer was used to capture the conductivity data with time. This data was processed by means of a spreadsheet to determine the centroid of the *Conductivity versus time* plot. The time interval between the moment of tracer injection and the centroid was taken to be the average fluid residence time between the injection port and the conductivity probe in the reactor. The standard deviation and the Vessel Dispersion Number (VDN), (Levenspiel 1972) was also calculated. The formulae used to calculate these three quantities are given below.

Time to centroid of conductivity trace, $\tilde{t}$:

$$\tilde{t} \cong \frac{\Sigma\ t_i\ C_i\ \Delta t_i}{\Sigma\ C_i\ \Delta t_i} \qquad \textbf{(D:1)}$$

where C_i = i th conductivity reading
t_i = time to i th reading
Δt = time interval between conductivity readings.

Standard deviation, σ:

$$\sigma^2 \cong \frac{\Sigma\ t_i^2\ C_i\ \Delta t_i}{\Sigma\ C_i\ \Delta t_i} - \tilde{t}^{-2} \qquad \textbf{(D:2)}$$

and the *Vessel Dispersion Number, VDN,* $\left(\frac{D}{u\,L}\right)$ was calculated from:

$$\sigma_\theta^2 = \frac{\sigma^2}{t^{-2}} = 2\frac{D}{uL} - 2\left(\frac{D}{uL}\right)^2 \times (1 - e^{-uL/D}) \qquad \textbf{(D:4)}$$

The distance between the port where the tracer was injected and conductivity probe is plotted against time (as measured to centroid of conductivity plot as discussed above). The *distance versus average time to centroid of trace* graph (shown in Figures D:2, D:5, D:8 and D:11), for each of the flow rates investigated, was linear. The slope representing the plug velocity at each particular flow rate.

Velocity versus flow rate is plotted in Figures D:3, D:6, D:9 and D:12 for each granule size respectively and is linear. Thus the velocity of flow through the reactor at any particular flow rate can be directly determined from the graph for a particular granule size. The inverse of velocity represents the time taken for a plug of fluid to pass through a meter length of reactor.

From Eq. 4:3 it can be seen that the slope of the *velocity versus flow rate* graph is proportional to some form of porosity. This porosity is not equivalent to that determined by the oven-drying procedure described in Chapter 4, but rather reflects the proportion of voids available to the fluid flow path at a particular flow rate and is called the apparent porosity.

Flow rate through reactor 3,0 ℓ/min

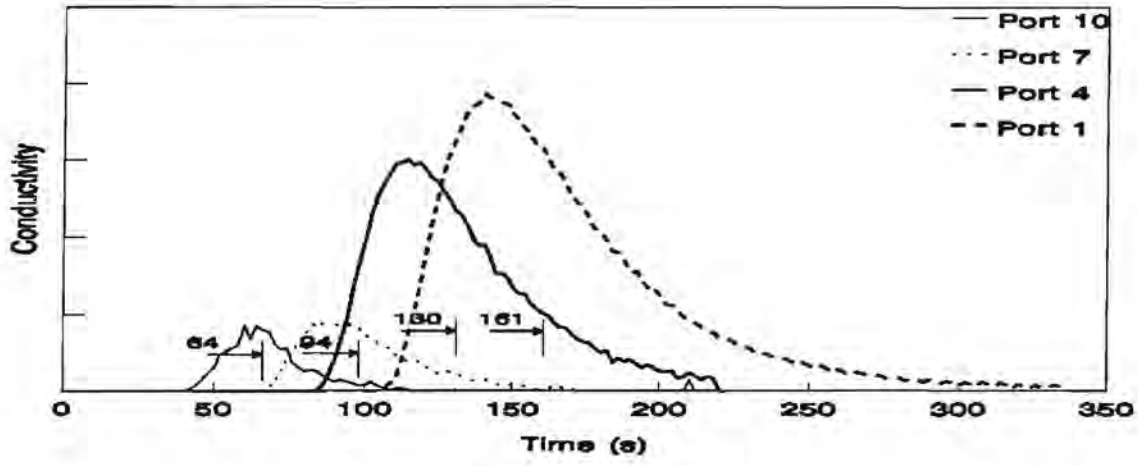

Flow rate through reactor 4,0 ℓ/min

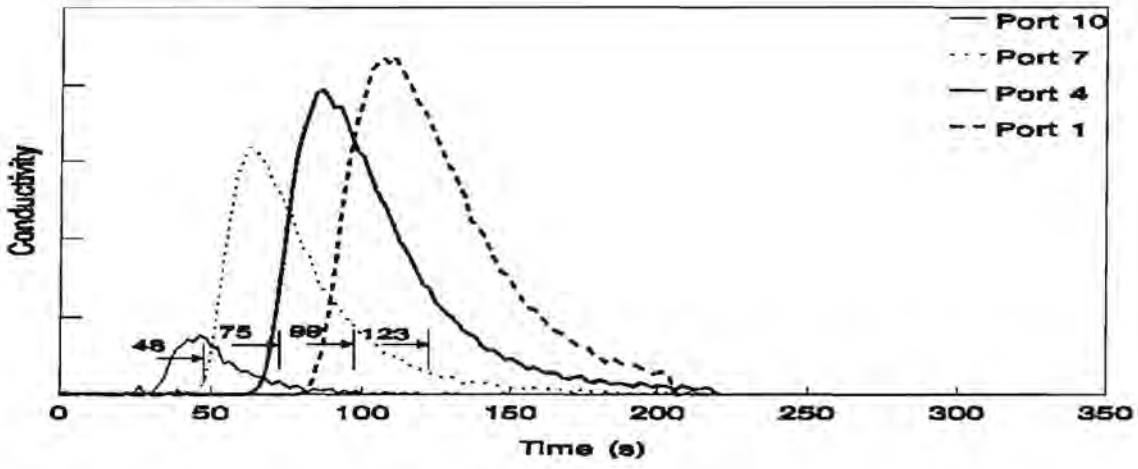

Flow rate through reactor 4,9 ℓ/min

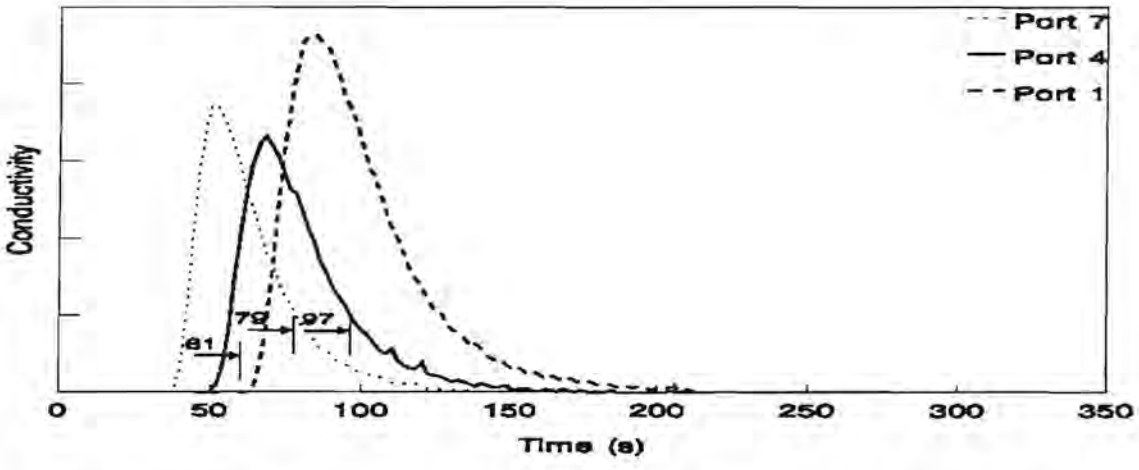

Figure D:1: *Conductivity versus Time* plots for **reactor containing 1,43mm granules.** Showing conductivity response due to KCl tracer injected at various ports, at various flow rates.

The time to the centroid of the KCl trace, its standard deviation and the dispersion coefficient for each trace measurement for the **1,43mm Bredasdorp limestone granules.**

Flow Rate (ℓ/min)	Trace injection at:	time (s)	σ (s)	D/uL
3,0	port 10	64	9,2	0,0102
	port 7	94	13,1	0,0096
	port 4	129	24,1	0,0173
	port 1	160	29,3	0,0166
4,0	port 10	48	8,5	0,0158
	port 7	75	16,4	0,0240
	port 4	99	19,2	0,0189
	port 1	123	23,7	0,0185
4,9	port 10			
	port 7	61	14,1	0,0264
	port 4	79	16,3	0,0214
	port 1	97	20,1	0,0213

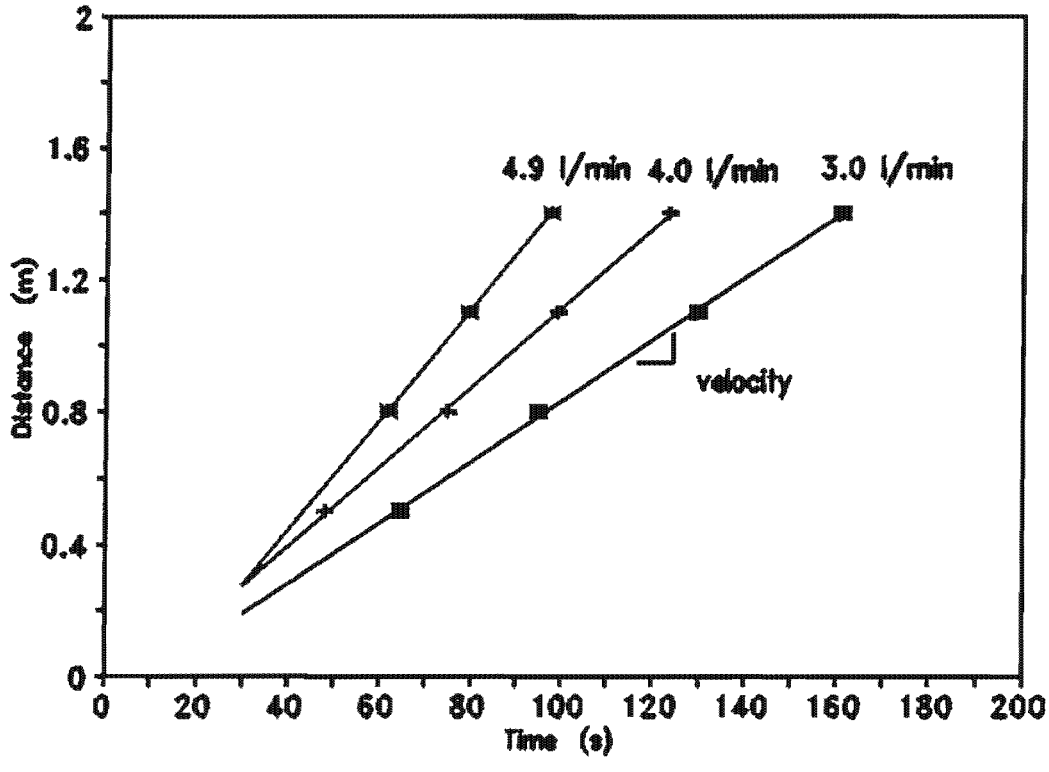

Figure D:2: *Distance versus average time to centroid of trace* graph for **1,43mm Bredasdorp limestone granules**, with best fit line.

Regression analyses to determine the average plug velocities through the reactor, using the average times (based on the centroid of the trace), and the various flow rates.

Flow rate (ℓ/min)	velocity (m/s)	time per unit length of reactor (s)	Regression coefficient
3,0	0,00923	108,70	0,9992
4,0	0,01196	84,03	0,9994
4,9	0,01667	60,24	0,9999

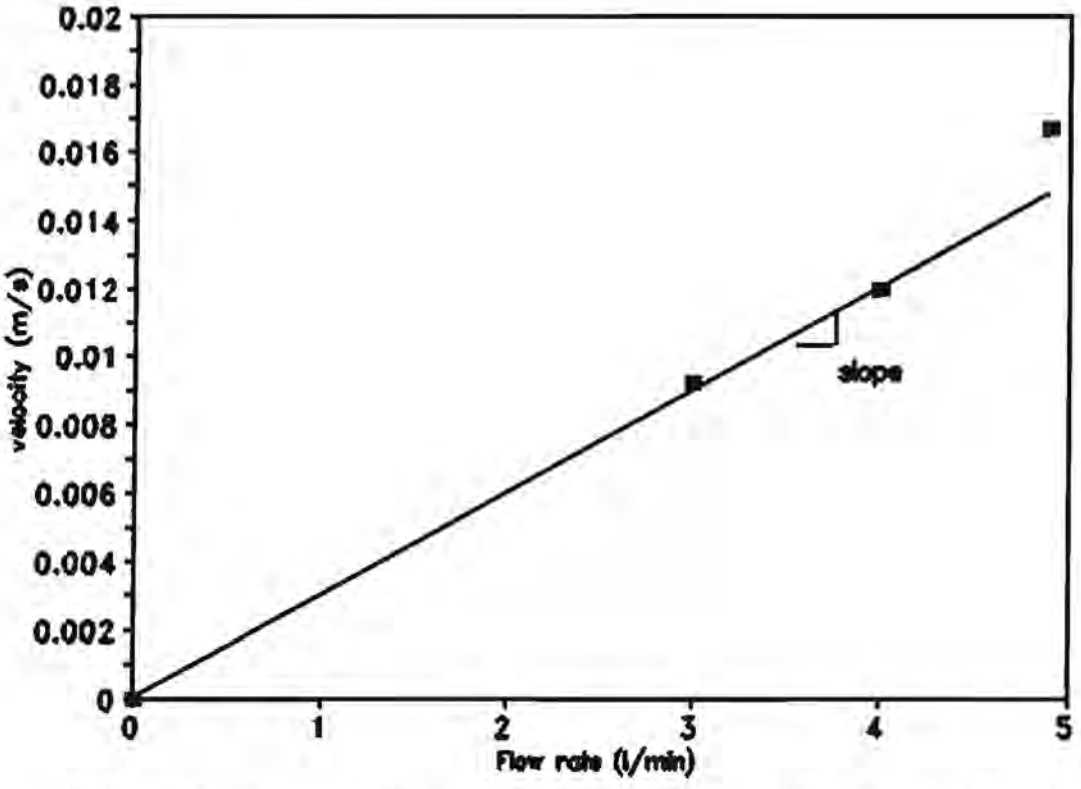

Figure D:3: *Velocity versus Flow rate* graph for **1,43mm Bredasdorp limestone granules**, with best fit line.

Regression analysis to determine the slope of the *velocity of plug versus flow rate* plot.

Regression coefficient	:	0,9995
Slope	:	0,00301 ($m.s^{-1}/\ell.min^{-1}$)
Apparent porosity	:	0,639

Flow rate through reactor 3,0 ℓ/min

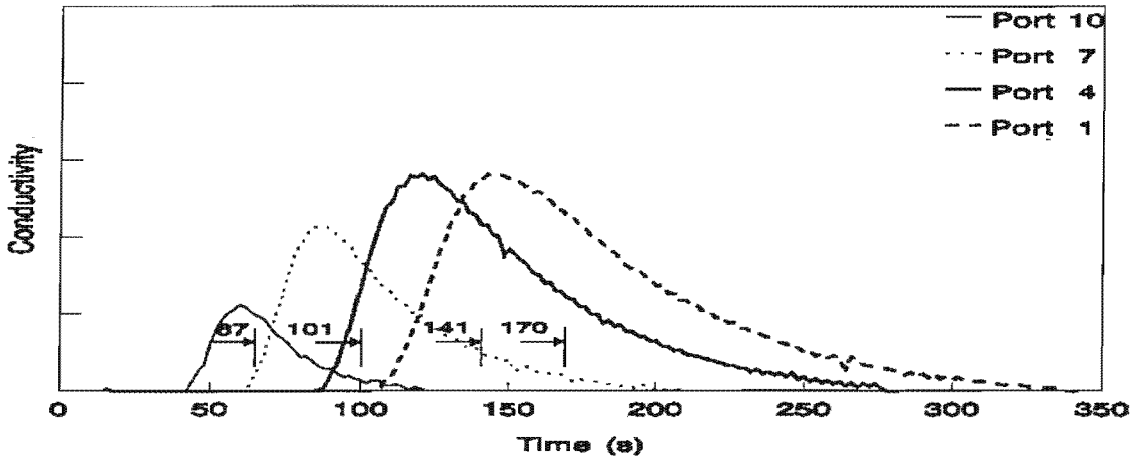

Flow rate through reactor 4,0 ℓ/min

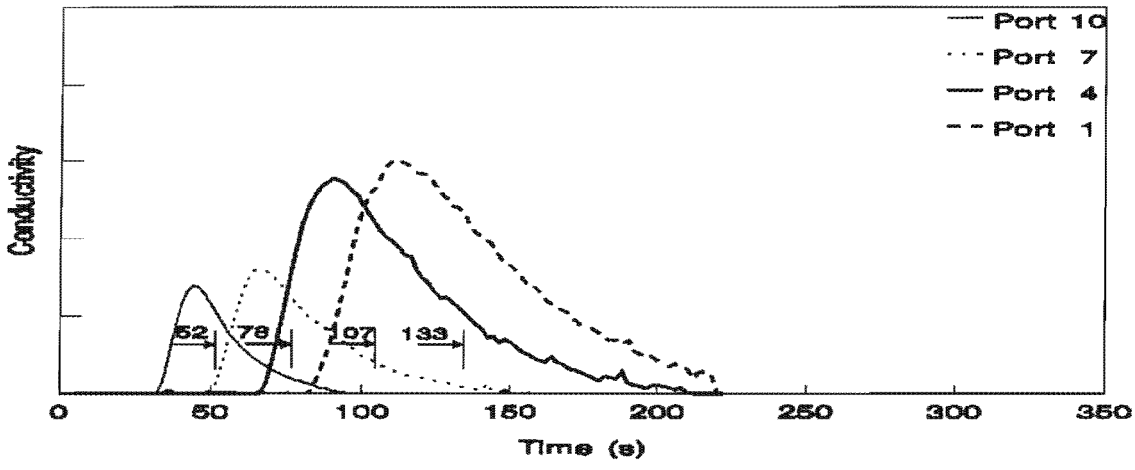

Flow rate through reactor 4,9 ℓ/min

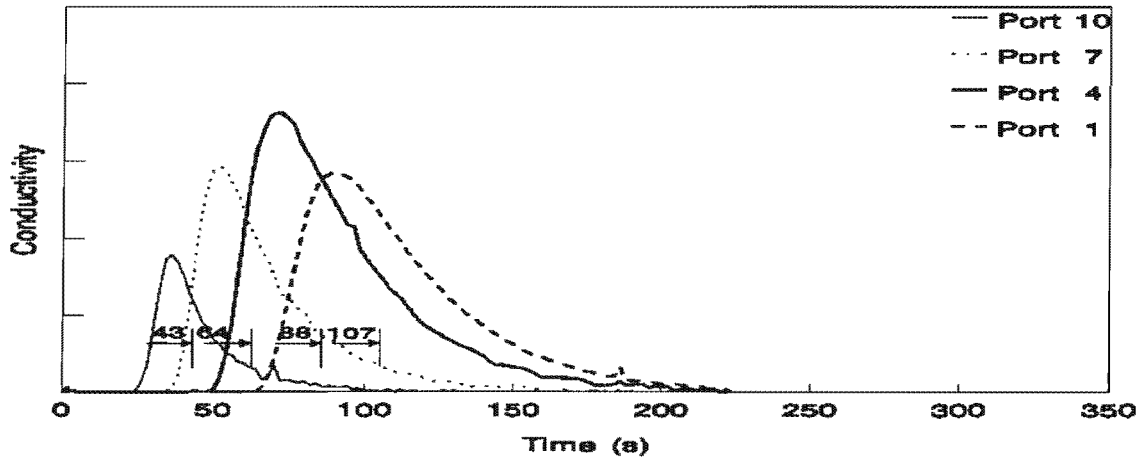

Figure D:4: *Conductivity versus Time* plots for **reactor containing 3,55mm granules.** Showing conductivity response due to KCl tracer injected at various ports, at various flow rates.

The time to the centroid of the KCl trace, its standard deviation and the dispersion coefficient for each trace measurement for the **3,55mm Bredasdorp limestone granules.**

Flow Rate (ℓ/min)	Trace injection at:	time (s)	σ (s)	D/uL
3,0	port 10	67	12,8	0,0184
	port 7	101	21,8	0,0231
	port 4	141	29,6	0,0221
	port 1	170	33,8	0,0198
4,0	port 10	52	10,9	0,0225
	port 7	78	15,8	0,0205
	port 4	107	22,9	0,0231
	port 1	133	28,5	0,0229
4,9	port 10	43	10,5	0,0300
	port 7	64	16,7	0,0342
	port 4	88	24,5	0,0327
	port 1	107	23,6	0,0243

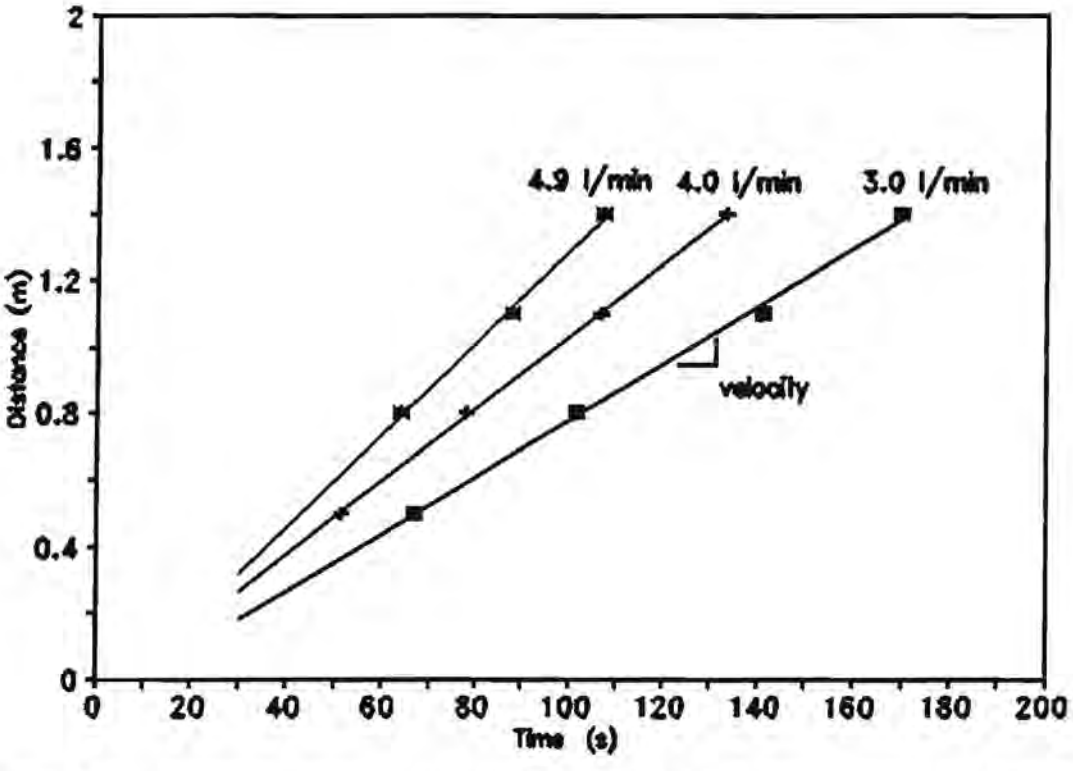

Figure D:5: *Distance versus average time to centroid of trace* graph, for **3,55mm Bredasdorp limestone granules,** with best fit lines.

Regression analyses to determine the average plug velocities through the reactor, using the average times (based on the centroid of the plug trace), and the various flow rates.

Flow rate (ℓ/min)	velocity (m/s)	time per unit length of reactor (s)	Regression coefficient
3,0	0,00859	117,65	0,9970
4,0	0,01095	91,74	0,9997
4,9	0,01384	72,46	0,9985

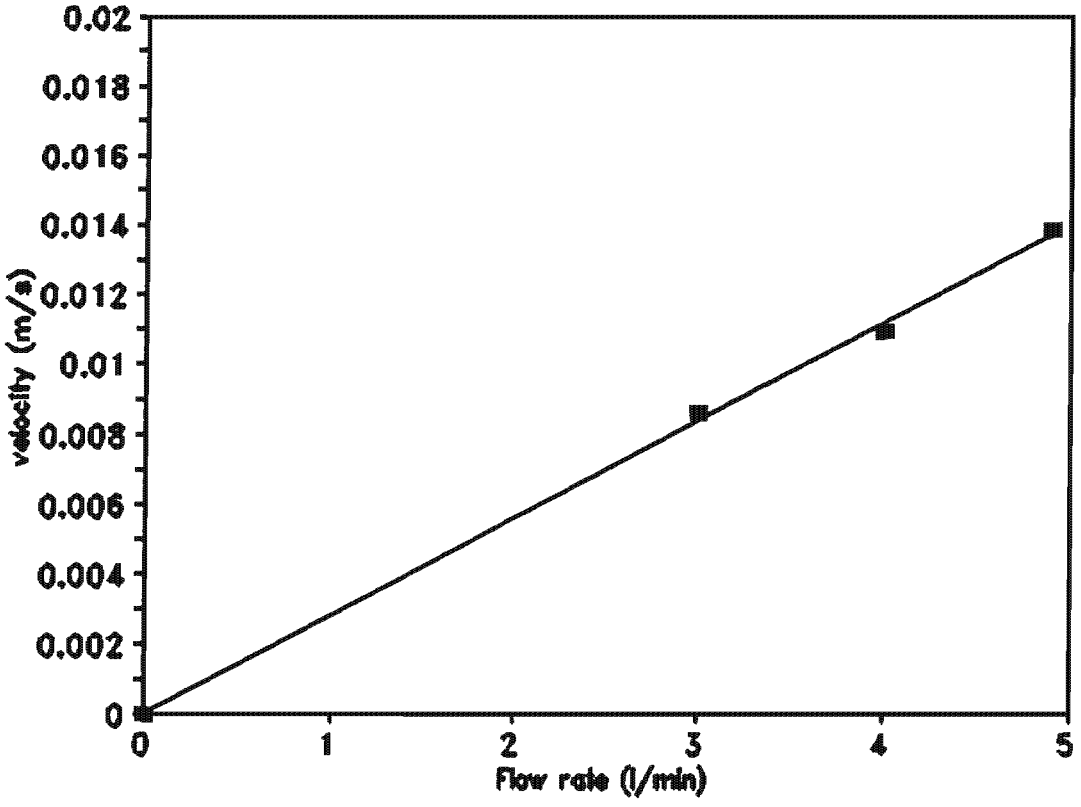

Figure D:6: *Velocity versus Flow rate* graph for **3,55mm Bredasdorp limestone granules**, with best fit line.

Regression analysis to determine the slope of the *velocity versus flow rate* graph.

Regression coefficient	:	0,9989
Slope	:	0,00280 ($m.s^{-1}/\ell.min^{-1}$)
Apparent porosity	:	0,688

Flow rate through reactor 2,9 ℓ/min

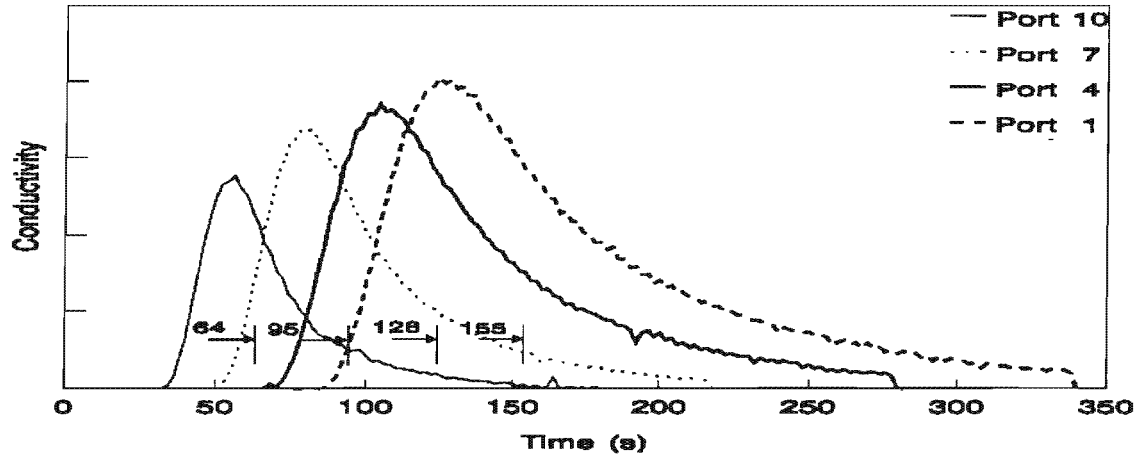

Flow rate through reactor 3,9 ℓ/min

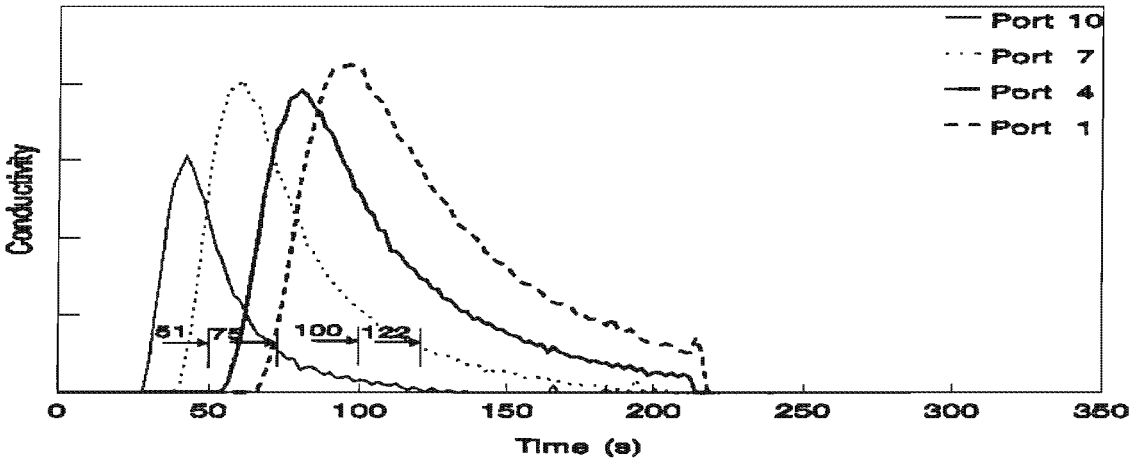

Flow rate through reactor 4,8 ℓ/min

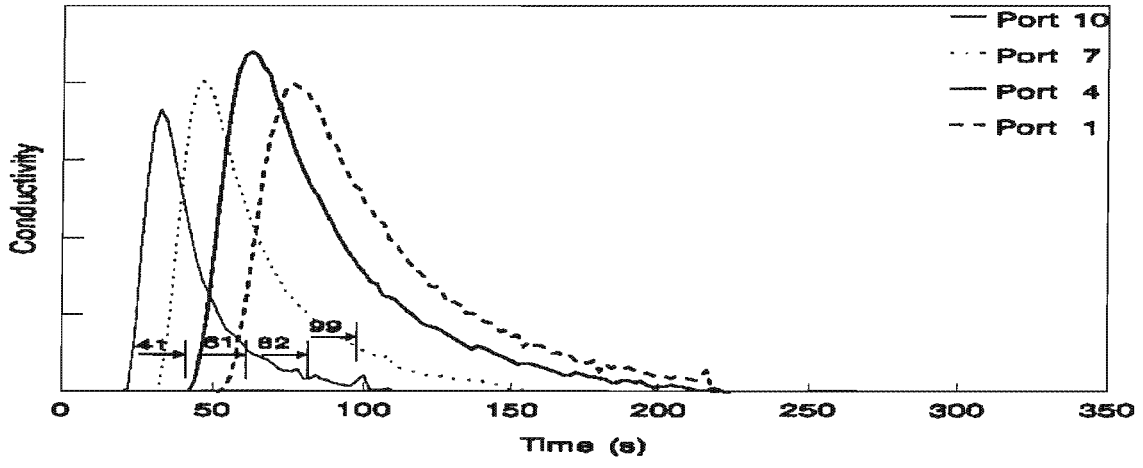

Figure D:7: *Conductivity versus Time* plots for **reactor containing 5,7mm granules.** Showing conductivity response due to KCl tracer injected at various ports, at various flow rates.

The time to the centroid of the KCl trace, its standard deviation and the dispersion coefficient for each trace measurement for the **5,7mm Bredasdorp limestone granules.**

Flow Rate (ℓ/min)	Trace injection at:	time (s)	σ (s)	D/uL
3,0	port 10	64	16,1	0,0321
	port 7	95	24,5	0,0332
	port 4	128	32,2	0,0319
	port 1	155	38,5	0,0309
4,0	port 10	51	14,0	0,0382
	port 7	75	22,1	0,0437
	port 4	100	27,7	0,0380
	port 1	122	34,1	0,0393
4,9	port 10	41	12,5	0,0469
	port 7	61	19,3	0,0503
	port 4	82	24,9	0,0465
	port 1	99	28,4	0,0411

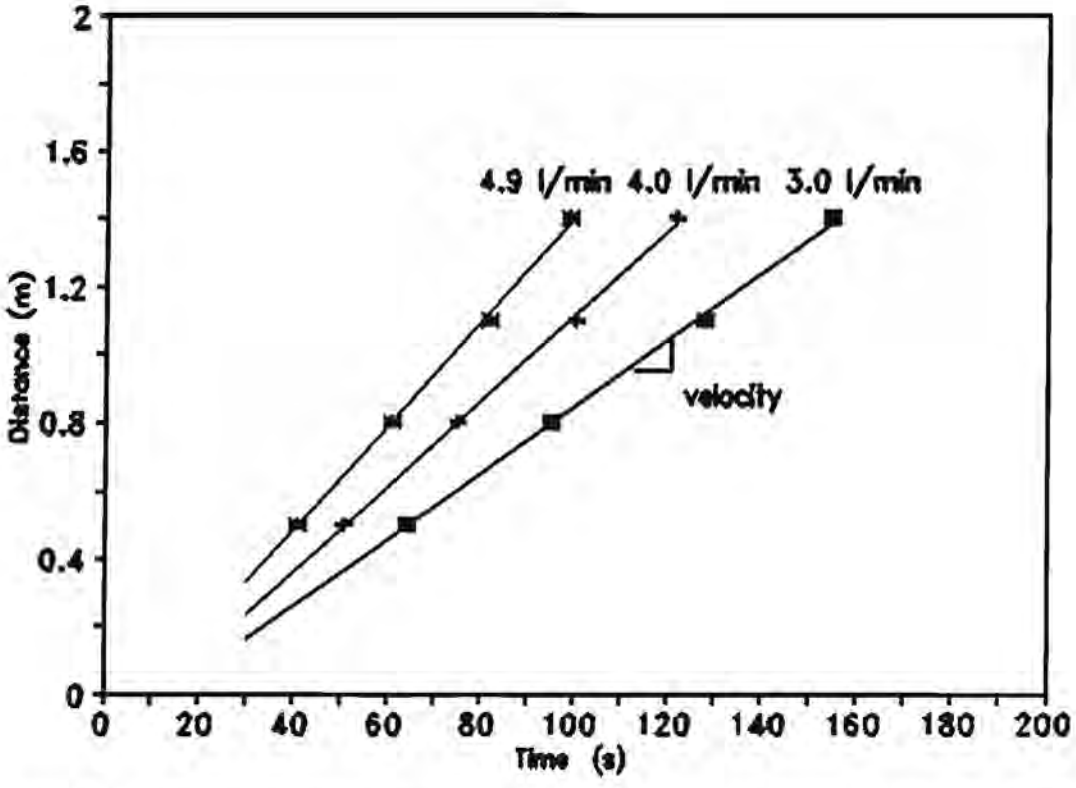

Figure D:8: *Distance versus average time to centroid of trace* graph, for **5,7mm Bredasdorp limestone granules**, with best fit lines.

Regression analyses to determine the average plug velocities through the reactor, using the average times (based on the centroid of the trace), and the various flow rates.

Flow rate (ℓ/min)	velocity (m/s)	time per unit length of reactor (s)	Regression coefficient
3,0	0,00980	102,04	0,9986
4,0	0,01253	80,00	0,9987
4,9	0,01531	65,36	0,9984

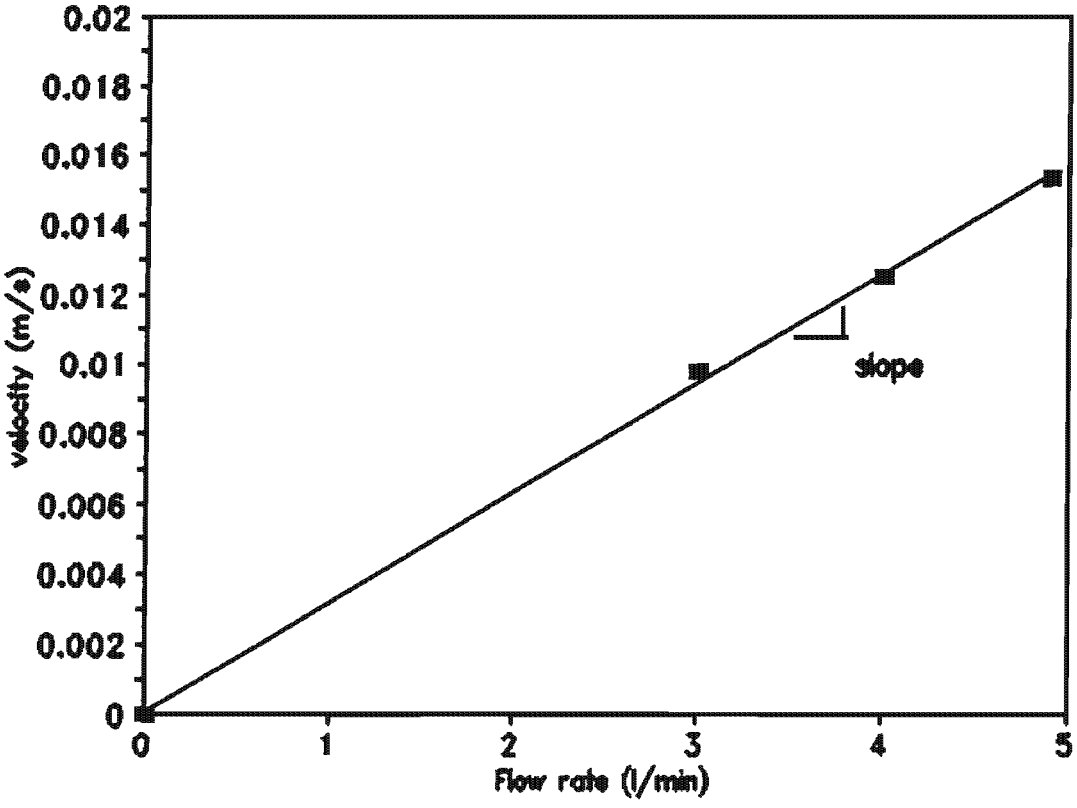

Figure D:9: *Velocity versus Flow rate* graph for **5,7mm Bredasdorp limestone granules**, with best fit line.

Regression analysis to determine the slope of the *velocity versus flow rate* graph.

Regression coefficient : 0,9990
Slope : 0,00313 ($m.s^{-1}/\ell.min^{-1}$)
Apparent porosity : 0,615

Flow rate through reactor 2,9 ℓ/min

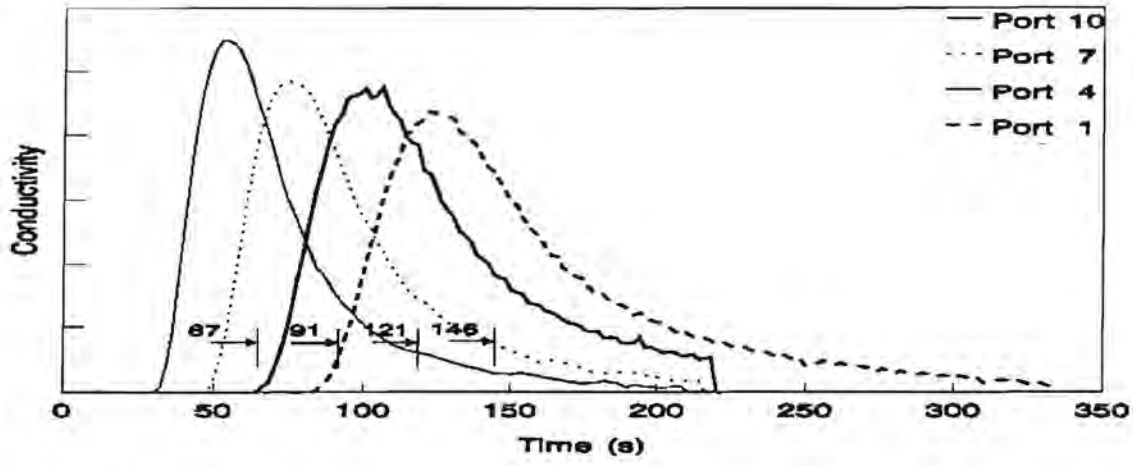

Flow rate through reactor 3,9 ℓ/min

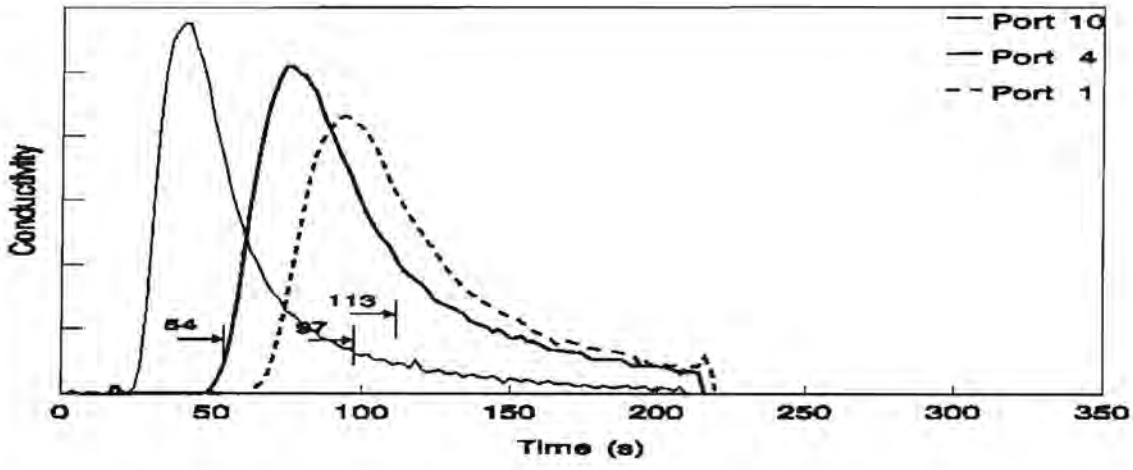

Flow rate through reactor 4,8 ℓ/min

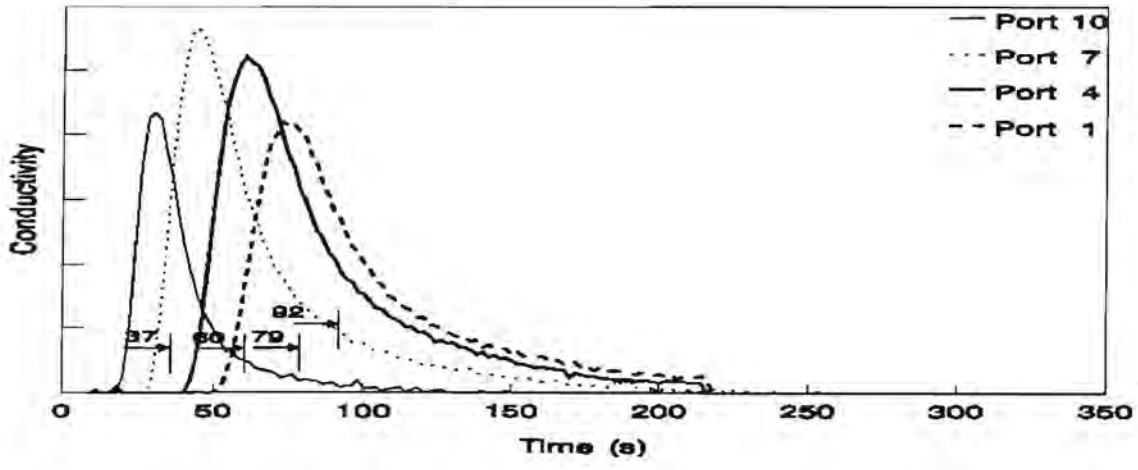

Figure D:10: *Conductivity versus Time* plots for **reactor containing 8,05mm granules.** Showing conductivity response due to KCl tracer injected at various ports, at various flow rates.

The time to the centroid of the KCl trace, its standard deviation and the dispersion coefficient for each trace measurement for the **8,05mm Bredasdorp limestone granules.**

Flow Rate (ℓ/min)	Trace injection at:	time (s)	σ (s)	D/uL
3,0	port 10	67	21,6	0,0518
	port 7	91	25,2	0,0385
	port 4	121	31,6	0,0343
	port 1	146	34,1	0,0273
4,0	port 10	54	20,1	0,0700
	port 7			
	port 4	97	28,7	0,0442
	port 1	113	28,7	0,0321
4,9	port 10	37	12,0	0,0518
	port 7	60	21,8	0,0661
	port 4	79	25,2	0,0505
	port 1	92	25,2	0,0373

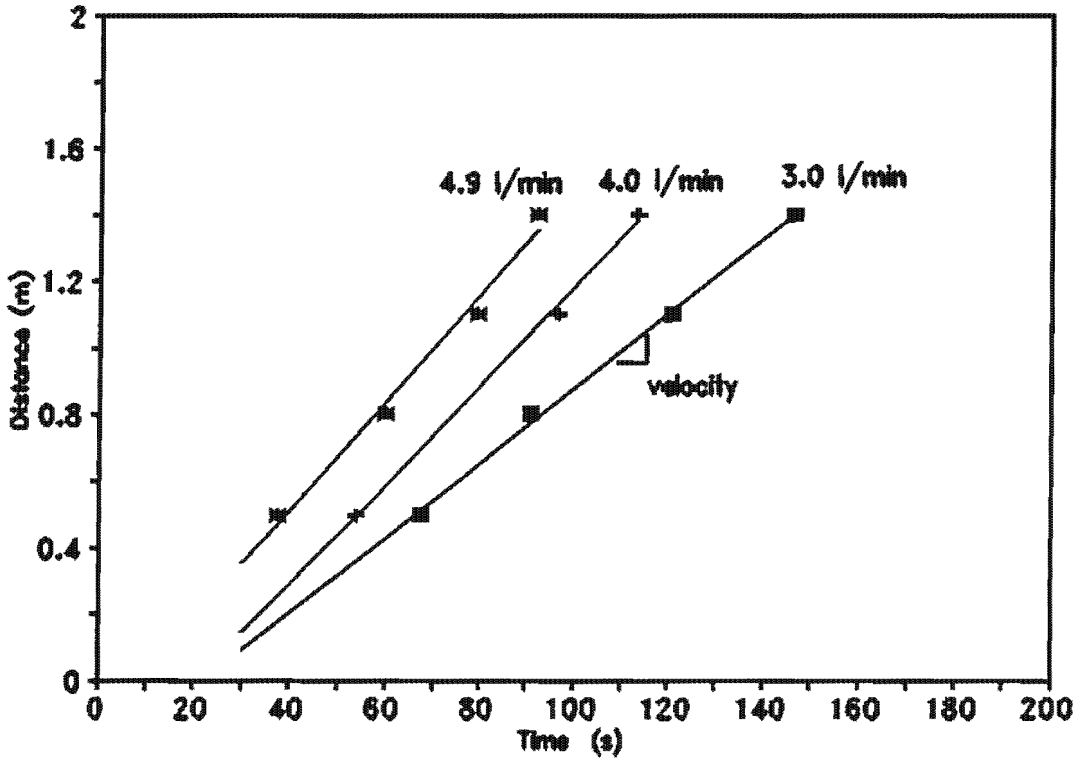

Figure D:11: *Distance versus average time to centroid of trace* graph, for **8,05mm Bredasdorp limestone granules**, with best fit lines.

Regression analyses to determine the average plug velocities through the reactor, using the average times (based on the centroid of the trace), and the various flow rates.

Flow rate (ℓ/min)	velocity (m/s)	time per unit length of reactor (s)	Regression coefficient
3,0	0,01125	89,29	0,9982
4,0	0,01486	67,57	0,9967
4,9	0,01608	62,50	0,9863

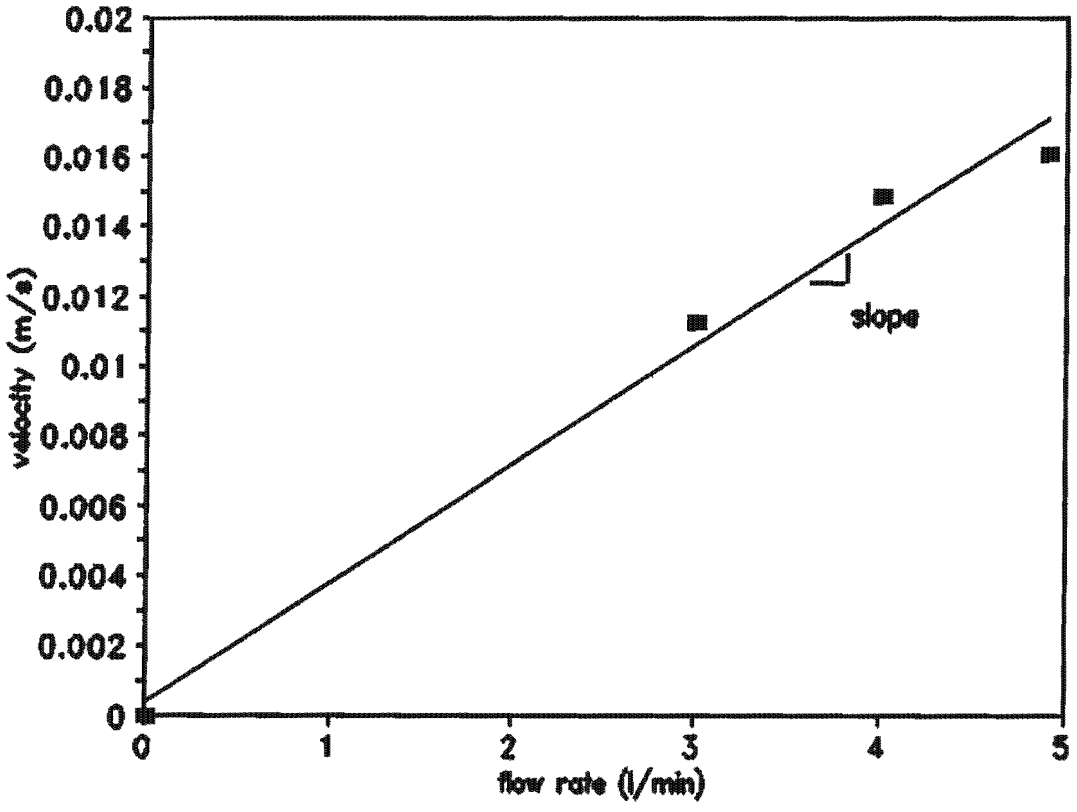

Figure D:12: *Velocity versus Flow rate* graph for **8,05mm Bredasdorp limestone granules**, with best fit line.

Regression analysis to determine the slope of the *velocity versus flow rate* graph.

Regression coefficient : 0,9859
Slope : 0,00342 ($m.s^{-1}/\ell.min^{-1}$)
Apparent porosity : 0,564

APPENDIX E

ALGORITHM USED TO DETERMINE $k_{compound}$

The algorithm used to determine the compound rate constant, $k_{compound}$, referred to in Chapter 4 is set out below.

Algorithm used to determine $k_{compound}$

Step 1: The average solution ionic strength is determined from the measured conductivity values at each port, using Eq. 2:9. Although the solution ionic strength increases with total dissolved solids, the solution ionic strength remains low throughout the experimental range. The variation in solution ionic strength does not cause any significant variability between the results obtained if using the average or the actual ionic strength at each port.

Step 2: Making use of the average solution ionic strength and the temperature at which the experiment was conducted, the mono- and divalent activity coefficients (f_m and f_d) are calculated using Eq. 2:5. Apparent equilibrium constants for the carbonate (k_{c1}' and k_{c2}') and water (k_w') systems are then calculated using Appendix A. Using the Truesdell and Jones formulation, Eq. 3:5, the apparent solubility product for calcium carbonate ($K'_{sp\ c}$) is calculated.

Step 3: The Acidity at each port is calculated from measured Alkalinity and pH values. It has been shown that the Acidity value of a plug of water remains unaltered as it passes through the reactor. In order to obtain the best estimate of the solution Acidity an average of the calculated Acidities is determined and this is used as the solution Acidity.

Step 4: The incremental step length, Δh, along the length of the reactor, at which the water quality parameters are to be calculated must be decided upon. This distance must be sufficiently small to ensure that the Runge-Kutta method returns predicted values at an acceptable level of accuracy. The time interval, Δt in which the plug of water passes through this Δh is calculated from

$$\Delta t = \frac{\Delta h}{\bar{v}} \qquad \text{(E:1)}$$

where v is obtained from Figure 4:2 for the appropriate granule size and flow rate.

Step 5: a) The port which is to be used as the starting point for the numerical prediction is identified. The pH at that port is determined from the average Acidity calculated over all the ports (Acidity must remain constant) and the Alkalinity measured at the port.
b) The $[CO_3^{2-}]$ at the initial port can be calculated from pH in (a) and the measured Alkalinity, using Eq. 4:10.

Step 6: An initial compound rate constant, $k_{compound}$, is assumed for use in the model.

Step 7: a) Calculate the Runge-Kutta factors given below, for the three simultaneous ordinary differential equations, Eq. 4:13, Eq. 4:14 and Eq. 4:15 at port n for the rate constant assumed in 6 above.

Runge-Kutta factors for the calcium rate equation

$$\begin{aligned}
kr_{1Ca} &= \Delta t\ f_1\ (t_{(n)}, [Ca^{2+}]_{(n)}, Alk_{(n)}, Acid_{(n)}, \text{constants}) \\
kr_{2Ca} &= \Delta t\ f_1\ (t_{(n)} + \frac{\Delta t}{2}, [Ca^{2+}]_{(n)} + \frac{kr_{1Ca}}{2}, Alk_{(n)} + \frac{kr_{1Alk}}{2}, Acid_{(n)} + \frac{kr_{1Acid}}{2}, \text{constants}) \\
kr_{3Ca} &= \Delta t\ f_1\ (t_{(n)} + \frac{\Delta t}{2}, [Ca^{2+}]_{(n)} + \frac{kr_{2Ca}}{2}, Alk_{(n)} + \frac{kr_{2Alk}}{2}, Acid_{(n)} + \frac{kr_{2Acid}}{2}, \text{constants}) \\
kr_{4Ca} &= \Delta t\ f_1\ (t_{(n)} + \Delta t, [Ca^{2+}]_{(n)} + kr_{2Ca}, Alk_{(n)} + kr_{2Alk}, Acid_{(n)} + kr_{2Acid}, \text{constants})
\end{aligned} \qquad \text{(E:2)}$$

Runge-Kutta factors for the Alkalinity rate equation

$$\begin{aligned}
kr_{1Alk} &= \Delta t\ 2\ f_1\ (t_{(n)}, [Ca^{2+}]_{(n)}, Alk_{(n)}, Acid_{(n)}, \text{constants}) \\
kr_{2Alk} &= \Delta t\ 2\ f_1\ (t_{(n)} + \frac{\Delta t}{2}, [Ca^{2+}]_{(n)} + \frac{kr_{1Ca}}{2}, Alk_{(n)} + \frac{kr_{1Alk}}{2}, Acid_{(n)} + \frac{kr_{1Acid}}{2}, \text{constants}) \\
kr_{3Alk} &= \Delta t\ 2\ f_1\ (t_{(n)} + \frac{\Delta t}{2}, [Ca^{2+}]_{(n)} + \frac{kr_{2Ca}}{2}, Alk_{(n)} + \frac{kr_{2Alk}}{2}, Acid_{(n)} + \frac{kr_{2Acid}}{2}, \text{constants}) \\
kr_{4Alk} &= \Delta t\ 2\ f_1\ (t_{(n)} + \Delta t, [Ca^{2+}]_{(n)} + kr_{2Ca}, Alk_{(n)} + kr_{2Alk}, Acid_{(n)} + kr_{2Acid}, \text{constants})
\end{aligned} \qquad \text{(E:3)}$$

Runge-Kutta factors for the Acidity rate equation

$$kr_{1Acid} = \Delta t\, f_2\,(t_{(n)}, [Ca^{2+}]_{(n)}, Alk_{(n)}, Acid_{(n)}, constants) = 0$$

$$kr_{2Acid} = \Delta t\, f_2\,(t_{(n)} + \frac{\Delta t}{2}, [Ca^{2+}]_{(n)} + \frac{kr_{1Ca}}{2}, Alk_{(n)} + \frac{kr_{1Alk}}{2}, Acid_{(n)} + \frac{kr_{1Acid}}{2}, constants) = 0$$

$$kr_{3Acid} = \Delta t\, f_2\,(t_{(n)} + \frac{\Delta t}{2}, [Ca^{2+}]_{(n)} + \frac{kr_{2Ca}}{2}, Alk_{(n)} + \frac{kr_{2Alk}}{2}, Acid_{(n)} + \frac{kr_{2Acid}}{2}, constants) = 0$$

$$kr_{4Acid} = \Delta t\, f_2\,(t_{(n)} + \Delta t, [Ca^{2+}]_{(n)} + kr_{2Ca}, Alk_{(n)} + kr_{2Alk}, Acid_{(n)} + kr_{2Acid}, constants) = 0$$

(E:4)

b) Use the Runge-Kutta factors in the formulae below to determine the Alkalinity and calcium concentrations at the subsequent port (n+1), noting that the Acidity remains constant.

$$[Ca^{2+}]_{(n+1)} = [Ca^{2+}]_{(n)} + \frac{1}{6}\left\{kr_{1Ca} + 2\,kr_{2Ca} + 2\,kr_{3Ca} + kr_{4Ca}\right\}$$

$$Alk_{(n+1)} = Alk_{(n)} + \frac{1}{6}\left\{kr_{1Alk} + 2\,kr_{2Alk} + 2\,kr_{3Alk} + kr_{4Alk}\right\}$$

$$Acid_{(n+1)} = Acid_{(n)} + \frac{1}{6}\left\{kr_{1Acid} + 2\,kr_{2Acid} + 2\,kr_{3Acid} + kr_{4Acid}\right\} = Acid_{(n)}$$

(E:5)

c) The pH at port (n+1) is determined from the average Acidity and the Alkalinity determine in 7 b) above, using a trial and error approach to solving Eq. 2:23 (a computer program was written for this purpose).
d) The $[CO_3^{2-}]$ at port (n+1) is then determined, using Eq. 4:10 and making use of the pH and the Alkalinity determined above.
e) Repeat from step 7 a) until the desired end port is reached.

Step 8: Calculate the sum of the squares of the difference between the experimentally observed values and those predicted by the model (7 above) for Alkalinity, ie. $\Sigma(Alk_{obs}-Alk_p)^2$, calcium, ie. $\Sigma(Ca_{obs}-Ca_p)^2$ and pH, ie. $\Sigma(pH_{obs}-pH_p)^2$ at each port.

Step 9: The procedure is repeated from step 6 above for another assumed rate constant, $k_{compound}$, until a minimum value for $\Sigma(Alk_{obs}-Alk_p)^2$ is found. The minimization algorithm is omitted for brevity, but numerous numerical methods exist which could be used to determine this minimum.

APPENDIX F

RESULTS OF DISSOLUTION EXPERIMENTS

The results of the investigation into the dissolution of Bredasdorp limestone granules (see Chapter 4) are reported in the following pages. The measured parameters are Alkalinity and calcium concentrations reported in mg $CaCO_3/\ell$, pH (pH units) and conductivity reported in mS/m. Alkalinity minus calcium, A.M.C., and Acidity are calculated from the measured parameters.

Note that the sampling ports are numbered sequentially from the bottom (inlet) of the reactor.

Experiment number: 1

media	: Bredasdorp limestone	Flow meter scale reading	: 7,0
granule size	: 8,05 mm	Loading rate	: 10,50 m/hr
water	: Acidified tap water	Temperature	: 23,8 °C

Port	Alkalinity mg $CaCO_3/\ell$	Calcium mg $CaCO_3/\ell$	pH	Conductivity mS/m	A.M.C. mg $CaCO_3/\ell$	Acidity mg $CaCO_3/\ell$
influent	- 3,02	40,6	4,07	18,48	-43,6	20,1
1	0,33	44,5	4,87	16,95	-44,2	20,4
2	1,39	45,0	5,50	16,87	-43,6	22,0
3	2,98	47,9	5,83	17,07	-44,9	19,2
4	4,26	49,0	6,09	17,25	-44,7	18,0
5	5,08	50,0	6,23	17,43	-44,9	18,5
6	6,74	51,0	6,39	17,67	-44,3	17,5
7	7,42	52,0	6,50	17,82	-44,6	18,5
8	8,78	53,0	6,59	18,03	-44,2	18,7
9	10,17	53,9	6,71	18,22	-43,7	19,0
10	11,00	54,9	6,77	18,36	-43,9	17,6
11	12,32	55,5	7,00	18.55	-43,2	17,6
12	12,74	56,0	7,05	18,83	-43,3	19,0
13	13,50	57,5	7,02	18,75	-44.0	17,7
14	14,32	58,0	7,25	18,84	-43.7	
effluent						

Calculated compound rate constant, $K_{DC\ compound}$: 0,0072

Experiment number: 2

media	: Bredasdorp limestone	Flow meter scale reading	: 7,0
granule size	: 8,05 mm	Loading rate	: 10,50 m/hr
water	: Acidified tap water	Temperature	: 23,4 °C

Port	Alkalinity mg $CaCO_3/\ell$	Calcium mg $CaCO_3/\ell$	pH	Conductivity mS/m	A.M.C. mg $CaCO_3/\ell$	Acidity mg $CaCO_3/\ell$
influent	- 4,85	40,0	4,02	17,59	-44,9	24,8
1	0,33	42,0	4,78	15,73	-41,7	- 0,6
2	- 0,07	45,5	5,66	15,75	-45,6	3,6
3	0,96	46,5	6,19	15,92	-45,5	5,4
4	2,30	47,0	6,50	15,82	-44,7	7,0
5	3,14	49,0	6,55	16,13	-45,9	14,0
6	6,88	50,5	6,62	16,15	-43.6	7,5
7	5,11	50,5	6,97	16,39	-45,4	7,8
8	5,11	52,8	6,91	16,64	-47,7	9,7
9	6,94	53,0	7,04	16,74	-46.1	12,4
10	9.83	54,0	7,22	16,91	-44,2	11,7
11	9,38	54,2	7,23	17,06	-44,8	13,4
12	10,72	55,5	7,23	17,30	-44,8	12,7
13	10,40	56,0	7,28	17,35	-45.6	13,5
14	11,20	56,0	7,31	17,67	-44,8	
effluent						

Calculated compound rate constant, $K_{DC\ compound}$: 0,0062

Experiment number: 3

media	: Bredasdorp limestone	Flow meter scale reading	: 25,0
granule size	: 8,05 mm	Loading rate	: 33,20 m/hr
water	: Acidified tap water	Temperature	: 23,7 °C

Port	Alkalinity mg $CaCO_3/\ell$	Calcium mg $CaCO_3/\ell$	pH	Conductivity mS/m	A.M.C. mg $CaCO_3/\ell$	Acidity mg $CaCO_3/\ell$
influent	-3,20	38,8	4,12	17,57	-42,0	
1	-1,61	40,0	4,59	16,36	-41,6	
2	-0,34	41,8	5,12	15,91	-42,1	
3	0,10	43,0	5,55	15,97	-42,9	1,5
4	1,53	43,8	5,97	16,10	-42,3	8,6
5	1,36	44,2	6,16	16,06	-42,8	5,4
6	2,07	44,8	6,31	16,28	-42,7	6,5
7	2,77	45,9	6,33	16,38	-43,1	8,4
8	3,50	46,2	6,48	16,61	-42,7	8,5
9	4,48	47,5	6,60	16,61	-43,0	9,3
10	4,86	47,5	6,75	16,78	-42,6	8,6
11	5,34	48,0	6,79	16,84	-42,7	9,1
12	6,04	48,9	6,84	16,78	-42,9	9,8
13	6,83	49,4	6,90	17,04	-42,6	10,5
14	6,88	50,0	6,94	16,84	-43,1	10,3
effluent						

Calculated compound rate constant, $K_{DC\ compound}$: 0,0133

Experiment number: 4

media	: Bredasdorp limestone	Flow meter scale reading	: 1,0
granule size	: 8,05 mm	Loading rate	: 2,94 m/hr
water	: Acidified tap water	Temperature	: 23,4 °C

Port	Alkalinity mg $CaCO_3/\ell$	Calcium mg $CaCO_3/\ell$	pH	Conductivity mS/m	A.M.C. mg $CaCO_3/\ell$	Acidity mg $CaCO_3/\ell$
influent	- 5,33	40,8	4,00	19,85	-46,1	
1	- 0,19	47,0	5,24	17,30	-47,2	
2	2,14	49,2	6,01	17,60	-47,1	11,2
3	3,14	52,0	6,20	17,72	-48,9	11,7
4	5,97	53,2	6,51	18,20	-47,2	13,9
5	7,93	55,0	6,67	18,44	-47,1	15,2
6	9,47	56,0	6,76	18,52	-46,5	16,5
7	10,82	57,0	6,81	18,92	-46,2	18,0
8	12.63	58,5	6,96	19,27	-45,9	18,5
9	15,03	61,0	7,13	19,68	-46,0	19,8
10	16,64	63,0	7,22	19,86	-46,4	20,9
11	18,35	64,0	7,25	20,60	-45,7	22,7
12	19,72	66,0	7,26	20,70	-46,3	24,3
13	21,74	67,9	7,28	20,95	-46,2	26,6
14	22,27	68,0	7,33	21,40	-45,7	26,7
effluent						

Calculated compound rate constant, $K_{DC\ compound}$: 0,0038

Experiment number: 5

media	: Bredasdorp limestone	Flow meter scale reading	: 9,9
granule size	: 8,05 mm	Loading rate	: 14,16 m/hr
water	: Acidified tap water	Temperature	: 22,1 °C

Port	Alkalinity mg $CaCO_3/\ell$	Calcium mg $CaCO_3/\ell$	pH	Conductivity mS/m	A.M.C. mg $CaCO_3/\ell$	Acidity mg $CaCO_3/\ell$
influent	-3,38	34,5	4,54	14,78	-37,9	
1	0,64	35,1	5,47	14,13	-34,5	10,4
2	1,33	37,0	6,14	14,31	-35,7	5,6
3	2,65	38,0	6,60	14,45	-35,4	5,6
4	4,39	39,0	7,02	14,64	-34,6	6,2
5	5,39	40,0	7,30	14,79	-34,6	6,6
6	6,05	40,5	7,53	14,86	-34,5	6,8
7	7,30	42,0	8,03	15,01	-34,7	7,5
8	7,58	42,5	8,37	15,20	-34,9	7,4
9	8,00	43,0	8,59	15,20	-35,0	7,6
10	8,19	43,2	8,72	15,36	-35,0	7,6
11	8,36	44,0	8,82	15,40	-35,6	7,6
12	8,47	44,1	8,88	15,46	-35,6	7,6
13	8,71	45,0	8,91	15,54	-36,3	7,7
14	8,63	46,0	8,90	15,62	-37,4	7,7
effluent	9,12	45,0	8,30	15,45	-35,9	9,1

Calculated compound rate constant, $K_{DC\ compound}$: 0,0094

Experiment number: 6

media	: Bredasdorp limestone	Flow meter scale reading	: 15,0
granule size	: 8,05 mm	Loading rate	: 20,59 m/hr
water	: Acidified tap water	Temperature	: 20,7 °C

Port	Alkalinity mg $CaCO_3/\ell$	Calcium mg $CaCO_3/\ell$	pH	Conductivity mS/m	A.M.C. mg $CaCO_3/\ell$	Acidity mg $CaCO_3/\ell$
influent	-5,76	34,7	3,90	17,08	-40,5	
1	-1,10	36,7	4,44	15,55	-37,8	
2	0,44	38,0	5,00	15,02	-37,6	20,8
3	1,44	40,0	5,77	15,02	-38,6	12,6
4	2,24	42,2	6,09	15,23	-40,0	10,5
5	3,43	42,7	6,36	15,29	-39,3	10,2
6	4,54	44,0	6,55	15,51	-39,5	10,3
7	5,77	44,5	6,77	15,61	-38,7	10,2
8	6,46	45,0	6,94	15,77	-38,5	9,8
9	7,95	46,0	7,08	15,77	-38,1	10,9
10	7,91	47,0	7,28	15,93	-39,1	9,8
11	11,09	47,5	7,46	15,95	-36,4	12,8
12	9,11	48,0	7,68	16,44	-38,9	9,9
13	9,40	48,4	7,96	16,13	-39,0	9,7
14	9,21	49,0	8,15	16,18	-39,8	9,3
effluent	9,95	49,7	7,67	16,11	-39,8	10,8

Calculated compound rate constant, $K_{DC\ compound}$: 0,0099

Experiment number: **7**

media	: Bredasdorp limestone	Flow meter scale reading	: 1,0
granule size	: 5,7 mm	Loading rate	: 2,94 m/hr
water	: Acidified tap water	Temperature	: 24,1 °C

Port	Alkalinity mg $CaCO_3/\ell$	Calcium mg $CaCO_3/\ell$	pH	Conductivity mS/m	A.M.C. mg $CaCO_3/\ell$	Acidity mg $CaCO_3/\ell$
influent	- 4,76	41,5	4,04	19,28	-46,3	
1	3,07	49,0	6,46	18,06	-45,9	7,7
2	6,78	52,0	7,12	17,99	-45,2	9,0
3	8,94	55,0	7,57	18,43	-46,1	9,9
4	10,39	57,5	7,95	18,62	-47,1	10,7
5	11,64	57,0	8,26	18,58	-45,4	11,6
6	13,32	59,5	8,42	18,70	-46,2	13,0
7	12,55	58,0	8,53	18,87	-45,5	12,1
8	12,82	58,8	8,67	18,79	-46,0	12,1
9	13,05	59,5	8,62	18,86	-46,5	12,4
10	13,70	59,0	8,65	18,83	-45,3	13,0
11	13,27	59,0	8,70	18,87	-45,7	12,4
12	13,23	59,5	8,72	18,94	-46,3	12,4
13	13,22	61,0	8,69	18,95	-47,8	12,4
14	14,05	61,0	6,70	18,97	-47,0	13,2
effluent	13,91	61,0	8,73	18,92	-47,1	13,0

Calculated compound rate constant, $K_{DC\ compound}$: 0,0026

Experiment number: **8**

media	: Bredasdorp limestone	Flow meter scale reading	: 24,0
granule size	: 5,7 mm	Loading rate	: 31,94 m/hr
water	: Acidified tap water	Temperature	: 24,3 °C

Port	Alkalinity mg $CaCO_3/\ell$	Calcium mg $CaCO_3/\ell$	pH	Conductivity mS/m	A.M.C. mg $CaCO_3/\ell$	Acidity mg $CaCO_3/\ell$
influent	- 4,71	38,8	4,04	19,55	-43,5	
1	- 0,01	44,5	5,07	19,63	-44,5	0,1
2	1,54	45,5	5,92	16,76	-44,0	9,6
3	2,47	47,5	6,41	17,06	-45,0	6,6
4	3.61	48,0	6,56	17,19	-44,4	7,9
5	4,85	50,2	6,89	17,29	-45,4	7,5
6	5,51	51,2	6,93	17,39	-45,7	8,3
7	6,47	51,0	7,10	17,59	-44,5	8,7
8	7,16	52,5	7,16	17,70	-45,3	9,3
9	8,06	52,2	7,30	18,06	-44,1	9,8
10	8,86	53,0	7,33	17,73	-44,1	10,6
11	9,77	53,2	7,44	17,92	-43,4	11,3
12	9,87	53,8	7,45	18,24	-43,9	11,3
13	10,40	54,0	7,59	18,13	-43,6	11,5
14	10,87	54,2	7,59	18,15	-43,3	12,0
effluent	12,18	55,2	7,70	18,06	-43,0	13,1

Calculated compound rate constant, $K_{DC\ compound}$: 0,0163

Experiment number: **9**

media	: Bredasdorp limestone	Flow meter scale reading	: 25,0
granule size	: 5,7 mm	Loading rate	: 33,20 m/hr
water	: Acidified tap water	Temperature	: 23,2 °C

Port	Alkalinity mg $CaCO_3/\ell$	Calcium mg $CaCO_3/\ell$	pH	Conductivity mS/m	A.M.C. mg $CaCO_3/\ell$	Acidity mg $CaCO_3/\ell$
influent	-5,19	40,3	4,01	16,74	-45,5	
1	- 0,47	45,6	4,55	15,19	-46,1	
2	1,01	49,0	5,52	14,87	-48,0	14,3
3	2,31	51,5	5,97	14,99	-49,2	13,0
4	3,53	50,0	6,35	15,13	-46,5	10,4
5	5,08	50,0	6,66	15,32	-44,9	9,9
6	6,18	52,0	6,88	15,07	-45,8	9,7
7	7,29	53,0	7,10	15,10	-45,7	9,8
8	8,20	53,0	7,28	15,40	-44,8	10,0
9	9,00	54,0	7,47	15,69	-45,0	10,3
10	9,61	55,0	7,65	15,51	-45,4	10,5
11	9,76	56,0	7,91	15,54	-46,2	10,2
12	10,54	57,0	8,12	16,06	-46,5	10,7
13	10,87	56,0	8,29	15,88	-45,1	10,8
14	11,51	57,0	8,41	16,10	-45,5	11,3
effluent	11,65	57,0	7,97	15,99	-45,4	12,0

Calculated compound rate constant, $K_{DC\ compound}$: 0,0181

Experiment number: **10**

media	: Bredasdorp limestone	Flow meter scale reading	: 19,0
granule size	: 5,7 mm	Loading rate	: 21,85 m/hr
water	: Acidified tap water	Temperature	: 23,8 °C

Port	Alkalinity mg $CaCO_3/\ell$	Calcium mg $CaCO_3/\ell$	pH	Conductivity mS/m	A.M.C. mg $CaCO_3/\ell$	Acidity mg $CaCO_3/\ell$
influent	- 8,91	48,3	3,84	17,59	-47,2	
1	- 2,27	43,5	4,29	15,50	-45,8	
2	0,35	46,5	4,96	14,70	-46,2	17,5
3	1,42	48,0	5,72	14,75	-46,6	13,2
4	3,35	50,0	6,19	15,07	-46,7	12,7
5	4,06	51,0	6,47	15,28	-46,9	10,0
6	6,01	52,0	6,67	15,38	-46,0	11,6
7	7,10	52,5	6,85	15,53	-45,4	11,4
8	8,04	54,0	7,02	15,72	-46,0	11,3
9	9,01	55,0	7,19	15,81	-46,0	11,5
10	9,53	56,0	7,32	15,93	-46,5	11,5
11	9,77	57,0	7,46	15,83	-47,2	11,2
12	10,37	57,0	7,66	16,09	-46,6	11,3
13	10,48	58,0	7,83	16,12	-47,5	11,0
14	11,18	58,0	7,99	16,30	-46,8	11,5
effluent	12,34	58,3	7,68	16,20	-46,0	13,4

Calculated compound rate constant, $K_{DC\ compound}$: 0,0149

Experiment number: 11

media	: Bredasdorp limestone	Flow meter scale reading	: 12,0
granule size	: 5,7 mm	Loading rate	: 16,81 m/hr
water	: Acidified tap water	Temperature	: 24,4 °C

Port	Alkalinity mg $CaCO_3/\ell$	Calcium mg $CaCO_3/\ell$	pH	Conductivity mS/m	A.M.C. mg $CaCO_3/\ell$	Acidity mg $CaCO_3/\ell$
influent	- 7,39	39,4	3,84	16,96	-46,8	
1	- 1,79	45,0	4,35	15,21	-46,8	
2	0,62	48,1	5,25	14,57	-47,5	15,9
3	2,00	49,8	5,88	14,78	-47,8	13,4
4	3,89	51,1	6,31	15,02	-47,2	12,1
5	5,52	52,8	6,60	15,21	-47,3	11,5
6	7,13	53,1	6,86	15,31	-46,0	11,4
7	8,69	54,0	7,06	15,42	-45,3	11,9
8	9,38	54,5	7,27	15,64	-45,1	11,5
9	10,51	55,0	7,44	15,80	-44,5	12,1
10	10,93	56,0	7,64	15,89	-45,1	11,9
11	11,64	55,0	7,84	16,02	-43,4	12,2
12	12,13	57,0	8,10	16,00	-44,9	12,3
13	12,72	58,0	8,30	16,13	-45,3	12,6
14	12,68	58,0	8,39	16,06	-45,3	12,4
effluent	12,99	59,0	8,40	16,10	46,0	12,7

Calculated compound rate constant, $K_{DC\ compound}$: 0,0128

Experiment number: 12

media	: Bredasdorp limestone	Flow meter scale reading	: 6,0
granule size	: 5,7 mm	Loading rate	: 9,24 m/hr
water	: Acidified tap water	Temperature	: 23,9 °C

Port	Alkalinity mg $CaCO_3/\ell$	Calcium mg $CaCO_3/\ell$	pH	Conductivity mS/m	A.M.C. mg $CaCO_3/\ell$	Acidity mg $CaCO_3/\ell$
influent						
1						
2	1,62	49,0	5,71	14,42	-47,4	15,4
3	3,17	49,8	6,20	14,68	-46,6	11,8
4	5,44	51,2	6,69	14,85	-45,8	10,2
5	7,17	52,3	7,09	15,01	-45,1	9,7
6	8,63	53,0	7,35	15,27	-44,4	10,3
7	9,89	51,0	7,66	15,39	-41,1	10,8
8	10,66	53,0	8,01	15,53	-42,3	10,9
9	11,19	54,0	8,35	15,65	-42,8	11,0
10	12,07	54,5	8,49	15,66	-42,4	11,7
11	12,26	55,0	8,58	15,70	-42,7	11,7
12	12,65	56,0	8,64	15,77	-43,4	12,0
13	12,81	56,0	8,66	15,78	-43,2	12,1
14	13,43	55,5	8,72	15,73	-42,1	12,6
effluent	13,06	55,3	7,97	15,69	-42,2	13,5

Calculated compound rate constant, $K_{DC\ compound}$: 0,0084

Experiment number: **13**

media	: Bredasdorp limestone	Flow meter scale reading	: 28,0
granule size	: 3,55 mm	Loading rate	: 36,99 m/hr
water	: Acidified tap water	Temperature	: 23,8 °C

Port	Alkalinity mg $CaCO_3/\ell$	Calcium mg $CaCO_3/\ell$	pH	Conductivity mS/m	A.M.C. mg $CaCO_3/\ell$	Acidity mg $CaCO_3/\ell$
influent	- 3,61	39,6	4,08	19,69	-43,2	
1	1,12	43,0	5,75	17,77	-41,9	9,8
2	2,53	46,0	6,36	18,05	-43,5	7,3
3	4,45	47,1	6,71	18,36	-42,7	8,2
4	6,08	49,0	6,94	18,52	-42,9	9,1
5	6,73	50,5	7,17	18,66	-43,8	8,7
6	8,54	52,0	7,25	18,77	-43,5	10,6
7	9,68	53,0	7,37	18,94	-43,3	11,4
8	11,02	54,2	7,47	19,29	-43,2	12,6
9	12,55	55,0	7,61	10,54	-42,5	13,8
10	12,77	56,0	7,63	19,57	-43,2	14,0
11	13,20	56,5	7,79	19,84	-43,3	14,0
12	14,09	56,5	7,79	19,84	-42,4	14,9
13	14,74	57,0	7,99	20,50	-42,3	15,2
14	15,44	58,0	7,94	20,50	-42,6	16,0
effluent	16,64	58,2	7,98	20,70	-41,6	17,2

Calculated compound rate constant, $K_{DC\ compound}$: 0,0265

Experiment number: **14**

media	: Bredasdorp limestone	Flow meter scale reading	: 28,0
granule size	: 3,55 mm	Loading rate	: 36,99 m/hr
water	: Acidified tap water	Temperature	: 24,2 °C

Port	Alkalinity mg $CaCO_3/\ell$	Calcium mg $CaCO_3/\ell$	pH	Conductivity mS/m	A.M.C. mg $CaCO_3/\ell$	Acidity mg $CaCO_3/\ell$
influent	-11,48	40,0	3,61	27,60	-51,5	
1	- 0,25	50,2	5,01	21,60	-50,5	
2	2,48	53,3	6,07	21,80	-50,8	11,5
3	4,65	56,4	6,31	22,00	-51,8	14,4
4	6,47	57,0	6,59	22,40	-50,5	13,6
5	7,92	58,8	6,71	22,70	-50,9	14,5
6	9,22	60,0	6,87	23,00	-50,8	14,5
7	10,32	61,0	7,00	23,20	-50,7	14,7
8	11,57	62,0	7,06	23,50	-50,4	15,8
9	13,18	64,0	7,18	23,60	-50,8	16,9
10	14,86	65,0	7,25	23,70	-50,1	18,4
11	14,98	66,2	7,35	24,00	-51,2	17,8
12	15,95	67,0	7,43	24,10	-51,1	18,4
13	16,62	68,0	7,55	24,30	-51,4	18,5
14	17,43	68,4	7,60	24,40	-51,0	19,2
effluent	18,01	68,5	7,70	24,60	-50,5	19,4

Calculated compound rate constant, $K_{DC\ compound}$: 0,0250

Experiment number: **15**

media	: Bredasdorp limestone	Flow meter scale reading	: 28,0
granule size	: 3,55 mm	Loading rate	: 36,99 m/hr
water	: Acidified tap water	Temperature	: 24,2 °C

Port	Alkalinity mg $CaCO_3/\ell$	Calcium mg $CaCO_3/\ell$	pH	Conductivity mS/m	A.M.C. mg $CaCO_3/\ell$	Acidity mg $CaCO_3/\ell$
influent	- 9,58	40,1	3,68	24,07	-49,7	
1	0,27	49,5	4,91	18,97	-49,2	15,1
2	1,76	53,0	5,97	18,99	-51.2	9,9
3	4,03	54,0	6,31	19,11	-50,0	12,5
4	5,43	56,0	6,62	19,37	-50,6	11,0
5	7,08	57,0	6,70	19,51	-49,9	13,1
6	8,50	58,0	6,92	19,85	-49,5	12,9
7	10,43	59,5	7,01	20,40	-49,1	14,8
8	11,53	61,0	7,08	20,50	-49,5	15,6
9	12,66	62,0	7,22	20,70	-49,3	15,9
10	13,70	62,5	7,29	20,50	-48,8	16,7
11	14,40	63,0	7,41	20,90	-48,6	16,7
12	15,20	63,2	7,42	21,10	-48,0	17,6
13	15,83	64,0	7,52	21,20	-48,2	17,8
14	16,32	65,0	7,49	21,40	-48,7	18,5
effluent	17,15	66,5	7,63	21,50	-49,4	18,8

Calculated compound rate constant, $K_{DC\ compound}$: 0,0267

Experiment number: **16**

media	: Bredasdorp limestone	Flow meter scale reading	: 24,9
granule size	: 3,55 mm	Loading rate	: 33,08 m/hr
water	: Acidified tap water	Temperature	: 23,7 °C

Port	Alkalinity mg $CaCO_3/\ell$	Calcium mg $CaCO_3/\ell$	pH	Conductivity mS/m	A.M.C. mg $CaCO_3/\ell$	Acidity mg $CaCO_3/\ell$
influent	-10,70	36,1	3,90	21,20	-46,8	
1	0,37	41,0	5,18	18,03	-40,6	11,2
2	2,60	44,5	6,10	18,12	-41,9	11,5
3	5,14	48,0	6,56	18,73	-42,9	11,2
4	7,09	49,0	6,76	18,72	-41,9	12,4
5	8,58	50,0	7,04	19,10	-41,4	11,9
6	9,96	52,0	7,17	19,09	-42,0	12,8
7	11,22	52,5	7,36	19,66	-41,3	13,3
8	12,10	54,0	7,54	19,86	-41,9	13,5
9	12,98	54,0	7,78	19,93	-41,0	13,8
10	13,58	54,6	7,94	20,60	-41,0	14,1
11	14,33	55,5	8,11	20,60	-41,2	14,5
12	14,86	55,0	8,22	19,88	-40,1	14,9
13	15,10	56,0	8,23	20,90	-40,9	15,1
14	15,72	56,0	8,20	20,30	-40,3	15,8
effluent	14,65	56,7	7,72	20,90	-42,1	15,7

Calculated compound rate constant, $K_{DC\ compound}$: 0,0245

Experiment number: **17**

media	: Bredasdorp limestone	Flow meter scale reading	: 19,9
granule size	: 3,55 mm	Loading rate	: 26,77 m/hr
water	: Acidified tap water	Temperature	: 21,9 °C

Port	Alkalinity mg $CaCO_3/\ell$	Calcium mg $CaCO_3/\ell$	pH	Conductivity mS/m	A.M.C. mg $CaCO_3/\ell$	Acidity mg $CaCO_3/\ell$
influent	-6,49	35,6	3,97	17,90	-42,1	
1	0,62	41,0	5,32	15,63	-40,4	14,0
2	3,03	44,1	6,19	16,00	-41,1	11,7
3	5,33	45,0	6,64	16,30	-39,7	10,7
4	7,33	45,5	7,04	16,49	-38,2	10,3
5	8,74	47,0	7,34	16,67	-38,3	10,5
6	9,85	49,5	7,54	16,91	-39,7	11,1
7	10,59	50,0	7,84	16,99	-39,4	11,2
8	11,28	51,0	8,19	17,00	-39,7	11,4
9	12,08	51,0	8,42	17,02	-38,9	11,8
10	12,50	51,8	8,51	17,17	-39,3	12,1
11	12,72	52,0	8,61	17,24	-39,3	12,2
12	12,96	53,0	8,64	17,23	-40,0	12,3
13	13,16	52,5	8,68	16,79	-39,3	12,5
14	13,22	53,0	8,66	17,43	-39,8	12,5
effluent	13,01	53,2	8,08	17,38	-40,2	13,3

Calculated compound rate constant, $K_{DC\ compound}$: 0,0198

Experiment number: **18**

media	: Bredasdorp limestone	Flow meter scale reading	: 22,4
granule size	: 3,55 mm	Loading rate	: 29,92 m/hr
water	: Acidified tap water	Temperature	: 22,8 °C

Port	Alkalinity mg $CaCO_3/\ell$	Calcium mg $CaCO_3/\ell$	pH	Conductivity mS/m	A.M.C. mg $CaCO_3/\ell$	Acidity mg $CaCO_3/\ell$
influent	-3,75	35,7	4,12	17,03	-39,5	
1	0,29	38,0	5,38	15,31	-37,7	5,8
2	3,10	42,5	6,31	15,64	-39,4	9,8
3	4,88	44,0	6,83	15,90	-39,1	8,0
4	6,60	45,0	7,21	16,74	-38,4	8,4
5	8,27	45,5	7,61	16,35	-37,2	9,1
6	8,88	46,0	8,12	16,45	-37,1	9,0
7	9,83	47,0	8,39	16,59	-37,2	9,6
8	10,11	50,0	8,54	16,61	-39,9	9,7
9	10,58	48,5	8,60	16,64	-37,9	10,1
10	10,80	48,5	8,67	16,73	-37,7	10,2
11	11,11	49,0	8,69	16,76	-37,9	10,4
12	11,13	49,5	8,70	16,81	-38,4	10,4
13	11,50	50,0	8,72	16,85	-38,5	10,7
14	11,42	51,0	8,68	16,84	-39,6	10,8
effluent	11,37	50,7	8,47	16,82	-39,3	11,1

Calculated compound rate constant, $K_{DC\ compound}$: 0,022

Experiment number: **19**

media	: Bredasdorp limestone	Flow meter scale reading	: 24,8
granule size	: 1,43 mm	Loading rate	: 32,95 m/hr
water	: Acidified tap water	Temperature	: 14,1 °C

Port	Alkalinity mg $CaCO_3/\ell$	Calcium mg $CaCO_3/\ell$	pH	Conductivity mS/m	A.M.C. mg $CaCO_3/\ell$	Acidity mg $CaCO_3/\ell$
influent	- 2,84	43,2	4,21	15,93	-46,0	
1	4,96	52,0	6,13	14,86	-47,0	23,6
2	7,24	55,0	6,40	15,21	-47,8	21,8
3	8,85	56,0	6,53	15,42	-47,2	22,0
4	10,08	57,0	6,65	15,55	-46,9	22,4
5	11,42	59,0	6,78	15,67	-47,6	21,0
6	12,83	60,0	6,88	15,91	-47,2	21,3
7	13,11	61,5	6,96	16,05	-48,4	20,3
8	15,06	61,0	7,06	16,19	-45,9	21,6
9	15,60	62,0	7,12	16,33	-46,4	21,5
10	16,58	62,0	7,21	16,37	-45,4	21,7
11	17,41	63,0	7,26	16,28	-45,6	22,2
12	17,87	65,0	7,33	16,51	-47,1	22,0
13	18,91	65,0	7,39	16,53	-46,1	22,7
14	19,32	65,0	7,45	16,67	-45,7	22,7
effluent	18,86	65,5	7,67	16,74	-46,6	20,8

Calculated compound rate constant, $K_{DC\ compound}$: 0,0217

Experiment number: **20**

media	: Bredasdorp limestone	Flow meter scale reading	: 19,9
granule size	: 1,43 mm	Loading rate	: 26,77 m/hr
water	: Acidified tap water	Temperature	: 14,8 °C

Port	Alkalinity mg $CaCO_3/\ell$	Calcium mg $CaCO_3/\ell$	pH	Conductivity mS/m	A.M.C. mg $CaCO_3/\ell$	Acidity mg $CaCO_3/\ell$
influent	- 3,78	35,0	4,09	15,02	-38,8	
1	4,06	45,0	6,36	13,56	-40,9	12,9
2	7,15	48,0	6,75	13,93	-40,9	13,5
3	8,53	48,0	6,93	14,22	-39,5	13,5
4	10,34	49,0	7,12	14,11	-38,7	14,2
5	11,25	51,0	7,25	14,35	-39,8	14,4
6	12,41	51,0	7,36	14,45	-38,6	15,1
7	13,37	53,0	7,46	14,43	-39,6	15,6
8	13,81	54,0	7,68	14,58	-40,2	15,2
9	14,39	55,0	7,76	14,51	-40,6	15,5
10	14,66	55,0	7,95	14,73	-40,3	15,3
11	15,64	56,0	8,12	14,62	-40,4	16,0
12	15,77	54,0	8,33	14,81	-38,2	15,8
13	16,67	56,0	8,42	14,86	-39,3	16,5
14	15,48	59,5	8,40	14,87	-44,0	15,4
effluent	16,08	57,3	7,83	14,83	-41,2	17,2

Calculated compound rate constant, $K_{DC\ compound}$: 0,021

Experiment number: **21**

media	: Bredasdorp limestone	Flow meter scale reading	: 14,9
granule size	: 1,43 mm	Loading rate	: 20,46 m/hr
water	: Acidified tap water	Temperature	: 14,5 °C

Port	Alkalinity mg $CaCO_3/\ell$	Calcium mg $CaCO_3/\ell$	pH	Conductivity mS/m	A.M.C. mg $CaCO_3/\ell$	Acidity mg $CaCO_3/\ell$
influent	- 3,08	32,0	4,40	12,65	-35,1	
1	4,03	40,0	7,00	12,20	-36,0	6,1
2	6,63	42,0	7,80	12,67	-35,4	7,1
3	7,58	43,0	8,47	12,89	-35,4	7,5
4	8,33	42,0	8,70	12,93	-33,7	8,0
5	9,11	42,0	8,85	13,00	-32,9	8,5
6	9,49	42,0	8,92	13,05	-32,5	8,7
7	8,79	43,0	8,96	12,89	-34,2	8,0
8	10,73	44,0	8,99	12,88	-33,3	9,7
9	12,98	44,0	9,02	13,02	-31,0	11,7
10	9,96	44,0	9,04	13,09	-34,0	8,9
11	9,96	44,0	9,05	12,89	-34,0	8,9
12	10,43	44,0	9,03	13,05	-33,6	9,3
13	10,43	43,1	9,06	13,18	-32,7	9,3
14	8,06	44,5	8,98	13,01	-36,4	7,3
effluent	10,78	44,8	7,94	13,01	-34,0	11,3

Calculated compound rate constant, $K_{DC\ compound}$: 0,014

Experiment number: **22**

media	: Bredasdorp limestone	Flow meter scale reading	: 24,8
granule size	: 8,05 mm	Loading rate	: 32,95 m/hr
water	: Rain water	Temperature	: 14,6 °C

Port	Alkalinity mg $CaCO_3/\ell$	Calcium mg $CaCO_3/\ell$	pH	Conductivity mS/m	A.M.C. mg $CaCO_3/\ell$	Acidity mg $CaCO_3/\ell$
influent	1,02	2,5	5,93	0,82	-1,5	7,3
1	1,50	3,5	5,77	0,73	-2,0	14,9
2	2,29	4,3	6,18	0,99	-2,0	10,2
3	2,98	4,6	6,49	0,95	-1,6	8,0
4	3,41	5,1	6,81	1,02	-1,7	6,2
5	4,41	5,5	7,24	1,27	-1,1	5,7
6	5,14	6,1	7,77	1,23	-1,0	5,6
7	5,76	6,9	8,23	1,46	-1,1	5,8
8	6,25	7,4	8,50	1,39	-1,2	6,1
9	6,73	8,0	8,74	1,56	-1,3	6,4
10	7,64	9,2	8,87	1,64	-1,6	7,1
11	8,16	9,1	8,94	1,55	-0,9	7,5
12	8,60	9,5	8,93	1,63	-0,9	7,9
13	8,97	9,7	8,84	1,79	-0,7	8,4
14	9,48	10,5	8,96	1,74	-1,0	8,7
effluent	8,50	9,1	8,14	1,61	-0,6	8,7

Calculated compound rate constant, $K_{DC\ compound}$: 0,0138

Experiment number: **23**

media	: Bredasdorp limestone	Flow meter scale reading	: 19,9
granule size	: 8,05 mm	Loading rate	: 26,77 m/hr
water	: Rain water	Temperature	: 12,8 °C

Port	Alkalinity mg $CaCO_3/\ell$	Calcium mg $CaCO_3/\ell$	pH	Conductivity mS/m	A.M.C. mg $CaCO_3/\ell$	Acidity mg $CaCO_3/\ell$
influent	0,64	2,7	5,89	0,81	-2,1	5,2
1	1,25	3,0	6,20	0,70	-1,8	5,4
2	1,99	5,6	6,56	0,82	-3,6	5,0
3	2,63	5,0	6,91	1,04	-2,4	4,4
4	3,63	5,5	7,38	1,11	-1,9	4,4
5	3,94	6,0	7,69	1,20	-2,1	4,4
6	4,70	6,4	8,15	1,18	-1,7	4,8
7	5,35	6,6	8,41	1,39	-1,3	5,3
8	5,57	7,2	8,72	1,30	-1,6	5,3
9	6,19	7,0	8,81	1,51	-0,8	5,8
10	6,35	8,0	8,92	1,55	-1,7	5,9
11	7,03	8,5	9,04	1,65	-1,5	6,3
12	7,56	8,6	9,11	1,70	-1,0	6,7
13	7,77	9,1	9,04	1,59	-1,3	7,0
14	8,28	9,1	8,91	1,75	-0,8	7,7
effluent	7,80	8,6	8,17	1,54	-0,8	8,0

Calculated compound rate constant, $K_{DC\ compound}$: 0,0101

Experiment number: **24**

media	: Bredasdorp limestone	Flow meter scale reading	: 9,9
granule size	: 8,05 mm	Loading rate	: 14,16 m/hr
water	: Rain water	Temperature	: 12,6 °C

Port	Alkalinity mg $CaCO_3/\ell$	Calcium mg $CaCO_3/\ell$	pH	Conductivity mS/m	A.M.C. mg $CaCO_3/\ell$	Acidity mg $CaCO_3/\ell$
influent	0,89	2,5	6,08	0,86	-1,6	4,9
1	1,71	3,6	6,67	0,95	-1,9	3,7
2	2,59	4,1	7,09	1,09	-1,5	3,7
3	3,49	5,0	7,53	1,08	-1,5	4,0
4	4,48	6,2	8,07	1,34	-1,7	4,6
5	4,90	6,9	8,69	1,25	-2,0	4,7
6	5,59	7,5	8,98	1,46	-1,9	5,1
7	6,60	8,0	9,19	1,47	-1,4	5,7
8	6,69	8,5	9,24	1,45	-1,8	5,6
9	7,19	8,4	9,34	1,80	-1,2	5,8
10	7,58	8,3	9,39	1,71	-0,7	6,0
11	7,73	8,6	9,43	1,75	-0,9	5,9
12	8,43	9,1	9,49	1,70	-0,7	6,3
13	8,58	9,1	9,41	1,85	-0,5	6,7
14	8,48	9,3	9,64	1,80	-0,8	5,6
effluent	8,80	9,4	8,94	1,76	-0,6	8,2

Calculated compound rate constant, $K_{DC\ compound}$: 0,0068

Experiment number: **25**

media	: Bredasdorp limestone	Flow meter scale reading	: 20,0
granule size	: 8,05 mm	Loading rate	: 26,90 m/hr
water	: Rain water	Temperature	: 13,9 °C

Port	Alkalinity mg $CaCO_3/\ell$	Calcium mg $CaCO_3/\ell$	pH	Conductivity mS/m	A.M.C. mg $CaCO_3/\ell$	Acidity mg $CaCO_3/\ell$
influent	1,43	2,3	6,27	2,02	-0,9	5,5
1	2,57	3,2	6,98	2,14	-0,6	4,0
2	3,35	3,9	7,52	2,40	-0,6	3,9
3	4,28	5,3	7,83	2,61	-1,0	4,6
4	5,31	6,4	8,47	2,51	-1,1	5,2
5	6,00	7,0	8,90	2,76	-1,0	5,5
6	6,82	7,4	9,00	2,76	-0,6	6,2
7	7,50	8,5	9,25	2,89	-1,0	6,2
8	7,84	9,0	9,33	2,98	-1,2	6,3
9	8,24	9,3	9,32	2,87	-1,1	6,7
10	8,91	9,5	9,41	3,10	-0.6	6,9
11	9,59	10,0	9,14	3,84	-0,4	8,4
12	10,27	10,9	9,48	2,80	-0.6	7,7
13	8,57	8,2	9,55	2,87	0,4	6,0
14	9,44	8,4	9,33	2,65	1,0	7,7
effluent	9,36	9,6	8,81	2,82	-0,2	8,8

Calculated compound rate constant, $K_{DC\ compound}$: 0,0121

Experiment number: **26**

media	: Bredasdorp limestone	Flow meter scale reading	: 10,0
granule size	: 5,7 mm	Loading rate	: 14,29 m/hr
water	: Table Mountain water	Temperature	: 19,4 °C

Port	Alkalinity mg $CaCO_3/\ell$	Calcium mg $CaCO_3/\ell$	pH	Conductivity mS/m	A.M.C. mg $CaCO_3/\ell$	Acidity mg $CaCO_3/\ell$
influent	4,61	4,7	6,54	9,34	-0,1	10,8
1	6,76	7,5	7,68	9,52	-0,7	7,4
2	8,64	9,0	7,35	9,75	-0,4	10,4
3	10,69	11,0	7,87	9,94	-0,3	11,3
4	11,62	11,0	8,15	10,07	0,6	11,8
5	12,63	12,0	8,44	10,17	0,6	12,4
6	13,66	12,0	8,72	10,22	1,7	12,9
7	14,38	13,0	8,83	10,36	1,4	13,4
8	15,38	14,0	8,93	10,52	1,4	14,0
9	15,74	15,0	9,02	10,52	0,7	14,0
10	16,41	16,0	9,07	10,59	0,4	14,4
11	16,82	18,0	9,05	10,71	-1,2	14,9
12	16,74	17,0	9,10	10,67	-0,3	14,6
13	16,96	17,0	9,12	10,61	-0,0	14,7
14	17,35	17,3	8,76	10,74	0,1	16,4
effluent						

Calculated compound rate constant, $K_{DC\ compound}$: 0,011

Experiment number: **27**

media	: Bredasdorp limestone	Flow meter scale reading	: 18,8
granule size	: 5,7 mm	Loading rate	: 25,38 m/hr
water	: Table Mountain water	Temperature	: 19,3 °C

Port	Alkalinity mg $CaCO_3/\ell$	Calcium mg $CaCO_3/\ell$	pH	Conductivity mS/m	A.M.C. mg $CaCO_3/\ell$	Acidity mg $CaCO_3/\ell$
influent	4,84	5,2	6,72	9,26	-0,3	9,1
1	6,15	6,8	6,99	9,36	-0,6	9,1
2	7,61	7,5	7,10	9,52	0,1	10,4
3	8,90	8,3	7,16	9,67	0,7	11,8
4	9,87	9,5	7,30	9,78	0,4	12,1
5	10,70	10,3	7,37	9,86	0,5	12,8
6	10,77	11,5	7,42	10,04	0,3	13,8
7	12,19	12,5	7,74	9,98	-0,3	13,1
8	13,43	13,0	7,86	10,00	0,4	14,2
9	13,72	13,3	7,84	10,10	0,5	14,5
10	14,22	14,0	7,76	10,26	0,2	15,3
11	14,30	15,0	7,78	10,42	-0,7	15,3
12						
13						
14						
effluent	15,96	15,6	8,77	10,50	0,4	15,0

Calculated compound rate constant, $K_{DC\ compound}$: 0,0138

Experiment number: **28**

media	: Bredasdorp limestone	Flow meter scale reading	: 14,9
granule size	: 5,7 mm	Loading rate	: 20,46 m/hr
water	: Table Mountain water	Temperature	: 14 °C

Port	Alkalinity mg $CaCO_3/\ell$	Calcium mg $CaCO_3/\ell$	pH	Conductivity mS/m	A.M.C. mg $CaCO_3/\ell$	Acidity mg $CaCO_3/\ell$
influent	6,29	6,8	6,84	10,62	-0.5	10,9
1	6,34	9,0	6,95	10,46	-2,7	10,0
2	8,48	10,0	7,24	10,66	-1,5	11,0
3	9,60	10,0	7,39	10,82	-0,4	11,6
4	10,47	11,0	7,66	10,88	-0,5	11,6
5	11,00	12,0	7,87	11,08	-1,0	11,7
6	11,82	13,0	8,28	11,08	-1,2	11,9
7	12,17	13,5	8,11	11,04	-1,3	12,5
8	13,29	14,0	8,54	11,24	-0,7	13,0
9	13,45	16,0	8,63	11,38	-2,6	13,0
10	14,25	17,0	8,72	11,37	-2,8	13,7
11	14,59	21,0	8,75	11,40	-6,4	13,9
12	14,51	17,0	8,87	11,53	-2,5	13,6
13	15,13	16,0	8,97	11,72	-0,9	13,9
14	15,28	17,3	8,45	11,53	-2,0	15,1
effluent						

Calculated compound rate constant, $K_{DC\ compound}$: 0,0085

Experiment number: **29**

media	: Bredasdorp limestone	Flow meter scale reading	: 25,0
granule size	: 5,7 mm	Loading rate	: 33,20 m/hr
water	: Table Mountain water	Temperature	: 12,8 °C

Port	Alkalinity mg $CaCO_3/\ell$	Calcium mg $CaCO_3/\ell$	pH	Conductivity mS/m	A.M.C. mg $CaCO_3/\ell$	Acidity mg $CaCO_3/\ell$
influent	4,39	5,6	6,75	10,38	-1,2	8,5
1	7,12	6,1	7,17	10,44	1,0	9,5
2	7,80	6,8	7,41	10,55	1,0	9,4
3	8,95	7,6	7,65	10,68	1,4	10,0
4	9,11	8,0	7,84	10,78	1,1	9,7
5	9,85	9,1	8,25	10,90	0,8	10,0
6	10,55	9,8	8,25	10,85	0,8	10,7
7	10,82	10,2	8,10	10,89	0,6	11,1
8	11,44	10,4	8,52	11,00	1,0	11,3
9	11,85	11,1	8,65	11,06	0,8	11,5
10	12,30	12,1	8,75	11,12	0,2	11,8
11	12,45	12,5	8,81	11,11	-0,1	11,8
12	12,51	13,0	8,92	11,15	-0,5	11,6
13	12,63	13,0	8,92	11,20	-0,4	11,7
14	12,80	12,4	7,85	11,23	0,4	13,7
effluent						

Calculated compound rate constant, $K_{DC\ compound}$: 0,011

Experiment number: **30**

media	: Bredasdorp limestone	Flow meter scale reading	: 24,9
granule size	: 5,7 mm	Loading rate	: 33,08 m/hr
water	: Table Mountain water	Temperature	: 14,8 °C

Port	Alkalinity mg $CaCO_3/\ell$	Calcium mg $CaCO_3/\ell$	pH	Conductivity mS/m	A.M.C. mg $CaCO_3/\ell$	Acidity mg $CaCO_3/\ell$
influent	-2,92	43,3	4,30	15,82	-46,2	
1	-0,26	45,0	4,76	14,80	-45,3	
2	1,39	47,0	5,54	14,64	-45,6	
3	2,43	48,1	5,89	14,62	-45,7	18,1
4	3,11	49,5	6,06	14,72	-46,4	16,6
5	3,71	50,0	6,20	14,66	-46,3	15,4
6	5,07	50,0	6,36	14,88	-44,9	16,1
7	5,71	51,0	6,17	15,06	-45,3	24,9
8	5,86	52,0	6,56	15,08	-46,1	13,9
9	7,03	53,0	6,64	15,28	-46,0	15,0
10	7,76	53,0	6,73	15,28	-45,2	14,9
11	8,04	56,0	6,80	15,30	-48,0	14,4
12	8,59	57,5	6,88	15,37	-48,9	14,2
13	8,91	58,0	6,96	15,58	-49,1	13,8
14	9,84	59,0	7,26	15,54	-49,2	12,5
effluent						

Calculated compound rate constant, $K_{DC\ compound}$: 0,0116